ABSTRACT

DIAGENETIC AND COMPOSITIONAL CONTROLS OF WETTABILITY IN SILICEOUS SEDIMENTARY ROCKS, MONTEREY FORMATION, CALIFORNIA

By

Kristina M. Hill

May 2015

Modified imbibition tests were performed on 69 subsurface samples from Monterey Formation reservoirs in the San Joaquin Valley to measure wettability variation as a result of composition and silica phase change. Contact angle tests were also performed on 6 chert samples from outcrop and 3 nearly pure mineral samples. Understanding wettability is important because it is a key factor in reservoir fluid distribution and movement, and its significance rises as porosity and permeability decrease and fluid interactions with reservoir grain surface area increase. Although the low permeability siliceous reservoirs of the Monterey Formation are economically important and prolific, a greater understanding of factors that alter their wettability will help better develop them. Imbibition results revealed a strong trend of decreased wettability to oil with increased detrital content in opal-CT phase samples. Opal-A phase samples exhibited less wettability to oil than both opal-CT and quartz phase samples of similar detrital content.

Subsurface reservoir samples from 3 oil fields were crushed to eliminate the effect of capillary pressure and cleansed of hydrocarbons to eliminate wettability alterations by asphaltene, then pressed into discs of controlled density. Powder discs were tested for wettability by dispensing a controlled volume of water and motor oil onto the surface and measuring the time required for each fluid to imbibe into the sample. The syringe and software of a CAM101 tensiometer were used to control the amount of fluid dispensed onto each sample, and imbibition completion times were determined by high-speed photography for water drops; oil drop imbibition was significantly slower and imbibition was timed and determined visually. Contact angle of water and oil drops on polished chert and mineral sample surfaces was determined by image analysis and the Young-Laplace equation. Oil imbibition was significantly slower with increased detrital composition and faster with increased silica content in opal-CT and quartz phase samples, implying decreased wettability to oil with increased detrital (clay) content. However, contact angle tests showed that opal-CT is more wetting to oil with increased detritus and results for oil on quartz-phase samples were inconsistent between different proxies for detritus over their very small compositional range. Water contact angle trends also showed inconsistent wetting trends compared to imbibition tests. We believe this is because the small range in bulk detrital composition between the "pure" samples used in contact angle tests was close to analytical error and because small-scale spatial compositional variability may be significant enough to effect wettability. These experiments show that compositional variables significantly affect wettability, outweighing the effect of silica phase.

DIAGENETIC AND COMPOSITIONAL CONTROLS OF WETTABILITY IN SILICEOUS SEDIMENTARY ROCKS, MONTEREY FORMATION, CALIFORNIA

A THESIS

Presented to the Department of Geological Sciences

California State University, Long Beach

In Partial Fulfillment

of the Requirements for the Degree

Master of Science in Geology

Committee Members:

Richard J. Behl, Ph.D. (Chair)
Matthew Becker, Ph.D.
Hilario Camacho Ph.D.

College Designee:

Robert D. Francis, Ph.D.

By Kristina M. Hill

B.S., 2009, California State University, Long Beach

May 2015

ProQuest LLC.
789 East Eisenhower Parkway
P.O. Box 1346
Ann Arbor, MI 48106 - 1346

ACKNOWLEDGEMENTS

Special thanks to Dr. Richard J. Behl, for never-ending dedication to excellence and truth in science. Your questions, ideas and guidance made this project a truly beneficial contribution to the geologic community. Your expectation of excellence from each student evinces your belief that each of us can always become more than what we are. Thanks to Drs. Matt Becker and Hilario Camacho for invaluable input; including methodology determination, critical editing assistance, and the reduction of my tested variables from roughly one million to only one-hundred thousand.

Additional thanks to Dr. Varenka Lorenzi and the staff at IIRMES, for phenomenal assistance with Soxhlet extraction of all core samples. With your kind and generous helpfulness I never felt like I was an obstacle or a burden in the lab, even as I weaved my work into your already busy schedules and tried not to break more than just the one Soxhlet. Thanks to Dr. Young-Seok Shon of the Chemistry Department for the generous and continually extended temporary donation of the CAM101 tensiometer and its specially designated computer. Many thanks to Dr. Bengt Allen of the Biology Department for tremendous assistance in using and understanding the appropriate statistical approaches for our study.

Thanks to Lisa Battig for recruiting me, first to God's team, and next to CSULB. I would not be the woman I am today without your godly, faithful, big-sisterly mentoring and I may never have made it to college without your encouragement.

Thanks to my parents for continually asking when I was graduating throughout my seven year, double major undergraduate education. Your persistent question echoed in the back of mind throughout my graduate education. Thank you both for always believing that I could do anything, and for proving it with your lifelong support in all the athletic, academic and spiritual pursuits that have shaped my life and character.

Above all, thanks to God for the inspiration, ability, and perseverance to complete this task. Without you I would never have the motivation to work hard for anything and I would have given up on life a long time ago. Your love, truth, faithfulness and power get me out of bed every morning and teach me to dream and work hard to make the greatest possible impact with my life. This thesis is dedicated to all the people I hope to serve and benefit by the future work made possible through this accomplishment. May you be many and spread far around the globe.

TABLE OF CONTENTS

Page

ACKNOWLEDGEMENTS iii

LIST OF TABLES vii

LIST OF FIGURES viii

CHAPTER

1. INTRODUCTION 1

2. BACKGROUND 4

    Wettability 4
    Standard Wettability Measurement Techniques 6
    Previous Work 9

3. MATERIALS AND METHODS 16

    Materials 16
    Methods 17

4. RESULTS 27

    X-Ray Diffraction 27
    Elemental Analysis 27
    Water Imbibition Tests 32
    Oil Imbibition Tests 34
    Water Contact Angle Tests 35
    Oil Contact Angle Tests 35
    Wettability Test Results vs. Composition 39

5. DISCUSSION 49

    Study Approach and Development 49
    Wettability Differences Between Silica Phase Groups 51
    Correlation Strength for Compositional Control of Test Results 51

CHAPTER Page

Overall Water Imbibition Assessment 57
Overall Oil Imbibition Assessment 58
Contact Angles 59
Principal Component Analysis 68
Multiple Regression Analysis 76
Comparison with Previous Work 80

6. CONCLUSIONS AND SYNTHESIS 83

7. FUTURE WORK 89

REFERENCES 91

LIST OF TABLES

TABLE Page

2.1. Dynamic Contact Angles of Water-Soaked Reservoir Minerals 13

2.2. Dynamic Contact Angles of Oil-Aged Reservoir Minerals 14

LIST OF FIGURES

FIGURE Page

2.1. Contact angle between a fluid, gas and solid 5

2.2. Examples of reservoir wettability 5

3.1. CAM101 tensiometer used for imbibition and contact angle tests 19

3.2. Soxhlet extraction for powdered core samples 19

3.3. Pressed discs of core samples for imbibition tests 20

3.4. Contact angle image capture from the CAM101 tensiometer software 20

3.5. XRD diffractogram of montmorillonite-bearing opal-A sample 24

3.6. Chart of montmorillonite weight percent vs. montmorillonite characteristic peak height at ~ 6° 2θ for opal-A samples 24

3.7. XRD diffractogram of montmorillonite-bearing opal-CT sample with a peak height at ~ 6° 2θ for opal-A samples 25

3.8. Chart of montmorillonite weight percent vs. montmorillonite characteristic XRD peak height at ~ 6° 2θ for opal-CT samples 25

4.1. Abundances by weight percent for major oxides from ICP-MS and ICP-IES analysis 29

4.2. Abundances by weight percent for minor oxides from ICP-MS and ICP-OES analysis 30

4.3. Elemental abundances in ppm from ICP-MS and ICP-OES analysis 31

4.4. Water imbibition rates by silica phase group for pressed discs from core samples 33

4.5. Oil imbibition rates by silica phase group for pressed discs from core samples 36

FIGURE Page

4.6. Water contact angle test results 37

4.7. Water contact angle tests displaying near average contact angle 38

4.8. Oil contact angle test results 39

4.9. Detritus in weight percent vs. oil contact angle 41

4.10. Biogenic & diagenetic silica in weight percent vs. oil contact angle 42

4.11. Potassium oxide in weight percent vs. oil contact angle 43

4.12. Titanium oxide in weight percent vs. oil contact angle 43

4.13. Water imbibition rate vs. montmorillonite clay weight percent 45

4.14. Oil imbibition rate vs. montmorillonite clay weight percent 46

4.15. Water imbibition rate vs. detritus weight percent 46

4.16. Oil imbibition rate vs. detritus weight percent 47

4.17. Water imbibition rate vs. biogenic & diagenetic silica weight percent 47

4.18. Oil imbibition rate vs. biogenic & diagenetic silica weight percent 48

4.19. Oil imbibition rate vs. magnesium oxide weight percent 48

5.1. Coefficients of determination for compositional variable abundances vs. imbibition rate test results for opal-A phase samples 52

5.2. Coefficients of determination for compositional variable abundances vs. imbibition rate test results for opal-CT phase samples 54

5.3. Moderate and significant R^2 correlations between oil imbibition times and opal-CT phase samples 55

5.4. Moderate R^2 correlations between oil imbibition times vs. Fe_2O_3, MgO, Na_2O, K_2O, Sc, and Al_2O_3 for opal-CT phase samples 55

5.5. Moderate R^2 correlations between oil imbibition times vs. TiO_2 and MnO for opal-CT phase samples 56

FIGURE Page

5.6. Moderate R^2 correlations between oil imbibition times vs. barium, zircon, and vanadium for opal-CT phase samples 56

5.7. Coefficients of determination for compositional variable abundances vs. imbibition rate test results for quartz phase samples 57

5.8. Coefficients of determination for compositional variable abundances vs. contact angle test results for opal-CT phase samples 61

5.9. Moderate R^2 correlations between water contact angles and element abundances for opal-CT phase samples 61

5.10. Moderate R^2 correlations between water contact angles and oxide abundances for opal-CT phase samples 62

5.11. Significant and moderate R^2 correlations between oil contact angles and oxide abundances for opal-CT phase samples 62

5.12. Significant and moderate R^2 correlations between oil contact angles vs. clay and detritus for opal-CT phase samples 63

5.13. Significant R^2 correlations between oil contact angles vs. silica-based compositional variables for opal-CT phase samples 63

5.14. Coefficients of determination for compositional variable abundances vs. contact angle test results for quartz phase samples 65

5.15. Moderate and significant R^2 correlations between water contact angles vs. compositional variables for quartz phase samples 66

5.16. Significant R^2 correlations between oil contact angles vs. silica-based variables and clay for quartz phase samples 66

5.17. Moderate R^2 correlations between oil contact angles vs. oxides for quartz phase samples..... 67

5.18. Moderate R^2 correlations between oil contact angles vs. compositional variables for quartz phase samples 67

5.19. Scree plot produced by PAST software PCA 69

5.20. Biplot produced by PAST software PCA 71

FIGURE Page

5.21. PC1 vs. H_2O imbibition 73

5.22. PC2 vs. H_2O imbibition 73

5.23. PC1 scores grouped by silica phase vs. oil imbibition rate..... 75

5.24. PC2 scores grouped by silica phase vs. oil imbibition rate..... 75

5.25. PC1 vs. water contact angle 77

5.26. PC2 vs. water contact angle 77

5.27. PC1 vs. oil contact angle..... 78

5.28. PC2 vs. oil contact angle..... 78

6.1. Water imbibition test trends for geologically significant compositional variables 85

6.2. Oil imbibition test trends for geologically significant compositional variables 86

6.3. Water contact angle test trends for geologically significant compositional variables 87

6.4. Oil contact angle test trends for geologically significant compositional variables 88

CHAPTER 1

INTRODUCTION

As petroleum provinces mature through standard oil field development practices, extractable reserves from high quality reservoirs are depleted beyond the ability of primary production techniques to retrieve. To balance this depletion in resources, exploration and production have increasingly looked to unconventional low-permeability reservoirs like tight sandstones and shales for additional reserves. Exploitation of these low-permeability rocks requires a more sophisticated understanding of the variables controlling migration, charge and extraction, including electrochemical relationships between the solid minerals and pore fluids, including wettability.

The state of California currently produces 7% of the nation's crude oil, making it one of the top domestic producers (U.S. Energy Information Administration [EIA], 2014). Within the state, the San Joaquin Valley is the most prolific oil-producing basin with current proved reserves at more than 100 million barrels of oil (MMBO) from 21 producing fields (Tennyson et al., 2012). The basin is home to the Midway Sunset, Kern River, and South Belridge fields, three of the top ten largest oil fields in the United States, all three of which produce from Monterey Formation reservoirs. Despite the vast and (highly sought after) oil reserves in the Monterey Formation reservoirs of the San Joaquin Valley, a significant amount of the original oil in place remains underground. Diatomite reservoirs have high porosities created by the interlocking matrix of diatoms,

sponge spicules and fine detritus (Garrison, 1992), but permeability values remain low– 0.1 to 10 millidarcies (mD) (Bhat & Kovscek, 1998). These rocks are composed largely of geologically unusual biogenic and diagenetic silica phases that have been little studied elsewhere. During silica diagenesis porosity and permeability are dramatically reduced, but in a complex, nonlinear fashion. Although oil has been produced from the Monterey for more than a century, most of the production was from higher-permeability, naturally fractured reservoirs. Only relatively recently has the need increased to understand production from the highly porous, but low-permeability rock matrix of diatomite and porcelanite. Thus, primary production from these siliceous reservoirs is difficult and still unperfected. Montgomery and Morea (2001) estimated that primary recoveries only range from 4-6% in the Buena Vista Hills field, even after decades of production, and that improved oil recovery methods (IOR) such as waterflood, acidization and artificial fracturing were only able to increase total recovery to between 6-12%.

Consequently, IOR techniques will be critical to unlocking the remaining reserves in the Monterey Formation reservoirs of California, and a greater understanding of the impacts of wettability will help in their development (Lemke and Schwochau, 1992). Wettability affects fluid distribution, saturations, relative permeability and capillary pressures—key properties of hydrocarbon reservoirs that allow us to exploit them effectively (Civan, 2004). Developing technologies rely increasingly on wettability measurements for secondary recovery methods (Odusina et al., 2012) and new methods of wettability alteration, including temperature change, surfactant and low salinity brine injection, and selective ions, are already being used to improve production in tight

sandstone reservoirs (Mohanty & Kathel, 2013). These methods can alter wettability of reservoirs from one fluid phase to another and increase spontaneous imbibition of oil.

Although changes in rock mineralogy, porosity, and permeability associated with silica diagenesis are fairly well known, little is understood about the impact of silica phase change and compositional variation of siliceous rocks on wettability. This study attempts to characterize and quantify those impacts by measuring wettability on Monterey Formation rocks covering a range of compositions, with special attention to the impact of silica phase and clay content to help understand fluid distribution and mobility in Monterey Formation reservoirs.

CHAPTER 2

BACKGROUND

Wettability

Wettability is the relative affinity between a surface and a fluid resulting from the hydrostatic intermolecular interactions between the two phases. The most basic expression of wettability is the contact angle θ (Figure 2.1), created when a drop of fluid is placed on a flat surface of a solid in the presence of a controlled third substance—often air, but sometimes a known liquid (Abdallah et al., 2007). Surfaces that are termed "water wet" or "water wetting" have a greater affinity for water molecules than the control fluid (e.g. oil, air). Water droplets on these "hydrophilic" surfaces lie flat, with a smaller contact angle theta between the fluid drop and the surface (Figure 2.1). Surfaces that are non-water wetting are termed "hydrophobic." In this case a drop of water would bead up to create a large contact angle θ, as shown in Figure 1.

In a petroleum reservoir, rock is considered "water wet" or water is termed the "wetting phase" when water is the primary or exclusive fluid in contact with the rock surface, while other phases, most commonly hydrocarbons, are not in contact with the rock surface, but are contained within the water-bound pore space (Figure 2.2). When the fluid positions are reversed, the rock is considered "oil wet" and oil is the "wetting phase." Wettability dramatically affects initial reservoir fluid distribution and multi-phase fluid flow through reservoir pore space over time. "Tight" (i.e., low permeability)

formations are more profoundly affected by the wetting phase than formations with higher porosity and permeability due to the higher proportion of fluid-rock surface area per fluid volume (Mohanty & Kathel, 2013).

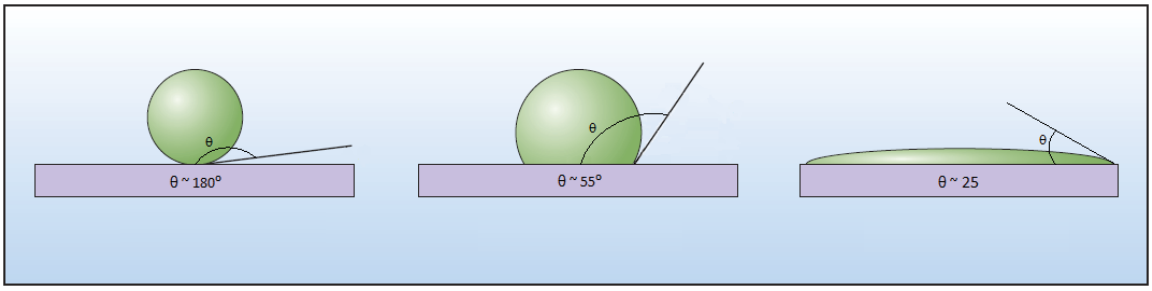

FIGURE 2.1. Contact angle between a fluid, gas and solid. Left: A large contact angle near 180° is created when a surface is non-wetting to a fluid. Center: A moderate contact angle is created when a surface is not strongly wetting to a fluid. Right: A small contact angle near 0° is created when a surface is strongly wetting to a fluid (Modified from Abdallah et al., 2007).

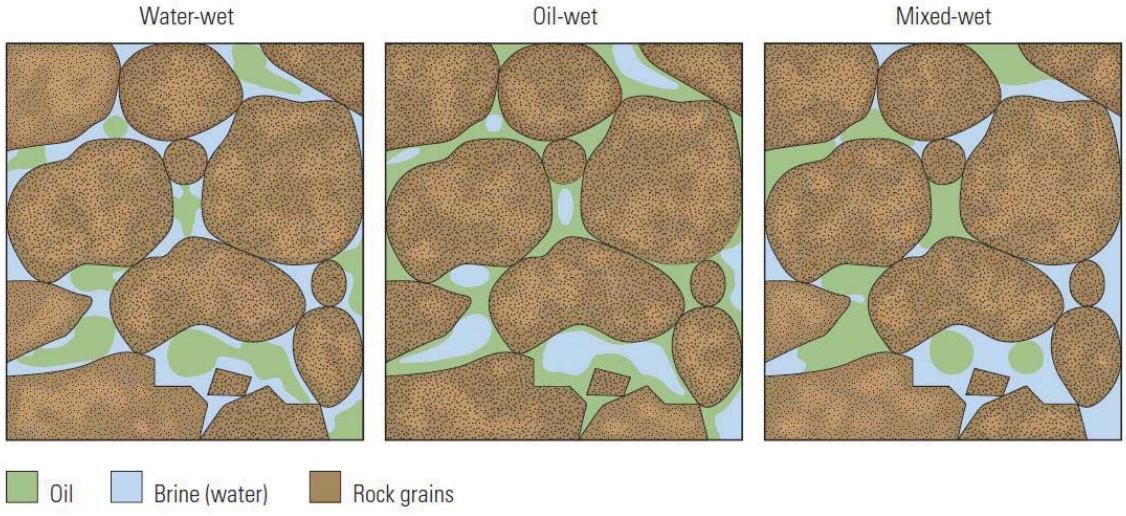

FIGURE 2.2. Examples of reservoir wettability. Left: In a water-wet reservoir (left) water molecules are contact with reservoir matrix grains and hydrocarbons are stored in the interstitial pore space surrounded by water. Center: In an oil wet reservoir (right) the positions are reversed and hydrocarbons are the phase in contact with reservoir grains. Right: In a mixed wet reservoir (center) both phases are in contact with reservoir rock grains (Modified from Abdallah et al., 2007).

Standard Wettability Measurement Techniques

The Amott-Harvey, Nuclear Magnetic Resonance (NMR), capillary rise, Wilhelmy plate, and contact angle methods for quantification of wettability were considered for use in this study because of their use in previous studies.

The Amott-Harvey test is widely used in the petroleum industry as an integral part of reservoir characterization. It is conducted by measuring both the spontaneous and forced imbibition rates of oil and water through a one-inch diameter core plug. After *in situ* hydrocarbons are removed from the plug it is flushed with water and then placed in a bath of oil. The amount of water in the sample that is spontaneously displaced by the oil under natural surface pressures is measured. The same test is conducted a second time with oil replacing the water as the displacing fluid. Next, the sample is once again flushed with water and placed in a centrifuge. A controlled amount of oil is forced through the sample at a capillary pressure determined by the speed and radius of the centrifuge. The capillary pressure required to force the entire amount of oil through the sample is also directly related to the wettability of the plug's solid material to the fluid tested. Spontaneous and forced imbibition measurements are combined to calculate an index value between -1 and 1, indicating the sample's wettability to oil and water, respectively.

The Amott-Harvey test was considered for use in this study because of its ubiquitous use in the petroleum industry as an integral part of reservoir characterization. However, of the Monterey Formation reservoir rocks, only diatomites of the opal-A silica phase would be suitable for this method of testing. Opal-CT and quartz-phase porcelanites have permeability values too low to allow the complete imbibition of tested

fluids in a reasonable time frame (Toronyi, 1997). The need for sufficiently high and comparable permeability values between all three silica phases eliminates the Amott-Harvey test as an effective approach for this study.

NMR logs are a relatively new and potentially effective tool, generally used to determine the amount of free and moveable water in a reservoir. NMR functions by sending a magnetic pulse through surrounding rock formations that causes polarized fluid molecules to spin. The amount of time required for fluid molecules in contact with rock surface to relax after stimulation is much shorter than the relaxation time of the bulk fluid not in contact with the reservoir. The fluid in contact with the reservoir is considered the "wetting phase" and is identified by its relaxation time (Freedman et al., 2003).

The capillary rise method is commonly used to measure the wettability of a powder to a fluid. Wettability by this method is determined by measuring the amount of fluid in a bath that spontaneously imbibes into a tube filled with the test powder, which is packed down and covered on the bottom by mesh or cheese cloth. The greatest challenge of this method is to control the packing of the powder in the tube so that the density of the sample powder is known and equivalent amongst all test samples. Some researchers have developed a mechanized way to control this packing density (Seth et al., 2001). The amount of fluid imbibed into the tube is commonly measured by visually marking the fluid height in the tube of packed powder. This can be problematic, as the height of the fluid may not be uniform around the circumference of the tube.

The Washburn method is similar, but uses a computer-monitored scale (Kirdponpattara et al., 2013). The amount of fluid imbibed into the packed tube is measured by the reduction in weight of the fluid bath, rather than by a semi-ambiguous

fluid height on the powder sample. This method uses the theoretical relationships between the mass of fluid absorbed and the powdered media to calculate a "contact angle" by the formula,

$$T = (\eta/C\rho 2\gamma \cos\theta)M2 \quad (1)$$

where T = time of contact, ρ = density of liquid, γ = surface tension of liquid, θ = contact angle, η = viscosity of liquid, C = material constant characteristic of solid sample, T = time after contact, M = mass of liquid adsorbed on solid, $C = rc\varepsilon 2(\pi R2)2/2$, rc = equivalent pore radius, ε = powder porosity and R = powder packing radius (Thakker et al., 2013).

The Wilhelmy plate method (Zelenev et al., 2011) is commonly used in the pharmaceutical field. In this method, a plate covered with the test material is lowered into a bath of a test fluid, and the contact angle between the surface of the fluid bath and the plate is measured as the contact angle.

The contact angle method is the most direct form of measurement of wettability of a surface to a fluid, and is the most ideal approach. The most common method of conducting this test is to use a goniometer or tensiometer, which employs a high-speed camera attached to a computer to take pictures of a drop of fluid on a leveled surface. This fluid drop is often administered by a measured syringe equipped to control the amount of fluid dispensed. Specialized software then analyzes the photos taken and uses the Young-Laplace equation to calculate the angle between the fluid drop and surface. The disadvantages of this method is that it requires a nonporous, smoothly polished, even surface that does not exist in most of the naturally occurring siliceous rocks of the

Monterey Formation (diatomite, diatomaceous mudstone, porcelanite, and siliceous mudstone). It is only available for nearly pure cherts or fracture-filling vein material.

Previous Work

The wettability of reservoir rocks is a key property affecting the quality and economic viability of a reservoir (Anderson, 1987) therefore, the factors affecting sandstone and carbonate reservoir wettability to water and oil have been widely studied (Barclay and Worden, 2000; Civan 2004; Fernø et al., 2011; Gupta & Mohanty, 2011; Karabakal and Bagci, 2004; Matyasik et al., 2010; Sayyouh et al., 1990; Shedid & Ghannam, 2004), as these are the most common hydrocarbon reservoir formation types in conventional petroleum systems. Little published research has yet been done on either the wettability of siliceous reservoir rocks, or of the importance of compositional variation within them. Temperature, fluid chemistry and rock mineralogy and secondary constituents such as clay, carbonates, clastics, organic material, etc., all may have significant impacts on formation wettability (Civan, 2004; Buckly, 1998; Kovcsek et al., 2010; Kumar et al., 2005; Lamparter et al., 2013; Lemke and Schwochau, 1992; Sayyouh et al., 1990).

Temperature

The impact of temperature on rock formation wettability has been studied relatively extensively compared to other variable controls of wettability. In general, reservoir rocks show increased wettability to oil with increased temperature. Madden and Strycker (1988) observed that Berea sandstone cores became increasingly water wet with increased temperature. Civan (2004) attempted to better constrain the predictability of wettability alteration with temperature change, by referencing previous studies of

isothermal capillary pressure effects in various sand-glass bead/air-water systems. The studies cited by Civan (2004) show the effect of temperature on wettability by relying on the indirect relationship between wettability and capillary pressure to infer wettability values rather than making any direct wettability measurements. For diatomaceous reservoir rocks, Kovcsek et al. (2010) reported an increase in spontaneous imbibition of water, or increased wettability to water, into diatomite cores with increased temperature.

Oil-Brine Chemistry

The chemical composition of the hydrocarbons and pore water present in a reservoir play a key role in the wettability of a reservoir to oil and water, as well as the length of time the formation is exposed to each fluid chemistry. Lemke and Schwochau (1992) used the Dynamic Wilhelmy Method, which measures advancing and receding contact angles by lowering a mineral slice into a fluid phase and measuring immersion depth plus acting surface forces, to demonstrate that mineral attraction to oil increases when the minerals are aged in hexadecane (a reproducible reservoir hydrocarbon substitute in this study) before conducting wettability tests, especially for calcite, limestone and dolomite. The same principle of increased wetting to a fluid after a 72 hour period of aging held true for the tested carbonate rocks and water.

Buckley (1998) describes two molecular interactions by which asphaltenes—the components of hydrocarbons that are aromatic, have a high molecular weight and propensity to aggregate—alter the wettability of reservoir rock to oil and water. The first of these two interactions, called "ionic" (acid/base and ion binding) interactions between asphaltenes and reservoir rock, most often increase the wettability of rock in a reservoir system to hydrocarbons. This effect can be reversed depending on the chemistry of the

formation water, however. In general, brines with a pH higher than 6.0 were more water wet, regardless of oil aging, while sample subjected to brines with pH below 6.0 were strongly influenced by asphaltenes to become increasingly oil wet with crude oil aging. The second type of molecular interactions are "colloidal" interactions between asphaltenes and reservoir rocks that increased rock wettability to oil, regardless of brine composition. Polar organic compounds in crude oils absorb onto mineral surfaces by collecting at water-oil interfaces and subsequently increase mineral wettability to oil at contact sites (Kumar et al., 2005). The presence of bitumen in reservoir rocks also increases rock wettability to oil, although, as with asphaltenes, this effect is less pronounced for siliciclastic reservoirs than carbonate ones (Lemke & Schwochau, 1992, as in Mann, 1994).

Chandrasekhar and Mohanty (2013) experimented with brine chemistry in limestone reservoir rocks in order to determine which brines improve oil recovery and found that oil-wet calcite plates became water wet in the presence of brine with high concentrations of Mg^{2+} and SO_4^{2-} ions. He attributes the increase in water-wet conditions to multi-ion exchange and mineral dissolution. Berg et al. (2010) demonstrated that lowering the salinity of formation water in sandstone reservoirs effectively expels hydrocarbons from formation clay particles as a result of increased water wetting from the salinity change. Finally, for siliceous sedimentary rocks, Takahashi and Kovscek (2010a) determined that both very high and very low pH brine solutions, compared to more neutral pH values, led to greater water wetting in siliceous shales of the Monterey Formation in the San Joaquin Basin, evidenced by greater oil productivity in spontaneous and forced imbibition tests.

Reservoir Mineral Wettability

Lemke and Schwochau (1992) quantified the contact angles of several common reservoir minerals, including quartz, calcite, limestone, dolomite, kaolin, albite and muscovite under three conditions: dry, aged in hexadecane for 72 hours at 20°C, and aged in hexadecane for 72 hours at 80°C. Wettability was determined by advancing and receding contact angles using the Dynamic Wilhelmy Method. Results for dry mineral contact angles are shown in Table 2.1. Albite, muscovite, kaolin, calcite and limestone show the greatest affinity for oil, in decreasing order, while quartz, calcite and dolomite were the most intrinsically water wet. Calcite, dolomite and limestone were the most affected by oil aging at 80°C and became strongly oil wet after treatment, while the remaining minerals were not significantly affected (Table 2.2).

As early as 1960, Moore (1960) documented that wet clay particles coating sand grains increase the wettability of their surrounding sands in reservoir rock by their inherent hydrophyllicity. Phyllosilicate clays such as smectites, illites and chlorites are permanently charged according to Schampera & Dultz (2011), in contrast with uncharged phyllosilicates talc and pyrophyllite. Charged phyllosilicates naturally bind layers of polar water molecules to their surface, and are water wet as a result.

Monterey Formation Wettability

Zhou et al. (2001) conducted a countercurrent imbibition study on a diatomite outcrop sample from the Grefco quarry in Lompoc, California. This study used a pump to circulate water through a partially oil-saturated core, then measured the amount of oil produced from the core. The cores tested strongly water wet.

TABLE 2.1. Dynamic Contact Angles of Water-Soaked Reservoir Minerals

Mineral	θ_A	θ_R
Quartz	17°	0°
Calcite (single crystal)	9°	0°
Limestone	15°	0°
Dolomite	9°	0°
Kaolin	18°	13°
Albite	21°	0°
Muscovite	19°	14°

Note: Advancing (θ_A), and receding (θ_R) contact angles measured on minerals, not subjected to oil aging (from Lemke and Schwochau, 1992).

Montgomery and Morea (2001) successfully measured the wettability of opal-CT samples from Antelope Shale reservoir cores using the Amott-Harvey method, despite common difficulties with this technique (Toronyi, 1997).

TABLE 2.2. Dynamic Contact Angles of Oil-Aged Reservoir Minerals

Mineral	θ_A	θ_R
Quartz	57°	55°
Calcite (single crystal)	138°	35°
Limestone	118°	49°
Dolomite	122°	48°
Kaolin	83°	47°
Albite	108°	52°

Note: Advancing (θ_A), and receding (θ_R) contact angles measured on minerals aged for 72 hours in hexadecane at 80ºC. Calcite, dolomite and limestone samples show the strongest response to oil aging, becoming strongly water wet (from Lemke and Schwochau, 1992).

The success of these tests is likely due to the sufficient, if low, porosity and permeability values of the tested samples. Opal-CT samples tested had an average porosity of 0.338 with mean permeability of 0.33mD, while opal-CT siltstones had mean porosities of 0.257 and average permeabilities of 0.69 mD. Their results describe high oil imbibition rates as a sign of strong water wetness, but refer to deZabala (1999) for a quantitative wettability index value of +0.78, where +1 is strongly water wet, -1 is strongly oil wet, and 0 is neutral (Abdallah et al., 2007). Toronyi (1997) characterized opal-CT phase samples from the Brown Shale unit of the Monterey Formation as water wet using a field dispersion test, but was unable to quantify the results. Due to the inability of the low

permeability rocks to channel fluids, lab wettability tests by the Amott-Harvey method were not obtained.

Takahashi and Kovscek (2010b) reported that Monterey Formation siliceous rocks (primarily quartz porcelanite) are either moderately oil-wet or mixed-wet, based on oil recovery by spontaneous countercurrent imbibition and by forced displacement. They also evaluated the effect of pH on wettability of these siliceous shales and reported contact angles for neutral pH brines at approximately 10°, using an augmented Young-Laplace equation to determine contact angles from measured surface forces.

Due to the diverse nature of Monterey Formation reservoirs and their composition of three distinct diagenetic silica phases, both the quantification of the wettability of each silica phase and the comparison between different secondary compositions within each phase are needed. Opal-A and opal-CT rocks are especially difficult to measure and poorly documented in wettability related literature. This study attempts to develop a reproducible method for testing and to produce initial measurements of wettability to advance current understanding.

CHAPTER 3

MATERIALS AND METHODS

Materials

A total of 69 subsurface samples from oil and gas well cores of Monterey Formation rocks were obtained for analysis of homogenized powders: 22 opal-CT and quartz phase samples were taken from two wells in the Elk Hills Field and 13 opal-CT and quartz phase samples are from one well in the Buena Vista Field. Thirty-four opal-A diatomite samples were taken from two wells in the Midway Sunset Field. These samples were chosen specifically to span all three silica phases and to encompass a broad range of compositions to be ground to powder, pressed into compact discs and used for contact angle and imbibition tests.

Nine samples of Monterey Formation rock from outcrop were chosen for silica phase, composition and impermeability. One sample of hydrothermal hyalite from Australia was obtained to provide an impermeable surface of opal-A silica. Four outcrop samples from beds and nodules of opal-CT chert, one opal-CT vein with minor quartz, and one sample of non-biogenic "ice cream opal" from Idaho, an opal-CT phase mineral were selected to provide non-porous samples for the opal-CT phase. Two quartz chert samples from bedded outcrops and one pure megacrystalline quartz sample were used to provide non-porous surfaces for the final silica phase. These samples were selected

specifically for contact angle tests on impermeable, polished, but otherwise unaltered surfaces.

Methods

The quantitative measurement of the wettability of powdered substances is important in numerous fields of study, including pharmaceutics, food, cosmetics and industrial granular solids, as well as being highly beneficial to petroleum geology and reservoir studies (Nowak et al., 2013; Susana et al., 2012; Depalo and Santomaso, 2013). Nonetheless, measurement of contact angles on powder samples is highly problematic. Pressed samples of powder are often permeable to fluid and therefore unable to produce stable contact angles in many fluid-surface experiments (Nowak et al., 2013).

In order to obtain reliable and relevant results, two methods of wettability measurement were employed. First, the relative wettability of Monterey Formation reservoir rocks was determined by measuring the rate of water and motor oil (which has a high enough viscosity to dispense in controllable amounts from the syringe of the CAM101 Tensiometer) imbibition into pressed discs of powders of known silica phase, size and density. Next, direct contact angle measurements were conducted with a tensiometer (a type of digital, optical goniometer) (Figure 3.1) on a separate set of solid, impermeable, polished, nearly pure hand samples of each silica phase: opal-A hyalite, opal-CT and quartz phase cherts and a non-biogenic crystalline quartz sample.

Opal-CT and quartz phase samples for powdered analysis were made available by industry and collected from a core warehouse. Opal-A diatomaceous samples were collected from a specialized storage facility where they were stored under refrigerated conditions. Samples were removed from core with hammer and chisel and transported in

zip-sealed plastic bags to CSULB for analysis. At CSULB, samples were ground in a ball mill and then stored in glass vials with plastic, air-tight lids. Given that the presence of hydrocarbons in a material is known to alter mineral wettability (Buckley, 1998), samples underwent hydrocarbon removal by Soxhlet extraction with methylene chloride. This method is proven to effectively remove more than 90% of hydrocarbons in sediment samples (Lau et al., 2014; Collister et al., 2004). For Soxhlet extraction, the 69 powdered core samples were baked dry at 50°C for ~18 hours—near the bottom of temperature ranges known to initiate diagenesis in smectites and siliceous sediment (Compton, 1991; Keller and Isaacs, 1985) then weighed and placed in a silicone thimble. Each sample thimble was placed in a glass Soxhlet, which was positioned over a vial of 200 ml of pure dichloromethane (DCM, or methylene chloride). Each vial-Soxhlet glassware combination set (Figure 3.2) was attached beneath a water-cooling system over metal heating grates. The heating grate was run for approximately sixteen hours, during which the heated DCM converted to gas and traveled up to the water cooler. The chilled DCM condensed and flowed into the sample-bearing Soxhlet. Hydrocarbons dissolved in the DCM and flowed through the porous silicone thimble, into the glass vial, where they remained until the extraction process was complete and the hydrocarbon bearing DCM waste was disposed of. After hydrocarbon extraction, each sample was baked dry at 50°C for ~18 hours in its silicone thimble and re-weighed to determine the mass of hydrocarbons removed. Finally, samples were returned to DCM rinsed glass vials with hexane-rinsed plastic lids.

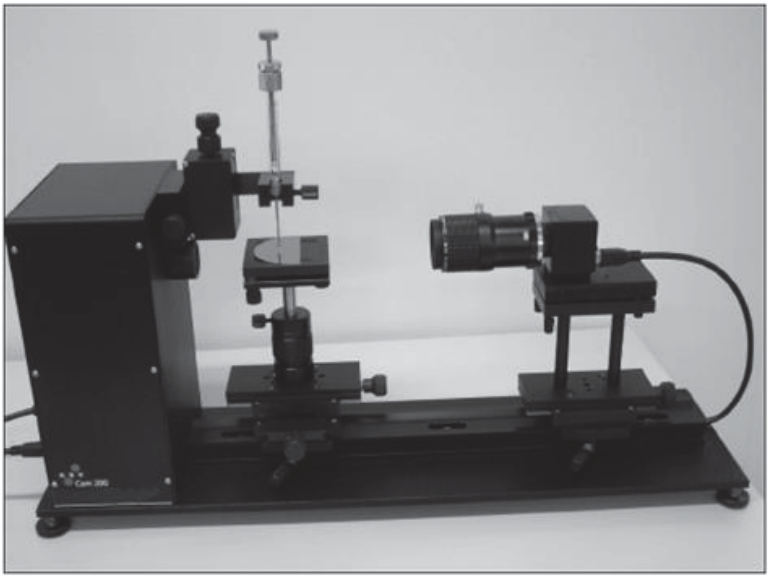

FIGURE 3.1. CAM101 tensiometer used for imbibition and contact angle tests.

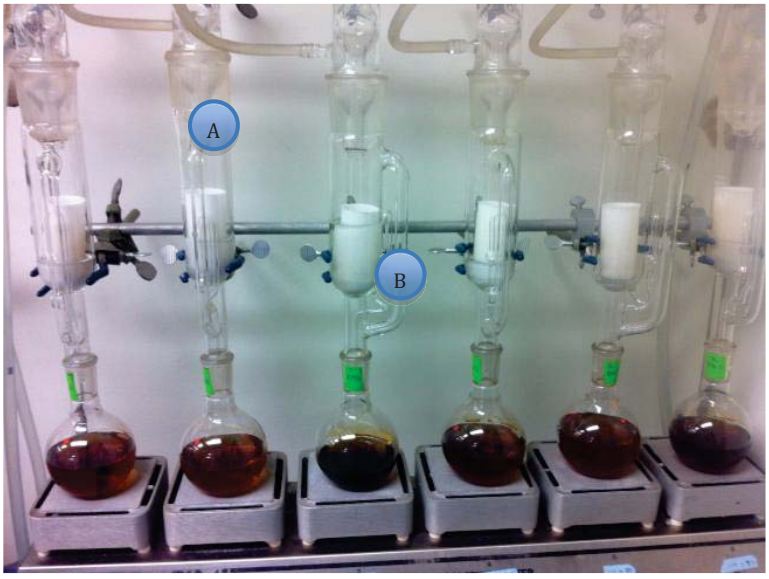

FIGURE 3.2. Soxhlet extraction for powdered core samples. A. White silicon thimbles filled with powdered core sample. B. Glass beakers filled with dichloromethane and hydrocarbons removed from each sample after extraction process is complete.

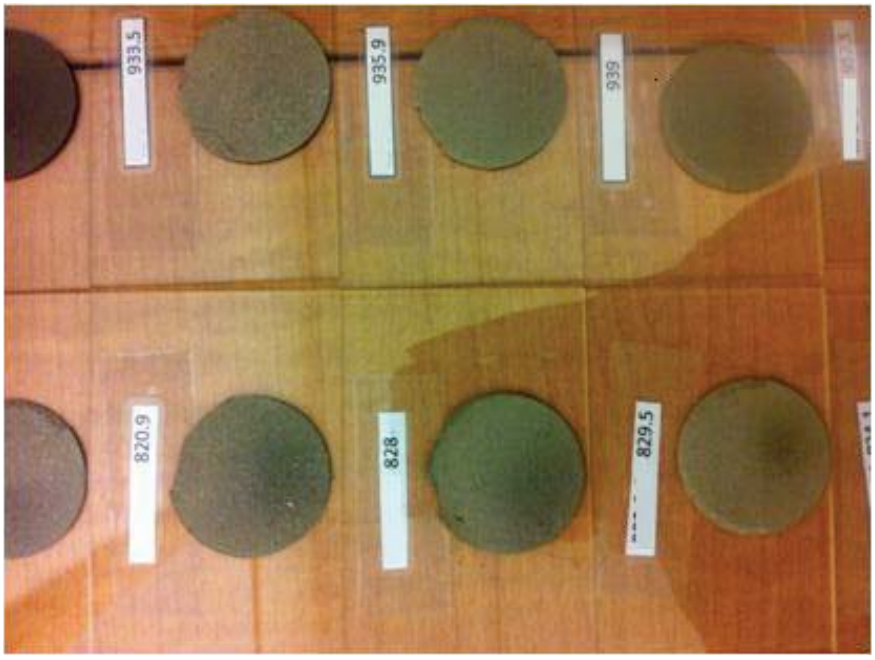

FIGURE 3.3. Pressed discs of core samples for imbibition tests.

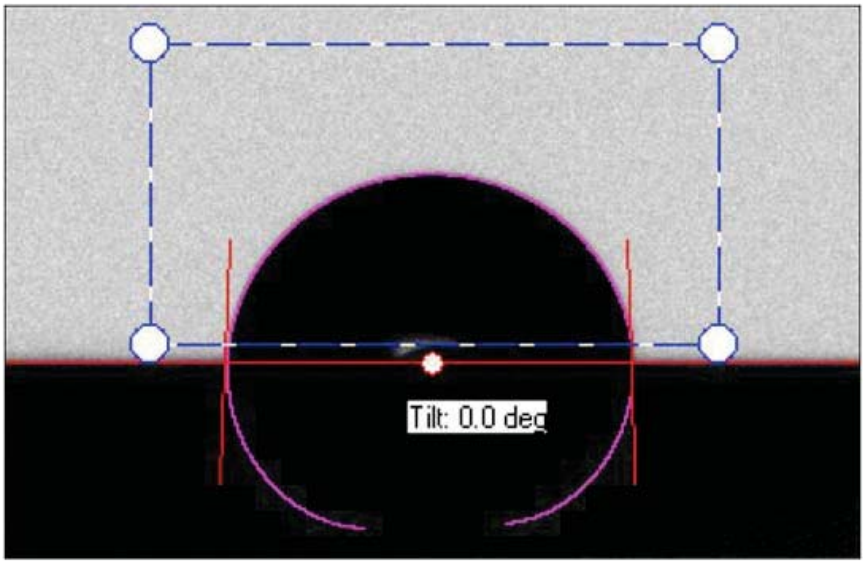

FIGURE 3.4. Contact angle image capture from the CAM101 tensiometer software.

For imbibition tests, 0.75 g (0.002 st.dev.) of each powdered core sample was pressed into a ~0.75mm thick disc (0.16 st. dev.) with a diameter of 3.175 cm with a hydraulic press at 10,000 lbs of pressure held for an average of one second (Figure 3.3). Pressed sample discs were then placed onto a glass slide with a small piece of double-sided adhesive tape to prevent sample discs from sliding (Figure 3.3). The sample slides were then placed onto the stage of a CAM101 tensiometer, where three to seven drops of distilled water and 3 drops of Castrol HD40 single grade motor oil were dispensed at different locations on each sample disc. For opal-CT and quartz samples, water tests and oil tests were conducted on separate pellets of identical sample and preparation as, due to lack of sample cohesiveness, sample discs frequently broke into pieces creating less continuous surface area for testing. Diatomite samples were highly cohesive, presumably due to higher clay content, and provided sufficient surface area for testing both water and oil droplet tests. Imbibition tests were recorded with a high-speed camera connected to CAM101 software for contact angle measurement (Figure 3.1). Due to the rapid imbibition times of water into core samples, an initial image capture speed of one photo per 0.199 seconds was set for the first 2 seconds in order to obtain high accuracy for measuring water imbibition times. Following images were taken at the slower rate of one image per second in order to prevent captured data from overwhelming the available disc space of the recording computer. Water imbibition tests were recorded by the CAM101 camera for 30 seconds. No water imbibition tests lasted longer than the observed period. Oil imbibition tests lasted up to four hours, so digital image recording was not a feasible method to observe test completion. After 30 seconds of CAM101 image capture, oil imbibition time was measured with an electronic timer and visual detection of oil sheen

on the sample surface with the aid of additional directed LED lighting and a hand lens. Water imbibition times were measured solely with the use of timed photos of the CAM101 software and visual detection of fluid above sample surface through the camera lens/photos.

Contact Angles

Each of the nine solid rock or mineral samples was cut and polished on a 6 μm-diamond grit polishing lap. Once polished, each sample was placed on the stage of a CAM101 tensiometer, where it was leveled and centered in front of a high-speed camera. An average of five drops each of Castrol HD40 and distilled water were dispensed at different locations on each sample, and images recorded at high speed of the fluid droplet until each drop reached a stable contact angle – about 30 seconds for water droplets and about 90 seconds for oil droplets. CAM101 software employed the Young-Laplace equation to calculate the contact angle between the fluid droplets and the sample surface in recorded images (Figure 3.4) (Rodríguez-Valverde et al., 2002).

X-Ray Diffraction

All core samples and hard rock samples were analyzed by X-ray diffractometer (XRD) to determine mineral composition and silica phase. Samples were measured in a Rigaku MiniFlex X-ray diffractometer, operated at 30 kV and 15 mA with X-rays generated from a copper anode target. Each sample was scanned from 5° to 45° 2θ at 0.2° steps for 1 second/step (Figure 3.5).

Montmorillonite Weight Percentage Calculations

Four measured mixtures of pure opal-A diatomite, montmorillonite and illite clay were analyzed in the x-ray diffractometer. Two mixtures contained 50% diatomite by

weight, one with 20% montmorillonite, 30% illite and the other with 20% illite, 30% montmorillonite. Another two measured mixtures contained 70% diatomite by weight. One of these contained 10% montmorillonite, 20% illite and the other with 10% illite, 20% montmorillonite. A coefficient of determination of $R^2 = 0.985$ was determined between the weight percent of montmorillonite and its characteristic peak height between 5.99 and 6.01 2θ. The resulting equation,

Montmorillonite wt% = 0.214 * (peak height at ~6 2θ) - 2.128

was applied to all diatomite samples (Figure 3.6).

An identical model was made for opal-CT samples with equal measurements by weight of montmorillonite and illite clays, but with pure opal-CT in place of opal-A diatomite. A coefficient of determination of 0.923 was established between the weight percent of montmorillonite and its characteristic peak height between 5.99 and 6.01 2θ (Figure 3.7). The resulting equation,

Montmorillonite wt% = 0.236 * (peak height at ~6 2θ) - 1.484

was applied to all opal-CT phase samples (Figure 3.8).

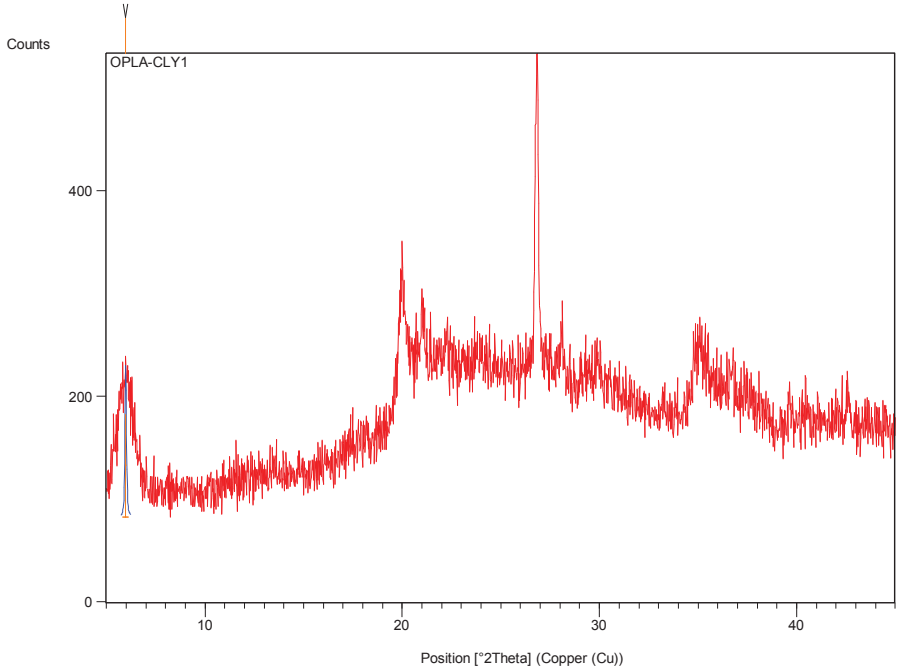

FIGURE 3.5. XRD diffractogram of montmorillonite-bearing opal-A sample. Peak height at approximately 6° 2θ measured for correlation with montmorillonite weight percent.

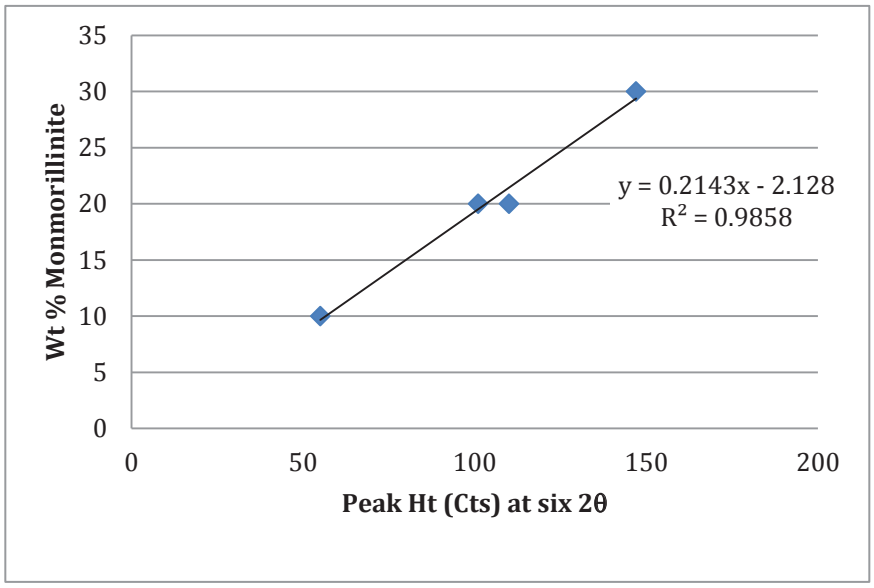

FIGURE 3.6. Chart of montmorillonite weight percent vs. montmorillonite characteristic peak height at ~ 6° 2θ for opal-A samples

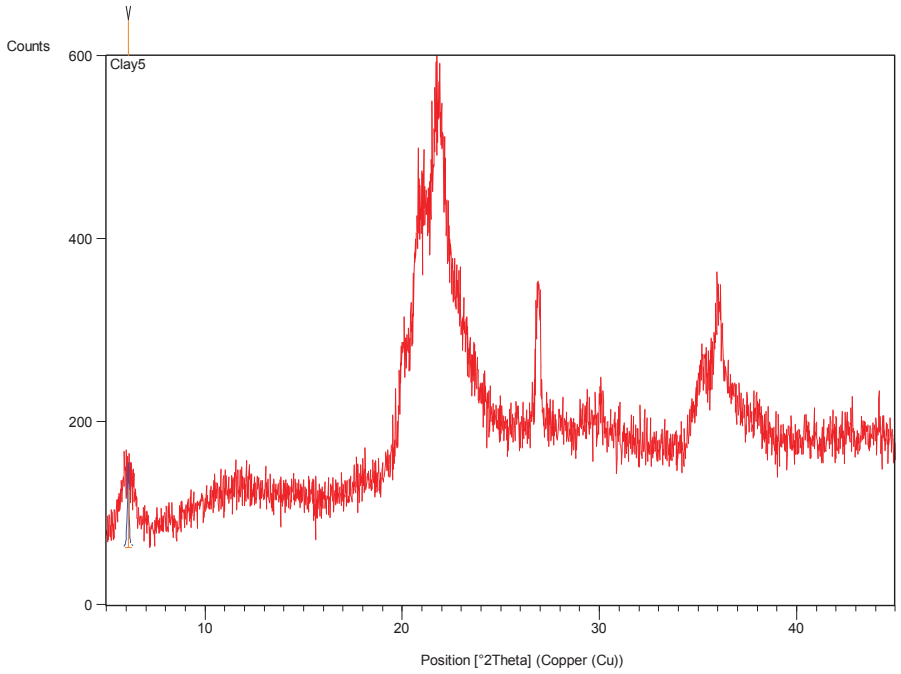

FIGURE 3.7. XRD diffractogram of montmorillonite-bearing opal-CT sample with a peak height at ~ 6° 2θ for opal-A samples.

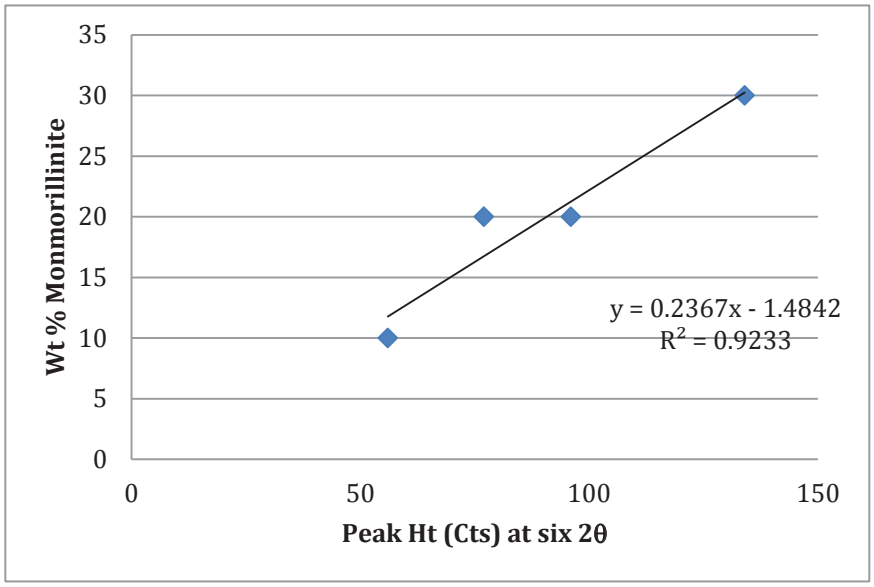

FIGURE 3.8. Chart of montmorillonite weight percent vs. montmorillonite characteristic XRD peak height at ~ 6° 2θ for opal-CT samples.

Chemical Analysis

All core, outcrop and mineral samples were sent to Actlabs, Canada, for Inductively Coupled Plasma (ICP) analysis to determine oxide and elemental abundances. Powdered sediment was fused with a flux of lithium tetraborate and lithium metaborate in an induction furnace. The resulting molten mixture was added to a solution of 5% nitric acid with an internal standard, and the samples run for select elements and oxides by a mixture of ICP-mass spectrometry and ICP-optical emissions spectroscopy.

Detritus, Biogenic and Diagenetic Silica Calculation

Isaac's (1980) equations for detritus and biogenic and diagenetic silica were applied to all samples, using the Al_2O_3 and SiO_2 abundances determined by Actlabs Fusion ICP analysis (Equations 1 and 2, below).

Equation 1. Detritus = $5.6 \times Al_2O_3$

Equation 2. Biogenic & Diagenetic Silica = $SiO_2 - (3.5 \times Al_2O_3)$

CHAPTER 4

RESULTS

X-Ray Diffraction

As intended in the sampling strategy, X-ray diffraction data confirmed that all three biogenic and diagenetic silica phases (opal-A, opal-CT and quartz) were sampled for this study. X-ray diffractograms reveal that the diagenetic silica in all samples from wells EH1 and EH2, both from the Elk Hills field, is primarily or entirely quartz phase. Of ten samples from well BV3 in the Buena Vista Field, the diagenetic silica from seven is primarily opal-CT with the 3 deepest samples being entirely quartz phase. All but one of the samples from wells MS4 and MS5, from the Midway Sunset Field, contain primarily biogenic opal-A phase silica. XRD results revealed that one sample from well MS5 was a siltstone and not a true diatomite. This sample was excluded from further analysis.

Elemental Analysis Results

Major Oxides, their Derivatives, and Clay Abundances

As intended, analysis of the subsurface Monterey Formation samples found them to be highly siliceous and composed of ~50-90 % silicon dioxide (SiO_2). Nonetheless, there is considerable variation in the concentration of major, minor and trace chemical components. Opal-A phase samples have a lower average abundance of SiO_2 compared to opal-CT and quartz phase sample groups. This relationship is reflected, if somewhat

diminished, in the calculated abundances of biogenic and diagenetic silica. Aluminum oxide abundances are comparable between all silica phase groups (0.08-13.06%), but slightly higher on average in the opal-A phase samples from Midway Sunset Field: 6.98% average for opal-A compared to 4.76 and 4.83 average for opal-CT and quartz, respectively. This relationship is replicated in calculated total detritus abundances. Opal-CT and Opal-A phase samples have more Fe_2O_3 than quartz phase samples in general (Figure 4.1).

Montmorillonite weight percentages were calculated from the x-ray diffractogram by measuring the peak height at approximately 6° 2θ. These values are not directly comparable with the oxide weight percentages determined with ICP-MS and ICP-OES. Calculated montmorillonite weight percentages (shown in Figure 4.1) are likely underestimated, but serve as an effective measure of relative abundance of clay between samples for the purpose of this study. The composite of the opal-A samples from Midway Sunset Field are distinct from both the opal-CT and quartz phase samples from Elk Hills and Buena Vista fields in that they contain a distinctly greater amount of montmorillonite clay with only a few exceptions (1.51-10.51% [7.56% mean], compared to 0-6.1% [4.0 % mean], respectively) (Figure 4.1).

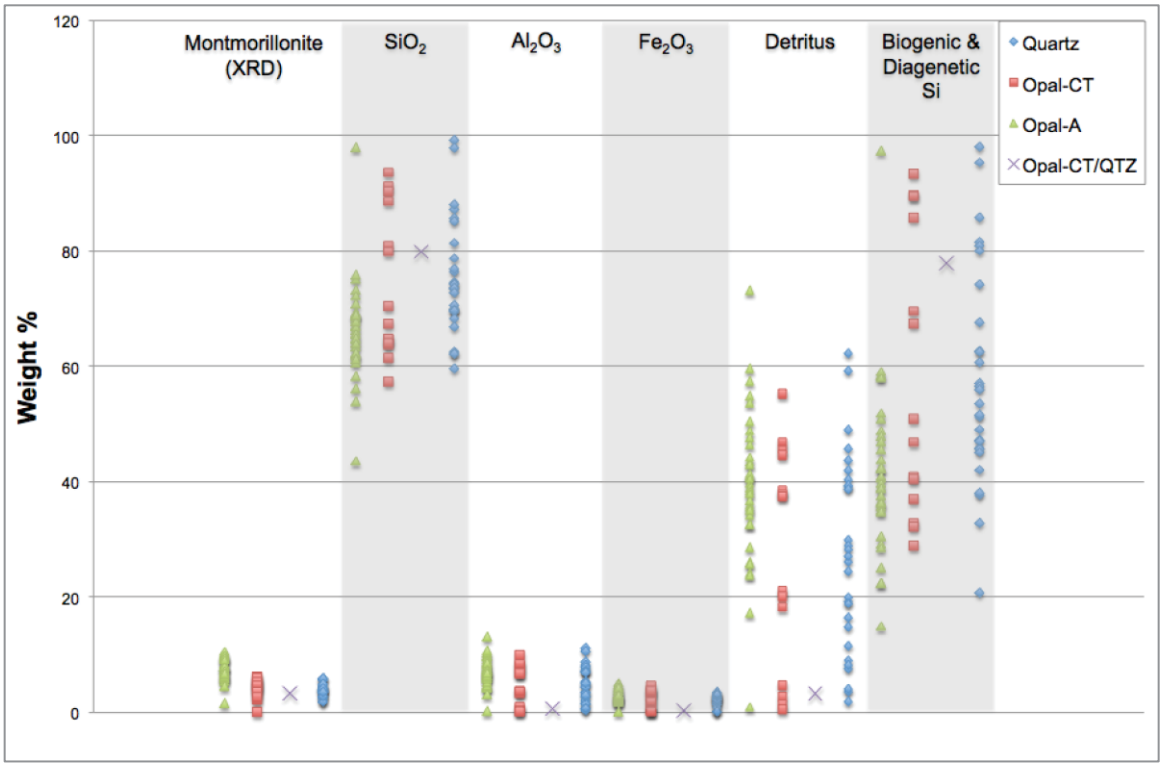

FIGURE 4.1. Abundances by weight percent for minor oxides from ICP-MS and ICP-OES analysis. Montmorillonite weight percent calculated from XRD peak height. Biogenic and diagenetic silica is equal to SiO_2 - (3.5*Al_2O_3) and detritus is equal to (5.6* Al_2O_3) from Isaac's (1980) equation for Monterey Formation rocks in the Santa Barbara Basin.

Minor Oxide Abundances

The ranges and mean abundances of minor oxides are comparable amongst each of the silica phase groups for MnO, MgO, NaO, K_2O, TiO_2, and P_2O_5 (generally 0-3 weight %). CaO is approximately twice as abundant as the other minor oxides, and notably more abundant on average in quartz phase samples than in opal-A and opal-CT phase samples (Figure 4.2).

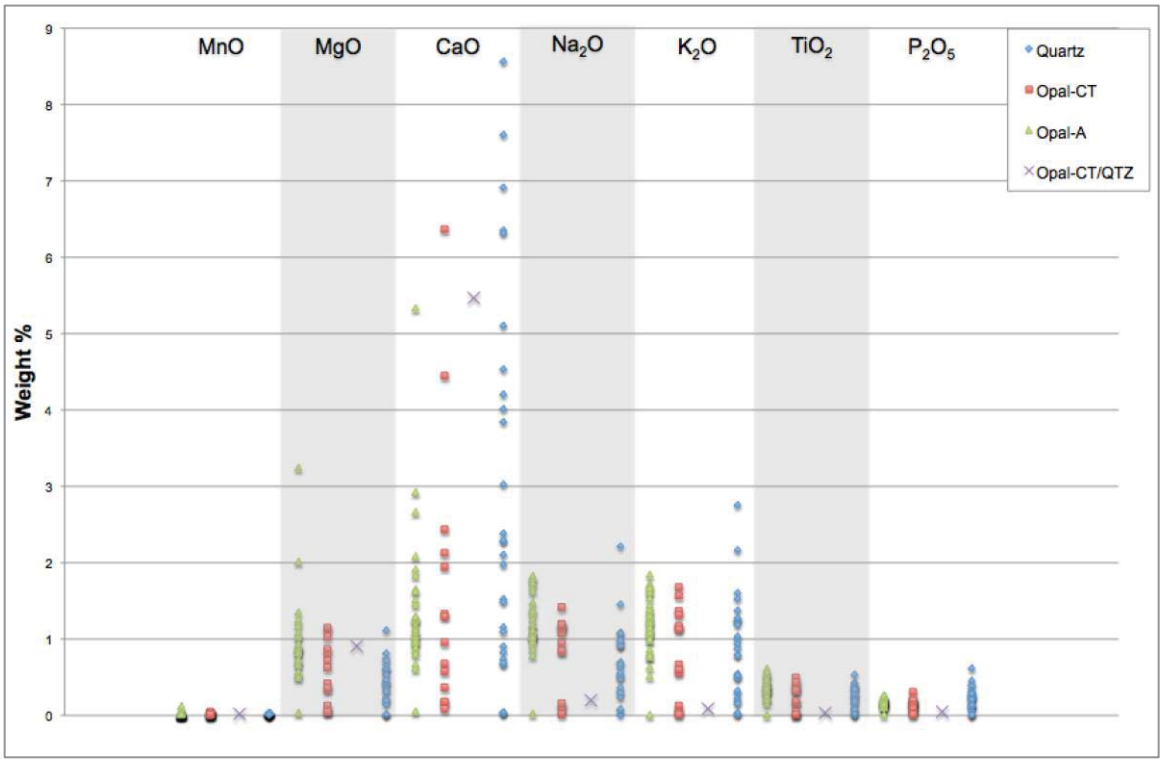

FIGURE 4.2. Abundances by weight percent for minor oxides from ICP-MS and ICP-OES analysis.

Trace and Minor Elemental Abundances

The elemental abundances of Sr, Y, SC, Zr, Be are comparable between silica phase groups in all samples (Figure 4.3). Barium is an order of magnitude more abundant than all other measured minor elements in most samples. However, there are also important compositional differences between samples of different silica phase. Barium is distinctly more abundant in the quartz phase samples from the Elk Hills Field than in the opal-A, opal-CT or mixed opal-CT/quartz phase groups. The range of

vanadium abundance in quartz phase samples is roughly twice as large as that of the opal-CT phase samples (2.5 – 603ppm compared to 2.5 – 329ppm, respectively). Opal-CT, likewise, has more than double the range of vanadium abundance in opal-A samples, which contain between 2.5 – 133 ppm.

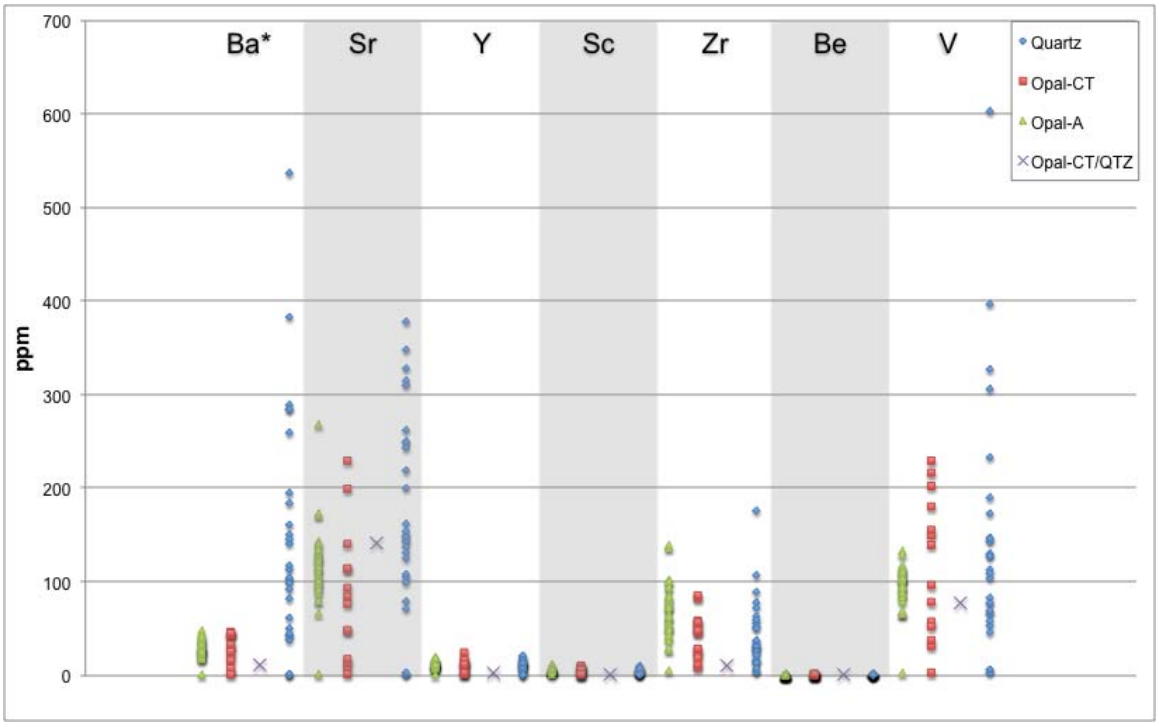

FIGURE 4.3. Elemental abundances in ppm from ICP-MS and ICP-OES analysis. Note: barium units are displayed in parts per thousand for display next to elements of lower abundances.

Water Imbibition Tests

Imbibition rates are reported as the average of 3-7 separate tests of each sample. The rate for imbibition of a single drop of water ranged from less than 5.22 µL/sec to 0.017 µL/sec (Figure 4.4).

Opal-A Phase Samples

All absorption rates measured range from 2.095 µL/sec to 0.017 µL/sec (Figure 4.4). 3% of samples tested absorbed the water droplets in faster than 1µL/sec seconds, averaged between separate tests. 15% of samples absorbed the water droplets between 0.5 and 1µL/sec. 27% of samples absorbed the water droplets between 0.2 and 0.5µL/sec. 27% of samples absorbed the water droplets between 0.1 and .2µL/sec. 18% of samples absorbed the water droplets between 0..05 and .1µL/sec. 6% of samples absorbed the water droplets between 0.02 and .05µL/sec, and 3% of samples absorbed the water droplets between 0.1 and .2µL/sec.

Opal-CT Phase Samples

All absorption rates measured range from 4.89 µL/sec to 0.255 µL/sec (Figure 4.4). 30% of samples absorbed the water droplets between 1 and 2µL/sec. 30% of samples absorbed the water droplets between 0.5 and 1µL/sec. 40% of samples absorbed the water droplets between 0.2 and .5µL/sec.

Quartz Phase Samples

All absorption rates measured range from 5.22 µL/sec to 0.017 µL/sec (Figure 4.4). 13% of samples tested absorbed the water droplets in faster than 2µL/sec seconds, averaged between separate tests. 9% of samples absorbed the water droplets between 0.5 and 1µL/sec. 9% of samples absorbed the water droplets between 0.5 and 1µL/sec. 27% of

samples absorbed the water droplets between 0.2 and 0.5µL/sec. 9% of samples absorbed the water droplets between 0.1 and .2µL/sec. 9% of samples absorbed the water droplets between 0..05 and .1µL/sec. 18% of samples absorbed the water droplets between 0.02 and .05µL/sec, and 5% of samples absorbed the water droplets between 0.1 and .2µL/sec.

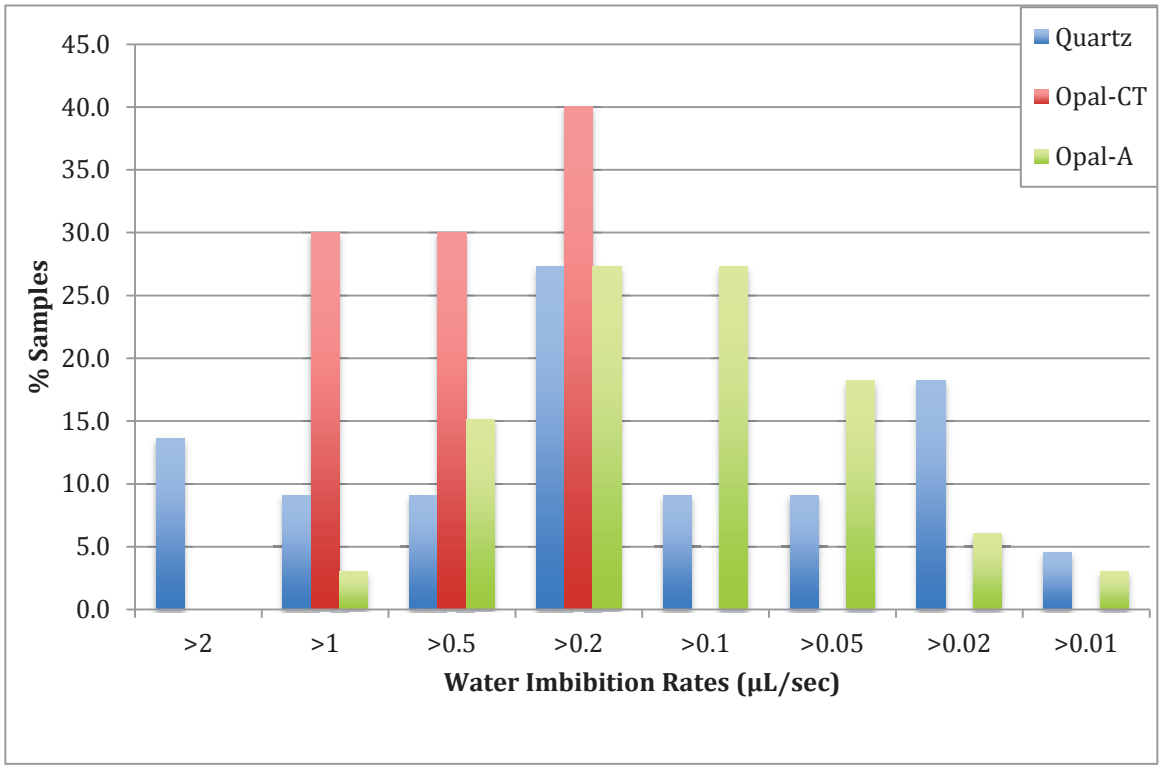

FIGURE 4.4. Water imbibition rates by silica phase group for pressed discs from core samples.

Oil Imbibition Tests

Imbibition rates are reported as the average of 3 tests of each sample. The rate for imbibition of a single drop of oil ranged from 0.10 µL/sec to 0.00067 µL/sec; in general, about an order of magnitude slower than that for water.

Opal-A Phase Samples

All absorption rates measured range from 0.0089 µL/sec to 0.00067 µL/sec (Figure 4.5). 3% of samples absorbed the water droplets between 0.005 and .01µL/sec. 6% of samples absorbed the water droplets between 0.002 and .005µL/sec. 67% of samples absorbed the water droplets between 0.001 and .002µL/sec. 24% of samples absorbed the water droplets between 0.0005 and .001µL/sec.

Opal-CT Phase Samples

All absorption rates measured range from 0.026 µL/sec to 0.0021 µL/sec (Figure 4.5). 10% of samples absorbed the water droplets between 0.02 and 0.05µL/sec. 20% of samples absorbed the water droplets between 0.01 and 0.2µL/sec. 40% of samples absorbed the water droplets between 0.005 and .01µL/sec. 30% of samples absorbed the water droplets between 0.002 and .005µL/sec.

Quartz Phase Samples

All absorption rates measured range from 00.10 µL/sec to 0.0027 µL/sec (Figure 4.5). 8% of samples tested absorbed the water droplets in faster than 0.05µL/sec seconds, averaged between separate tests. 17% of samples absorbed the water droplets between 0.02 and 0.05µL/sec. 46% of samples absorbed the water droplets between 0.01 and 0.2µL/sec. 17% of samples absorbed the water droplets between 0.005 and .01µL/sec. 13% of samples absorbed the water droplets between 0.002 and .005µL/sec.

Water Contact Angle Tests

As described above, contact angle measurements were made on polished surfaces of actual rocks – nonporous, nearly pure (79.8-99.2 % SiO2) siliceous sedimentary rocks (cherts) or hydrothermal precipitates (hyalite). Variability between individual measurements of contact angle of the same sample was high (Figure 4.6).

Opal-A Phase Samples

Fifteen tests on the opal-A Hyalite sample resulted in contact angles between 43.49° and 81.72°, for an average of 64.11° (Figure 4.7a).

Opal-CT Phase Samples

Ten to thirteen tests each on three opal-CT chert samples from outcrop and one pure mineral opal-CT vein sample resulted in contact angles between 17.63° and 89.23°, for an average of 49.26° (Figure 4.7b & c).

Mixed Opal-CT/Quartz Phase Sample

Five tests on a single mixed opal-CT and quartz sample from outcrop resulted in contact angles between 16.75° and 65.01°, for an average of 34.05°.

Quartz Phase Samples

Ten to eleven tests each on two quartz phase chert samples from outcrop and one pure mineral quartz sample resulted in contact angles between 28.66° and 81.35°, for an average of 58.89° (Figure 4.7d).

Oil Contact Angle Tests

Oil contact angle measurements were made on polished surfaces of the same nonporous, nearly pure (siliceous sedimentary rocks (cherts) or hydrothermal precipitates

(hyalite) tested for water. Variability between individual measurements of contact angle of the same sample was much lower than for water (Figure 4.8).

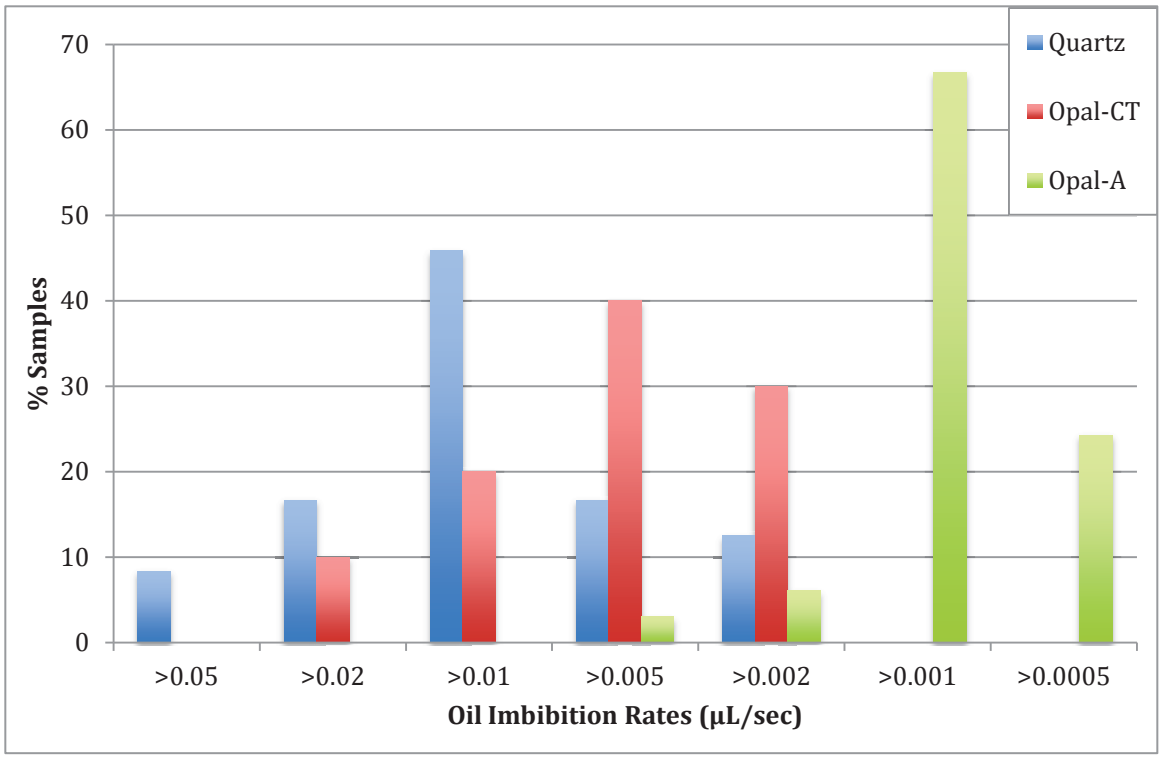

FIGURE 4.5. Oil imbibition rates by silica phase group for pressed discs from core samples.

Opal-A Phase Samples

Five tests on the opal-A hyalite sample resulted in contact angles between 7.56° and 9.19°, for an average of 8.56°.

Opal-CT Phase Samples

Four to five tests each on three opal-CT chert samples from outcrop and one opal-CT precipitate sample resulted in contact angles between 6.78° and 17.78°, for an average of 9.83°.

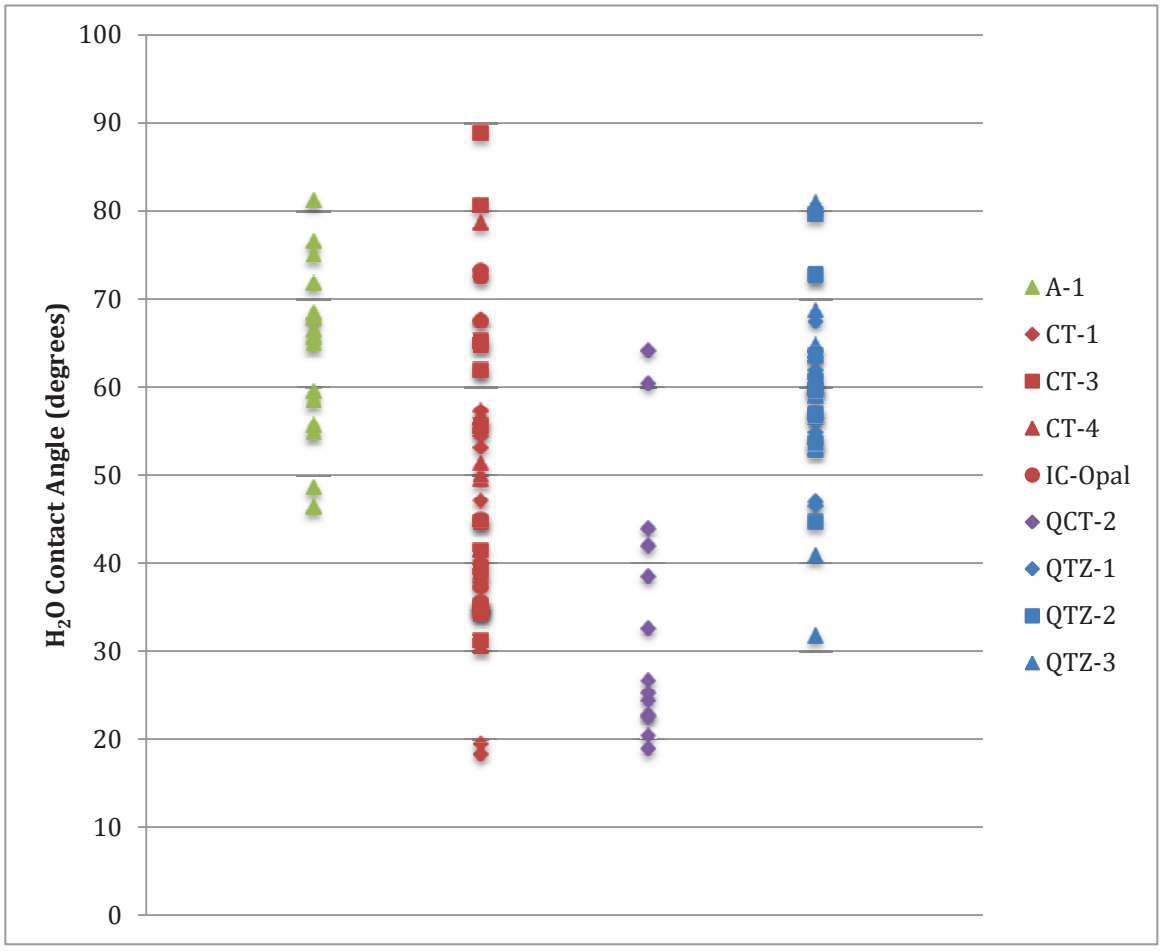

FIGURE 4.6. Water contact angle test results. Note that sample QCT-2 is an opal-CT/quartz mixed-phase sample.

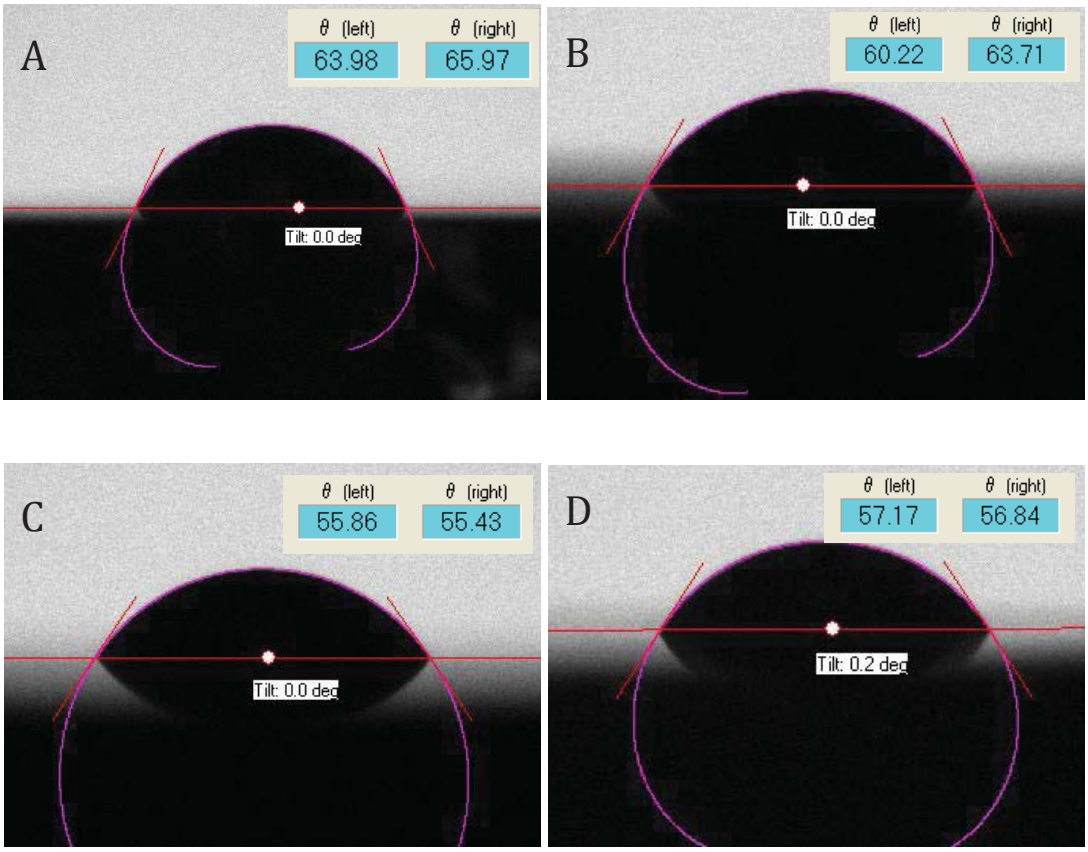

FIGURE 4.7. Water contact angle tests displaying near average contact angle. A: sample A-1, B: CT-3, C: CT-4, and D: QTZ-1.

Quartz Phase Samples

Four to five tests each on two quartz phase chert samples from outcrop and one pure mineral quartz sample resulted in contact angles between 8.35° and 11.97°, for an average of 9.85°.

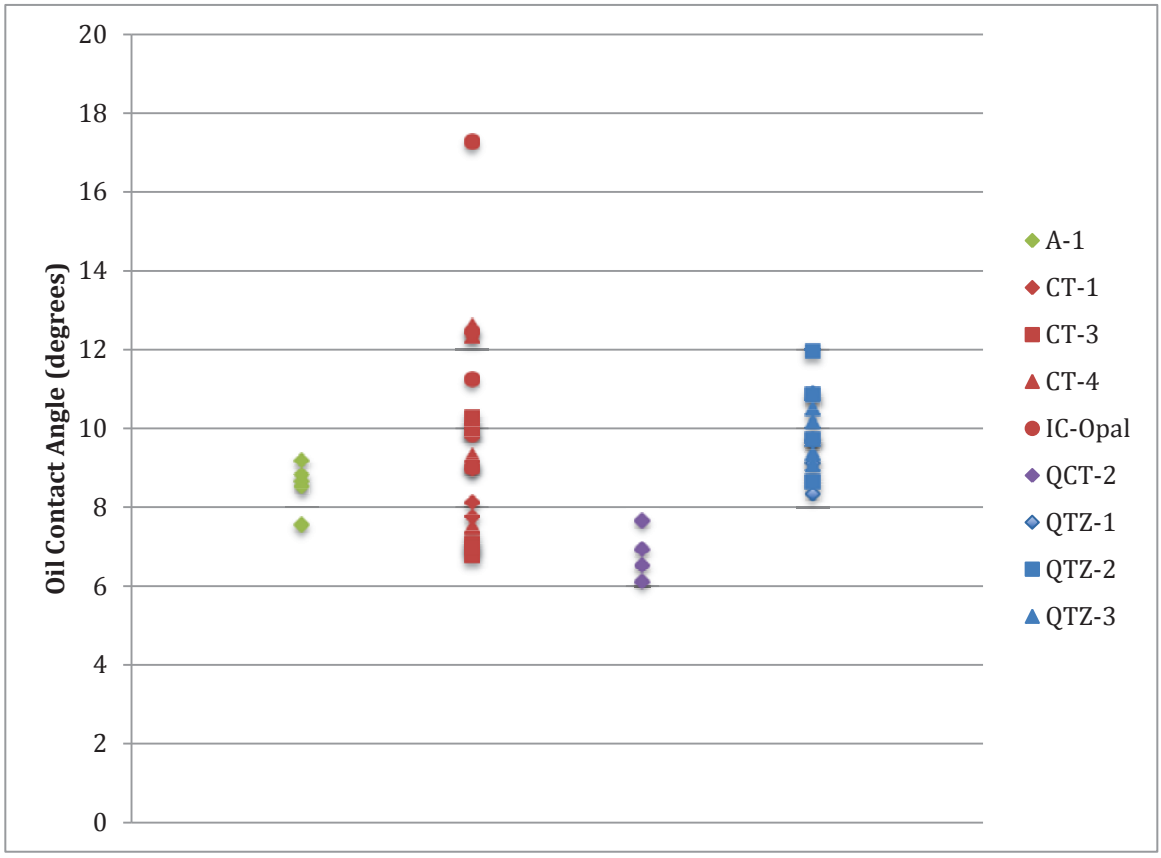

FIGURE 4.8. Oil contact angle test results. Note that sample QCT-2 is an opal-CT/quartz mixed-phase sample.

Wettability Test Results vs. Composition

Significant Relationships Between Contact Angle and Composition

Relationships between compositional variables and wettability of opal-CT phase rocks are demonstrated by the results of contact angle tests on three opal-CT chert samples from outcrop and one mineral precipitate sample, informally known as "Ice Cream Opal". Relationships between compositional variables and wettability of quartz

phase samples are shown by the contact angle results of 2 quartz chert samples from outcrop and one pure mineral quartz sample. Only one sample of impermeable opal-A was obtained for this study in the form of a hyalite hydrothermal precipitate sample. No relationships between opal-A sample composition and contact angle are attainable in this study because of only having the single sample of unique composition.

Perhaps the most important and compelling trend between composition and contact angle to emerge in this study is the near-linear increase in wettability to oil of opal-CT phase siliceous rocks with the increase in detritus by weight percent (Figure 4.9). Both detritus and biogenic/diagenetic silica abundances are calculated using Isaac's (1980) equations for Monterey Formation rocks from the Santa Barbara Basin. Quartz phase samples do not exhibit a discernible change in contact angle of oil with increase or decrease of detrital content. Quartz phase samples do exhibit a decrease in oil contact angle, however, with the increase of diagenetic silica (Figure 4.10). So, in contrast to the opal-CT samples, this implies that more pure siliceous rocks of the quartz phase tend to be more wetting to oil than less pure samples of similar composition.

Titanium and potassium oxides in opal-CT samples also showed strong trends of increasing wettability to oil with increase in the weight percent of those components (Figures 4.11 and 4.12).

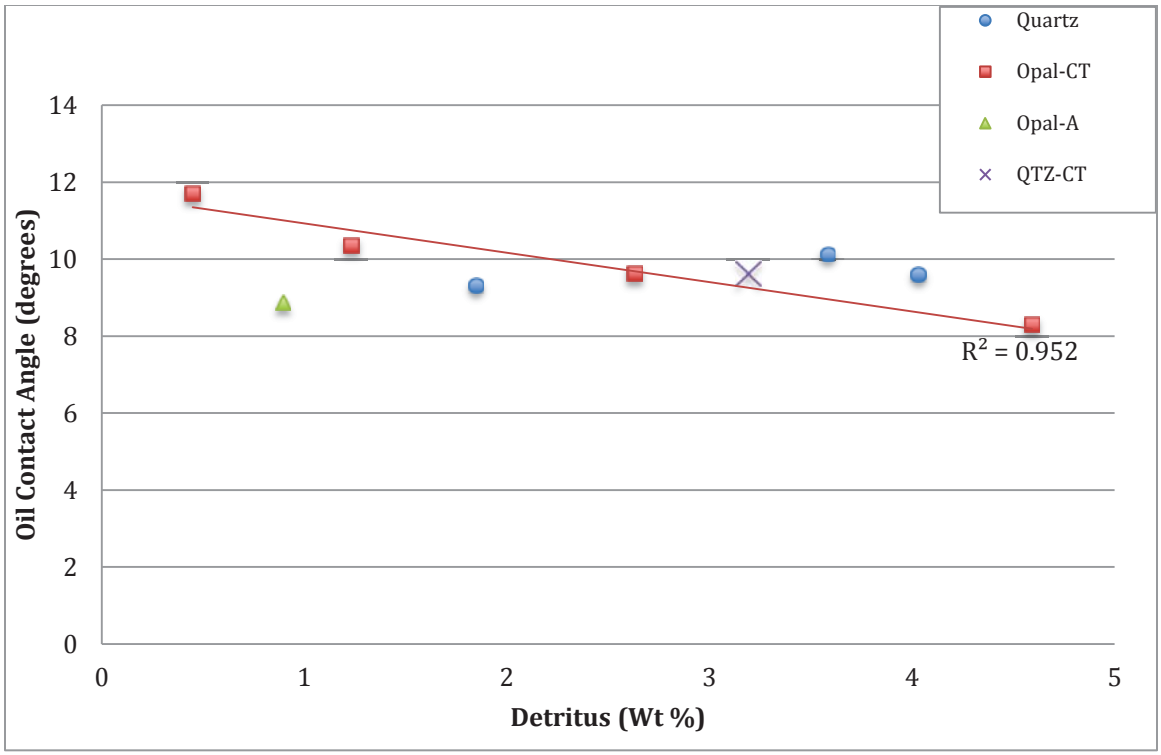

FIGURE 4.9. Detritus in weight percent vs. oil contact angle. Trend line shown for opal-CT phase samples only. Detritus is equal to ($5.6*Al_2O_3$) from Isaac's (1980) equation for Monterey Formation siliceous rocks in the Santa Barbara Basin.

Significant Relationships Between Imbibition and Composition

Some significant trends exist between wettability test results and compositional variables when samples from individual silica phase groups or distinct stratigraphic units are evaluated separately. No significant relationships were revealed in this study between compositional variables and test results when all samples are treated as a single group.

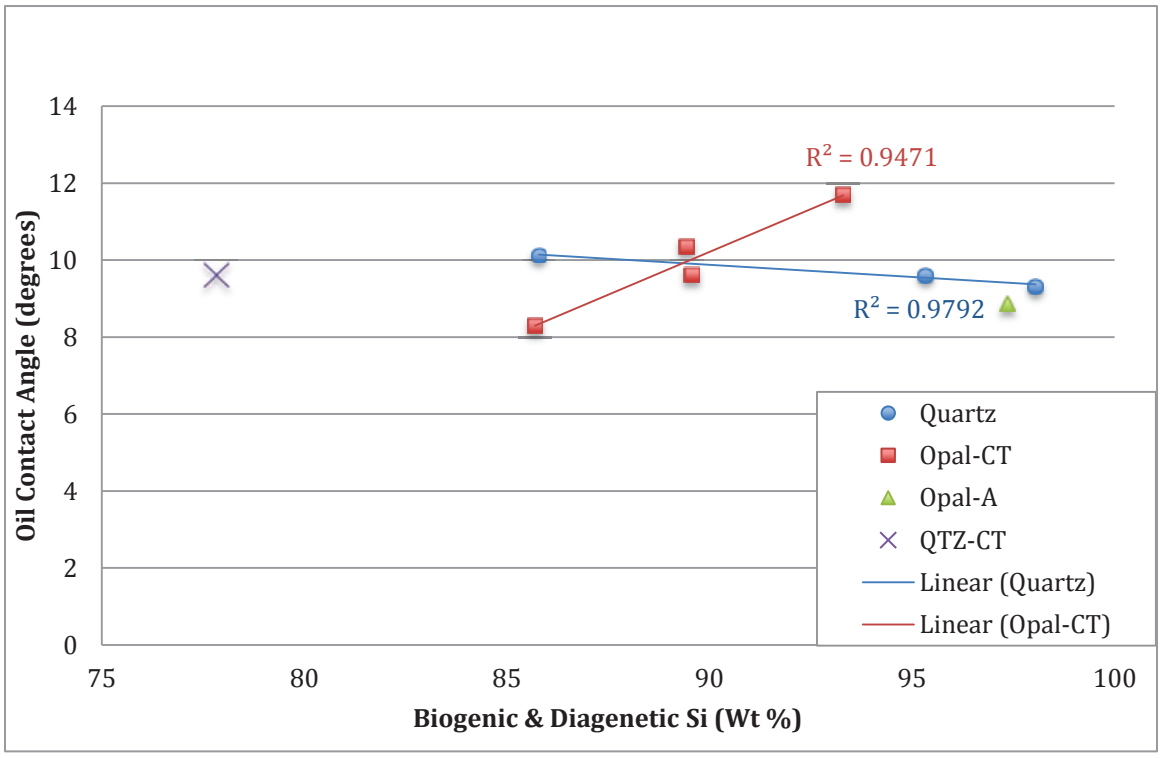

FIGURE 4.10. Biogenic & diagenetic silica in weight percent vs. oil contact angle. Trend lines shown for opal-CT and quartz phase samples. Biogenic and diagenetic silica is equal to SiO_2 - (3.5*Al_2O_3) from Isaac's (1980) equation for Monterey Formation siliceous rocks in the Santa Barbara Basin.

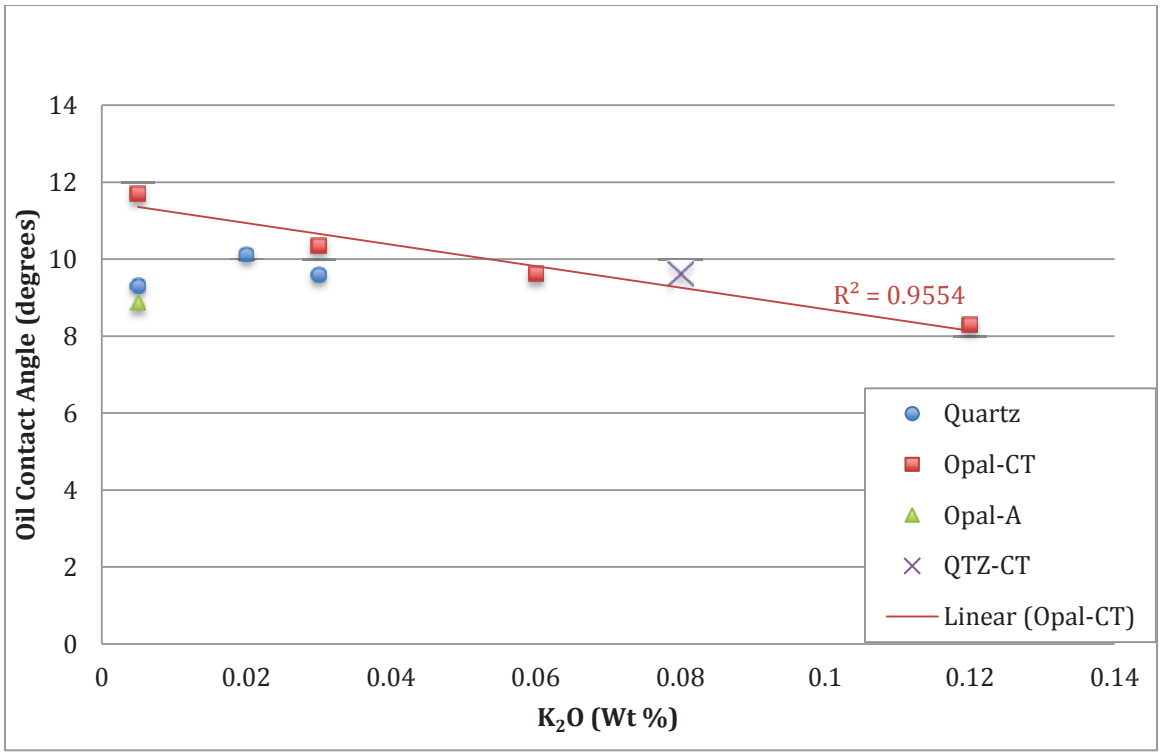

FIGURE 4.11. Potassium oxide in weight percent vs. oil contact angle. Trend line shown for opal-CT phase samples only.

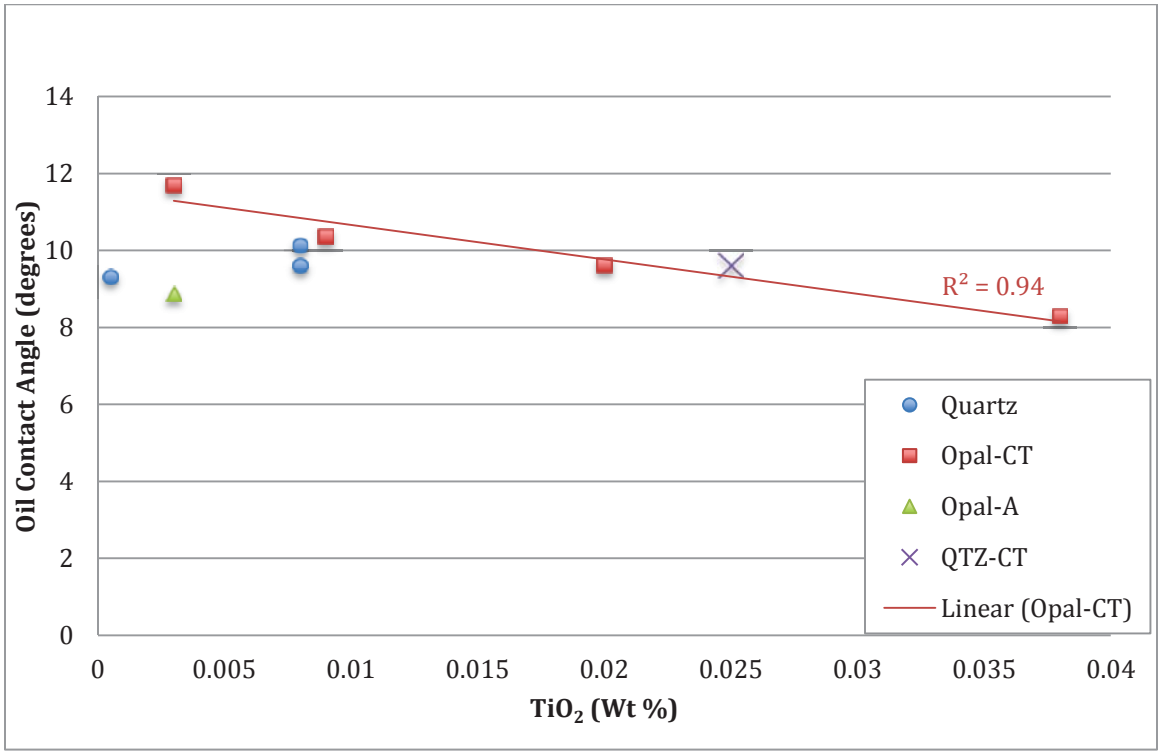

FIGURE 4.12. Titanium oxide in weight percent vs. oil contact angle. Trend line shown for opal-CT phase samples only.

Opal-A phase samples (Midway-Sunset field). Imbibition test results for opal-A phase samples demonstrate a random dispersion when plotted against all compositional variables (Figures 4.13, 4.14, 4.15, 4.16, 4.17 and 4.18). This indicates that the relative abundance of any single elemental component or oxide, including clay directly controls imbibition results of either oil or water. Water imbibition times were similar for opal-A and quartz phase samples, indicating that there is no difference between these two silica phases regarding their wettability to water as indicated by this test method (Figure 4.13). Oil imbibition times were distinctly longer for opal-A samples than samples of the opal-CT and quartz phase groups. Although the rates of oil imbibition rate of opal-A samples are an order of magnitude slower than opal-CT and quartz groups, the only compositional factor that distinguishes the opal-A group from the other silica phases is the weight percent of montmorillonite clay. However, the trend of decreasing wettability to oil with increasing weight percent of montmorillonite (Figure 4.14) is not discernible or statistically provable within the opal-A group itself.

Opal-CT phase samples (Buena Vista Field). Opal-CT phase samples do not exhibit any remarkable trends of water or oil imbibition rate with change in weight percent montmorillonite clay. There is a moderately strong correlation between oil and water wettability (as indicated by imbibition rate) and total detritus, as well as biogenic/diagenetic silica. Opal-CT core samples demonstrated increasing imbibition times for both oil and water tests with the increase in detritus among samples (Figures 4.15 and 4.16). Magnesium oxide produced the strongest relationship between oil imbibition rate and opal-CT sample composition, showing an increase in imbibition time, or decreasing wettability to oil, with the increase of MgO abundance (Figure 4.19).

Quartz Phase Samples (Elk Hills and Buena Vista Fields) No distinct trends are apparent between any compositional variables and water imbibition times. Relationships between oil imbibition times with compositional variables in the quartz silica phase sample group are identical to those of the opal-CT group, but weaker in correlation value (Figures 4.14 and 4.16).

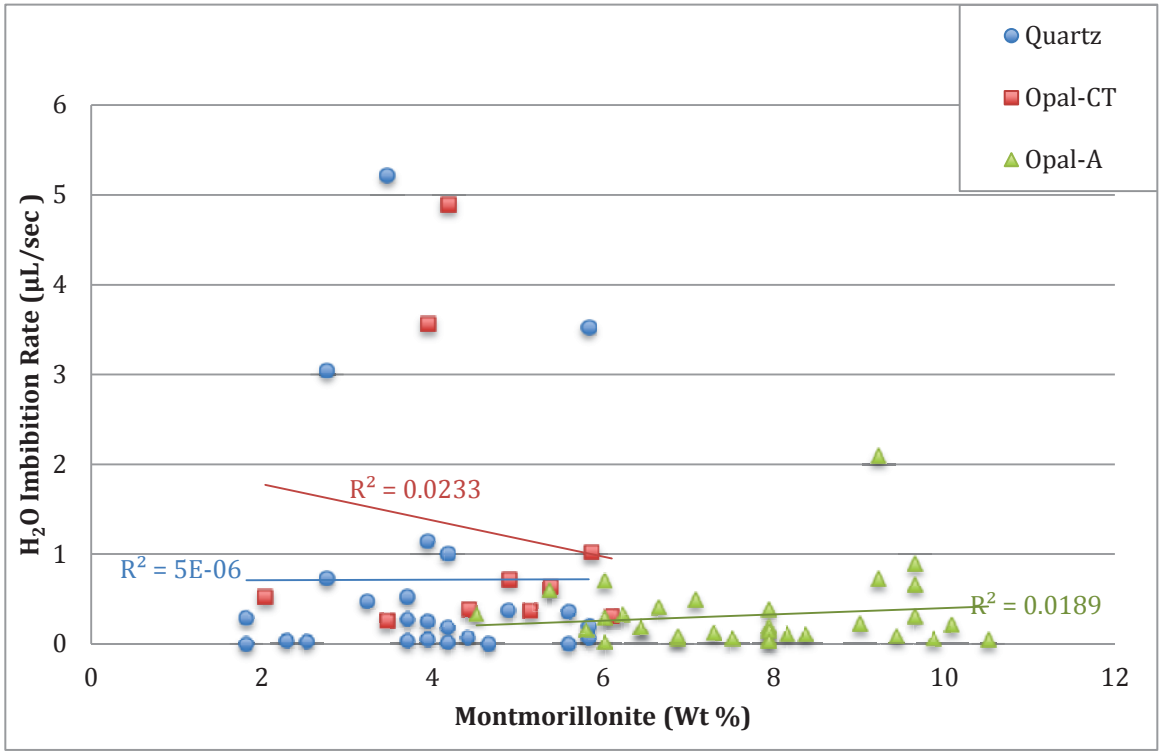

FIGURE 4.13. Water imbibition rate vs. montmorillonite clay weight percent. R^2 test correlation values shown for each silica phase group. Trend lines for each phase group are shown in colors corresponding to their respective symbols.

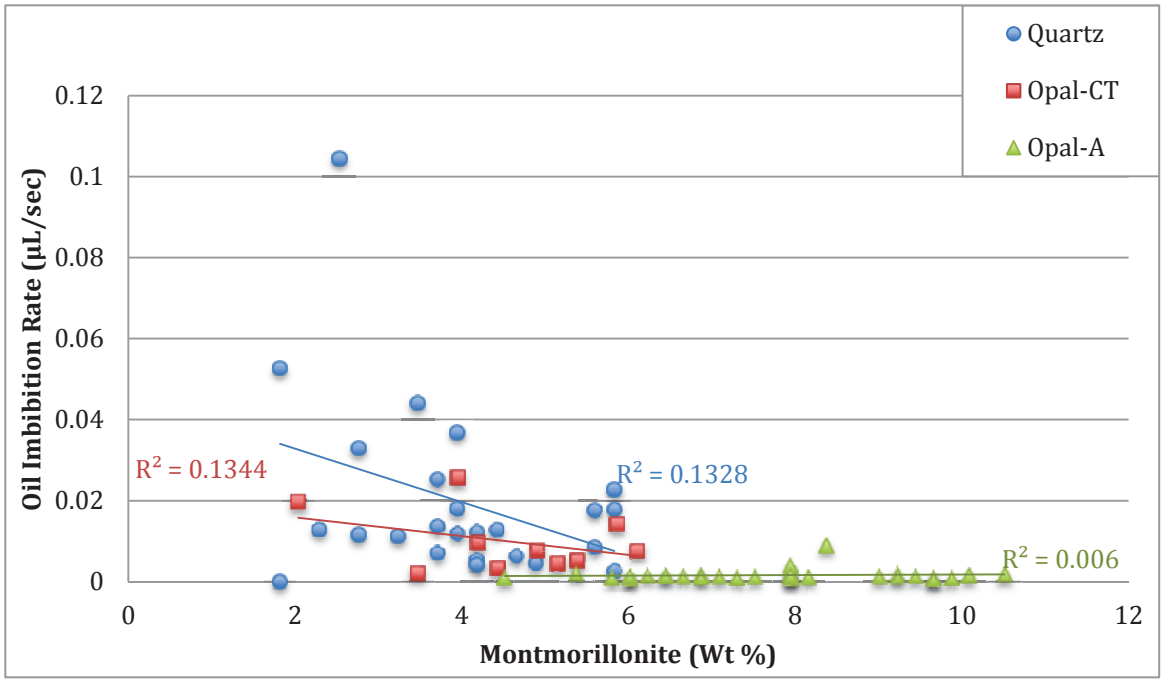

FIGURE 4.14. Oil imbibition rate vs. montmorillonite clay weight percent. R^2 test correlation values shown for each silica phase group. Trend lines for each phase group are shown in colors corresponding to their respective symbols.

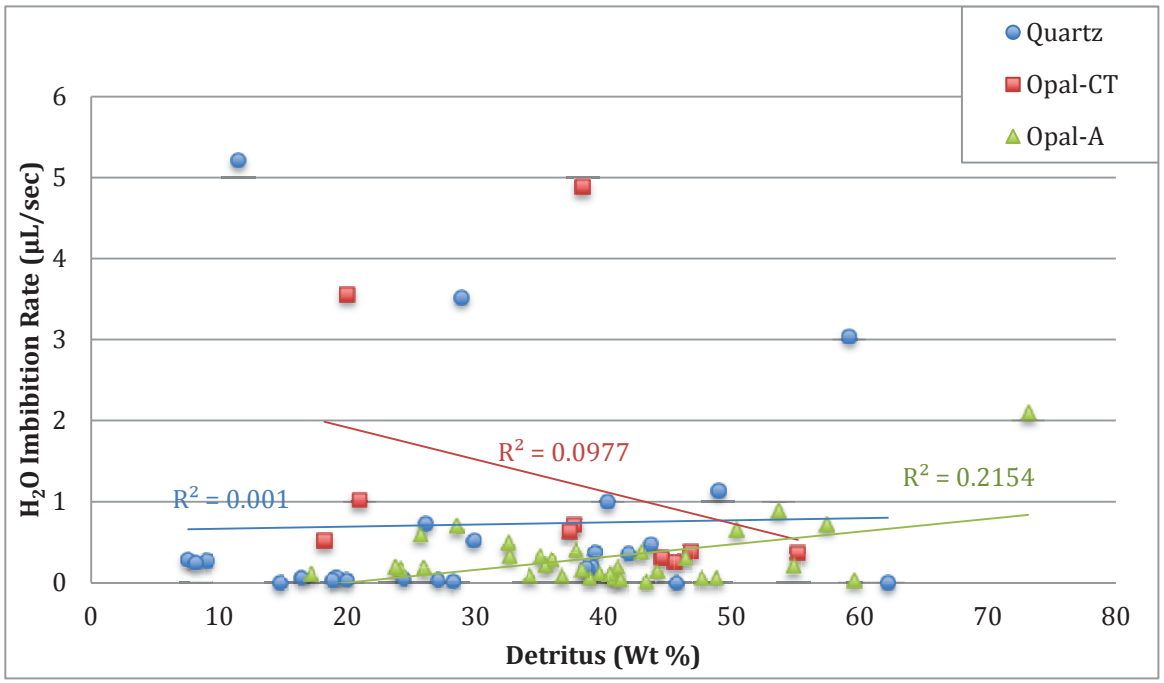

FIGURE 4.15. Water imbibition rate vs. detritus weight percent. R^2 test correlation values shown for each silica phase. Trend lines for each phase group are shown in colors corresponding to their respective symbols.

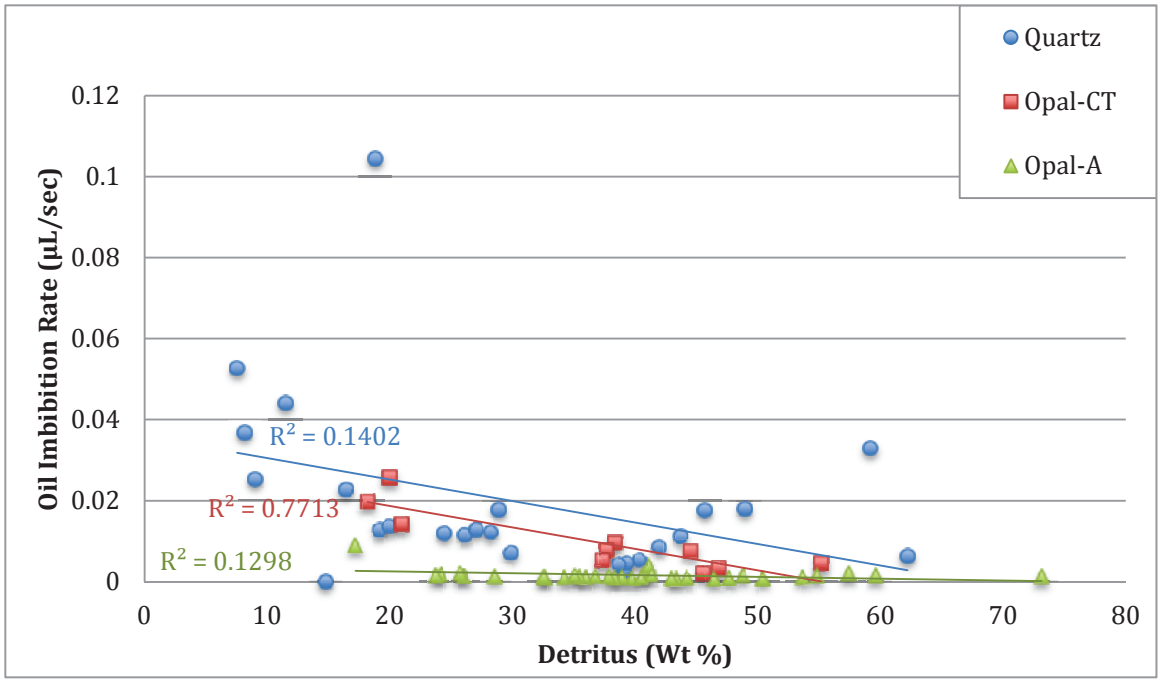

FIGURE 4.16. Oil imbibition rate vs. detritus weight percent. R^2 test correlation values shown for each silica phase. Trend lines for each phase group are shown in colors corresponding to their respective symbols.

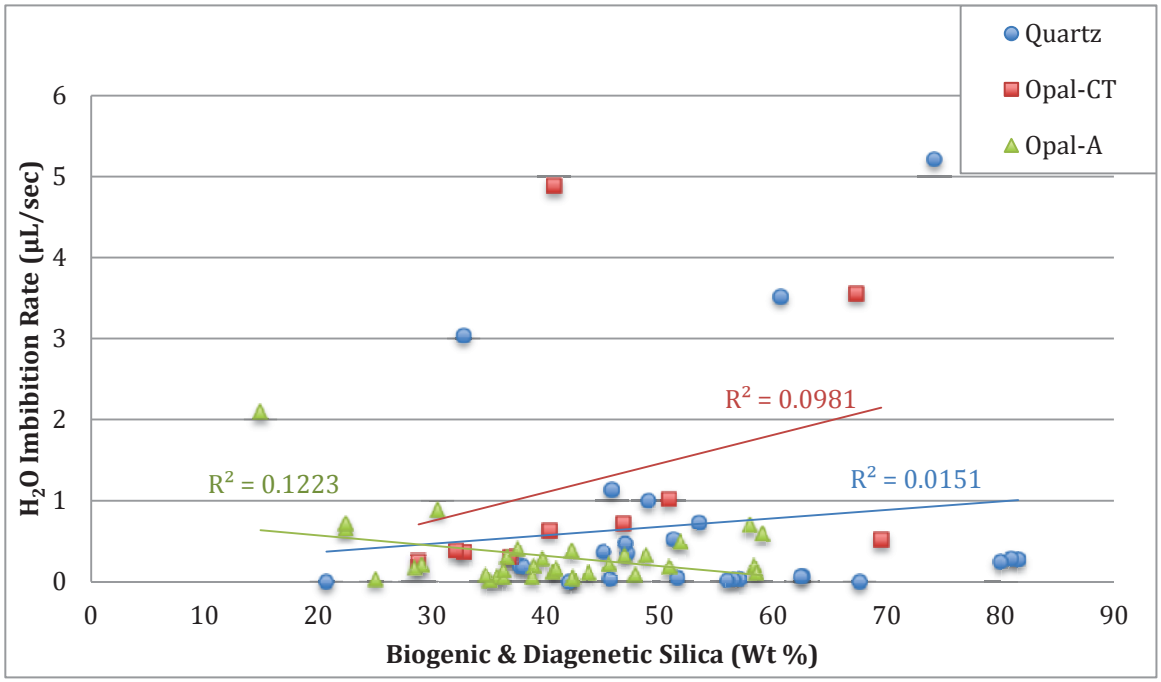

FIGURE 4.17. Water imbibition rate vs. biogenic & diagenetic silica weight percent. R^2 test correlation values shown for each silica phase. Trend lines for each phase group are shown in colors corresponding to their respective symbols.

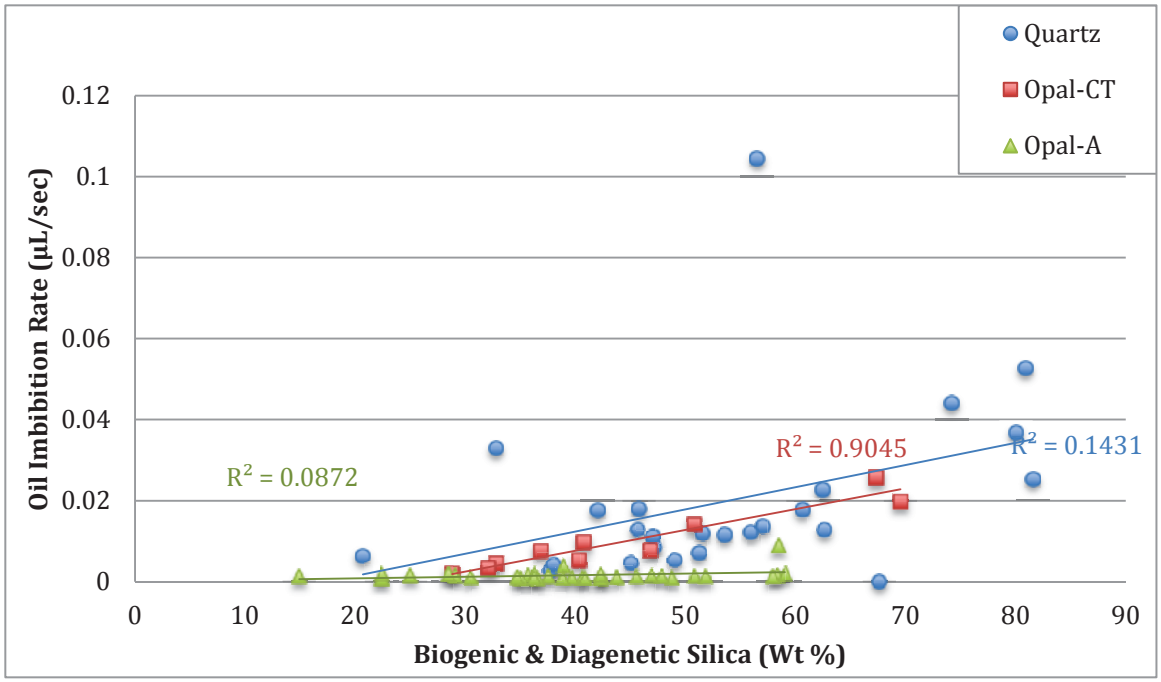

FIGURE 4.18. Oil imbibition rate vs. biogenic & diagenetic silica weight percent. R^2 test correlation values shown for each silica phase. Trend lines for each phase group are shown in colors corresponding to their respective symbols.

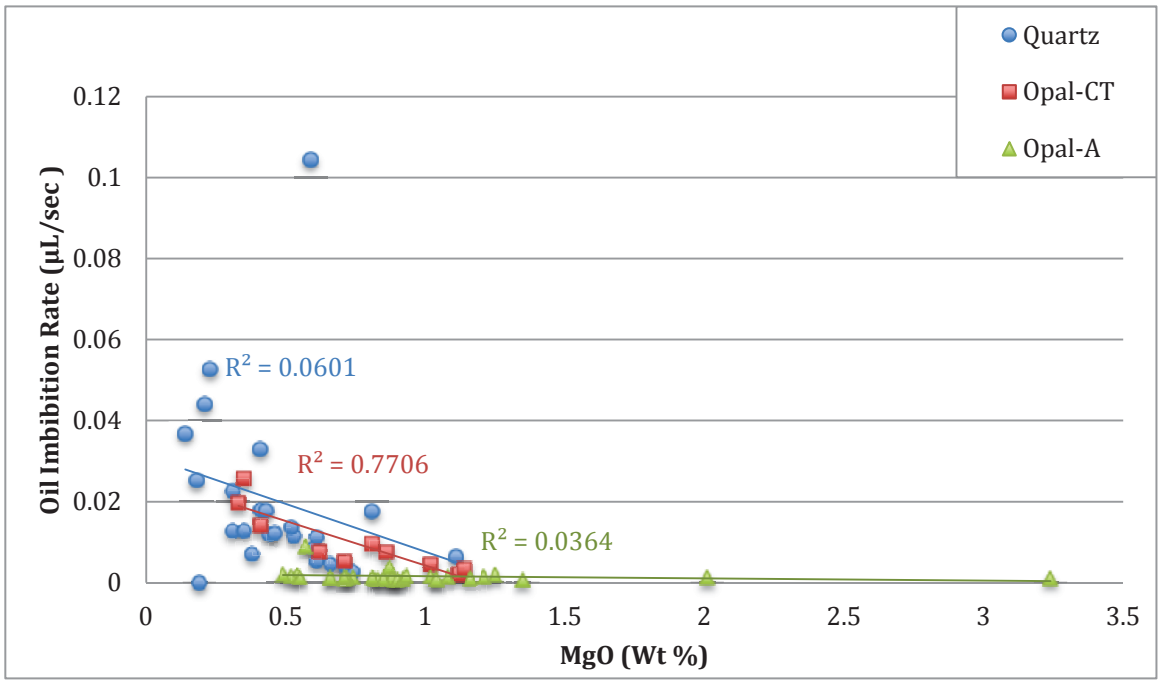

FIGURE 4.19. Oil imbibition rate vs. magnesium oxide weight percent. R^2 test correlation values shown for each silica phase. Trend lines for each phase group are shown in colors corresponding to their respective symbols.

CHAPTER 5

DISCUSSION

Study Approach and Development

Contact angle measurements are difficult to impossible to make on porous media where fluids are absorbed or influenced by capillary action (Nowak et al., 2013). The challenge was to use or develop a reliable, reproducible method for quantification of wettability in the highly porous clayey-siliceous reservoir rocks of the Monterey Formation. The initially proposed method to conduct this study was to perform contact angle tests on flat, impermeable discs of crushed and cleaned Monterey Formation reservoir core samples spanning a range of silica diagenesis and clay content. Preliminary tests quickly revealed that even 10,000 lbs of pressure under a hydraulic press were insufficient to render the powdered rock samples impermeable, and contact angle measurements could not be made on these samples. In order to achieve flat, impermeable surfaces for our tests, the samples were crushed to powder and sieved to finer than 62 microns and applied to glass slides with double-sided adhesive tape. Although Bachmann et al. (2000) were able to achieve reliable results by this method, it proved unreliable for our study. Samples covered and pressed onto the double-sided tape did not achieve a thorough enough coverage over the adhesive to prevent applied fluid drops from interacting with the adhesive in place of the sample powder although multiple application methods were attempted.

Although contact angle measurements could not be performed on natural or powdered and compressed diatomite and porcelanite samples, nearly pure solid samples of each of the three silica phases could be tested. One sample of hyalite, a hydrothermal precipitate of the opal-A mineraloid, large enough to conduct contact angle measurements on, was obtained from Australia. Multiple samples of very low-porosity, nearly impermeable, opal-CT and quartz phase chert were obtained from outcrop exposures of the Monterey Formation. All of these samples (opal-A, opal-CT and quartz) were slabbed and polished to provide surfaces on which contact angles could be measured and compared.

We developed a modified imbibition test, somewhat similar to the spontaneous imbibition part of the Amott-Harvey method, but using pressed powder pellets instead of core plugs. Precise parameter control provided by the hydraulic press and the tensiometer allowed for very reproducible experimental conditions. By pressing a consistent weight of rock sample powder, sieved to <62 microns, into a uniformly sized disk at 10,000 lbs of pressure, porosity differences and rock density differences between samples were minimized. It was possible to precisely control the volume of fluid dropped into each sample to 6.89 μL of oil with a standard deviation (σ) of 0.36, and 1.55μL, σ 0.3 for water. With these variables controlled and the force of gravity on a constant mass the only force acting on the fluid drop over the sample pellets, the rate of imbibition of each test fluid can be attributed to differences in the wettability of each sample to the fluid in question.

Wettability Differences Between Silica Phase Groups

Imbibition test results showed no statistically significant wettability difference between silica phase groups that was not better explained by clay and detrital input (See Figures 4.4 and 4.5 for histograms of imbibition distribution by phase). The lack of definitive separation between silica phase groups is described in detail under Multiple Regression Analysis, below.

Contact angle tests demonstrated differences in wettability between silica phase groups including direction and magnitude of wettability alteration (Figures 4.9, 4.10, 4.11, 4.12). However, the range of compositional variation was not much greater (or close to) the analytical error. Trends displayed in charts comparing contact angle test with composition thus require additional testing over a greater range of composition for conclusive determination of relationships.

Correlation Strength for Compositional Control of Test Results

Strength of relationships between wettability and compositional variables of the samples tested in this study were determined by three major statistical analyses: Coefficient of Determination (R^2), Principal Component Analysis, and Multiple Regression.

Coefficient of determination is a best-fit line applied to unique compositional variables plotted against wettability test results for each individual silica phase group. The goal of the regression test is to determine how much of the variance in the y value, or test result, is explained by the variance of x— in this case, a compositional variable. For this study, R^2 values are considered significant above 0.8. Values between 0.5 and 0.7 are considered moderately significant, and values below 0.5 are considered insignificant.

Significant values are marked in green, moderate values in yellow, and insignificant values in gray in the charts included in the discussion.

Opal-A phase samples

Variations in composition had a little to no impact on water or oil imbibition rates. All variables produced R^2 values less than 0.5 when compared to results of these wettability tests (Figure 5.1).

Opal-A H_2O Imbibition	
Variable	**R^2**
Sr	+ 0.309
Sc	+ 0.219
Detritus	+ 0.215
Fe_2O_3	+ 0.156
Ba	+ 0.137
Na_2O	+ 0.131
Biog-Diag Si	- 0.122
TiO_2	+ 0.119
Zr	+ 0.08
MgO	+ 0.068
V	+ 0.058
MnO	+ 0.057
K_2O	+ 0.052
CaO	+ 0.033
P_2O_5	+ 0.031
Montmorillonite	+ 0.018
Y	+ 0.008
SiO_2	- 0.005

Opal-A Oil Imbibition	
Variable	**R^2**
K_2O	- 0.162
TiO_2	- 0.135
Detritus	+ 0.129
Y	- 0.119
P_2O_5	- 0.107
Zr	- 0.107
Ba	- 0.088
Biog-Diag Si	+ 0.087
V	- 0.085
CaO	+ 0.076
Fe_2O_3	- 0.063
Na_2O	- 0.052
Sc	- 0.047
MgO	- 0.036
Sr	- 0.033
SiO_2	+ 0.009
Montmorillonite	+ 0.006
MnO	- 0.005

FIGURE 5.1a (LEFT) AND 5.1b (RIGHT). Coefficients of determination for compositional variable abundances vs. imbibition rate test results for opal-A phase samples. Variables are sorted in order of magnitude of correlation. R^2 values are considered significant above 0.8. Values between 0.5 and 0.7 are considered moderately significant, and values below 0.5 are considered insignificant. Significant values are marked in green, moderate values in yellow, and insignificant values in gray.

Opal-CT phase samples

All variables produced R^2 values less than 0.5 when compared to water imbibition rates (Figure 5.2a). In contrast, oil imbibition test results showed a clear influence of composition for some components (Figure 5.2b). Moderately significant correlation of oil imbibition rates with potassium oxide, silicon dioxide, detritus, magnesium oxide, titanium oxide, sodium oxide, ferric oxide, vanadium, manganese oxide, barium, zircon and scandium are reflected in R^2 values between 0.5 and 0.7. Biogenic and diagenetic silica has a positive, significant effect on oil imbibition rates, while silicon dioxide by itself, the primary component of biogenic and diagenetic silica, has a moderately positive effect on oil imbibition rate (Figures 5.3, 5.4, 5.5, and 5.6). The increase in oil imbibition rates with the increase in weight percent of silica indicates that the more purely siliceous the sample and free of contaminating elements, the more readily the sample imbibed oil. All non-siliceous compositional variables exhibit negative, moderate or insignificant relationships with oil imbibition rate. This indicates that the increase of these components in each sample tended to impede oil imbibition, increasing the time required for a controlled amount of oil to imbibe.

Quartz phase samples Variations in composition had a little to no impact on water or oil imbibition times. All variables produced R^2 values less than 0.5 when compared to results of these wettability tests (Figure 5.7).

Opal-CT H_2O Imbibition	
Variable	**R^2**
Na_2O	- 0.149
K_2O	- 0.109
Biog-Diag Si	+ 0.098
Detritus	- 0.097
TiO_2	- 0.095
MgO	- 0.082
Fe_2O_3	- 0.067
SiO_2	+ 0.066
Zr	- 0.065
V	- 0.064
Y	- 0.041
Montmorillonite	- 0.023
Sr	+ 0.014
MnO	- 0.013
CaO	+ 0.013
Sc	- 0.011
P_2O_5	- 0.007
Ba	0.000

Opal-CT Oil Imbibition	
Variable	**R^2**
Biog-Diag Si	+ 0.904
K_2O	- 0.783
SiO_2	+ 0.773
Detritus	- 0.771
MgO	- 0.770
TiO_2	- 0.738
Na_2O	- 0.726
Fe_2O_3	- 0.715
V	- 0.664
MnO	- 0.657
Ba	- 0.637
Zr	- 0.593
Sc	- 0.589
P_2O_5	- 0.493
Y	- 0.418
Sr	- 0.414
CaO	- 0.293
Montmorillonite	- 0.134

FIGURE 5.2a (LEFT) AND 5.2b (RIGHT). Coefficients of determination for compositional variable abundances vs. imbibition rate test results for opal-CT phase samples. Variables are sorted in order of magnitude of correlation. R^2 values are considered significant above 0.8. Values between 0.5 and 0.7 are considered moderately significant, and values below 0.5 are considered insignificant. Significant values are marked in green, moderate values in yellow, and insignificant values in gray.

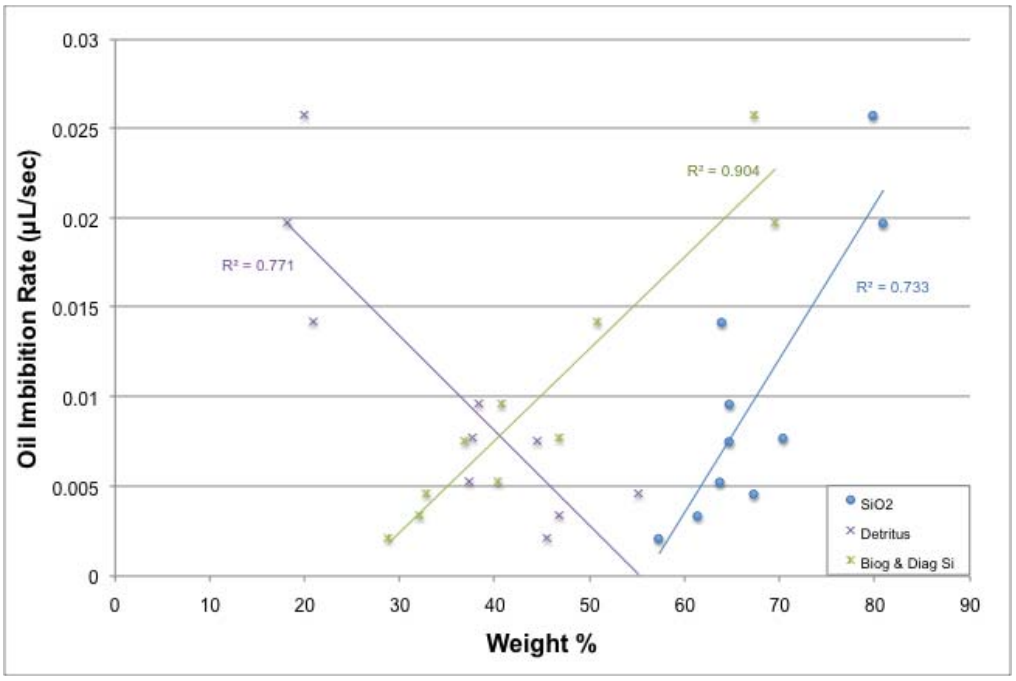

FIGURE 5.3. Moderate and Significant R^2 Correlations Between Oil Imbibition Times and Opal-CT Phase Samples. Note negative relationship between oil imbibition rate and detritus, while increase purity of siliceous content produced a positive relationship with oil imbibition rate.

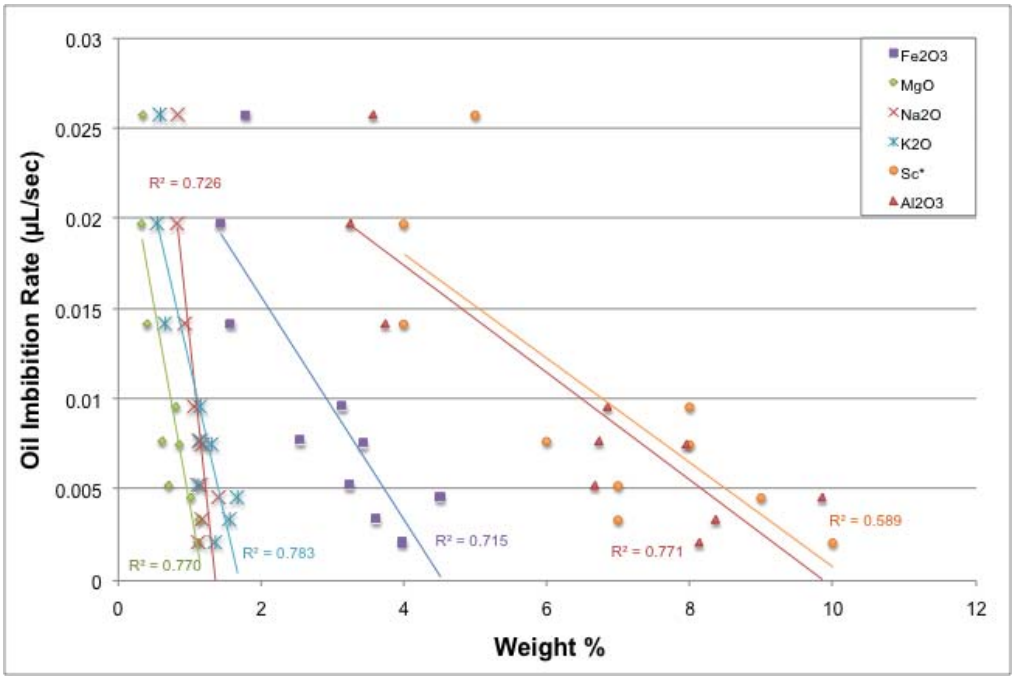

FIGURE 5.4. Moderate R^2 Correlations Between Oil Imbibition Times vs. Fe_2O_3, MgO, Na_2O, K_2O, Sc, and Al_2O_3 for Opal-CT Phase Samples. Note: Sc values are shown in ppm, plotted with oxide weight percents for display. Note negative relationship between oil imbibition rate and detritus-related variables.

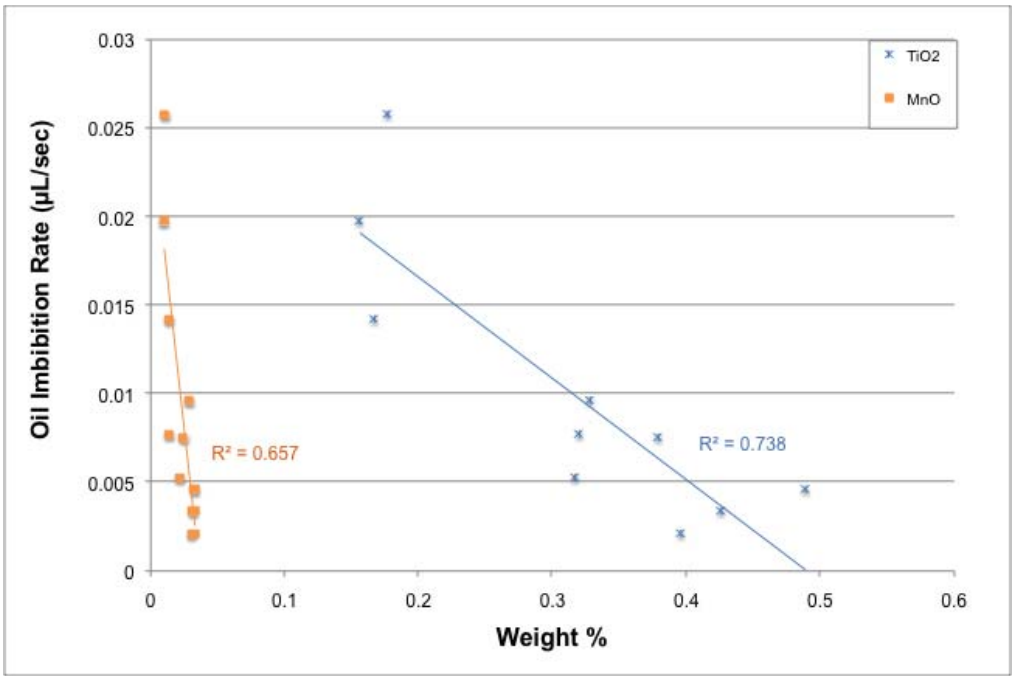

FIGURE 5.5. Moderate R^2 correlations between oil imbibition times vs. TiO_2 and MnO for opal-CT phase samples. Note negative relationship between oil imbibition rate and detritus-related variables.

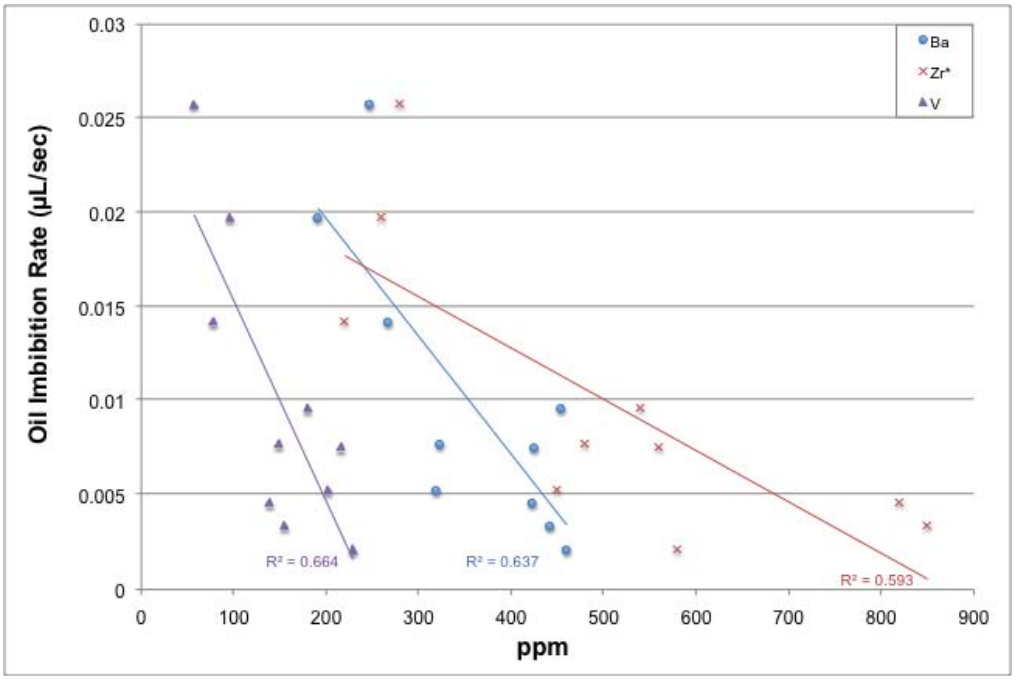

FIGURE 5.6. Moderate R^2 correlations between oil imbibition times vs. barium, zircon, and vanadium for opal-CT phase samples. Note negative relationship between oil imbibition rate and detritus-related variables.

Quartz H_2O Imbibition	
Variable	**R^2**
MnO	- 0.154
V	- 0.143
Sc	- 0.134
Fe_2O_3	- 0.131
CaO	- 0.126
Na_2O	+ 0.118
Y	- 0.096
SiO_2	+ 0.088
Sr	- 0.07
Zr	+ 0.069
MgO	- 0.059
P_2O_5	- 0.056
TiO_2	- 0.022
Ba	- 0.020
K_2O	+ 0.019
Biog-Diag Si	+ 0.015
Detritus	+ 0.001
Montmorillonite	0.000

Quartz Oil Imbibition	
Variable	**R^2**
TiO_2	- 0.178
Biog-Diag Si	+ 0.143
Detritus	- 0.140
Fe_2O_3	- 0.137
P_2O_5	- 0.136
Montmorillonite	- 0.132
CaO	+ 0.088
SiO_2	+ 0.084
K_2O	- 0.084
Sc	- 0.083
Sr	+ 0.081
Y	- 0.075
Ba	+ 0.064
MgO	- 0.060
Na_2O	- 0.036
Zr	- 0.028
MnO	0.000
V	0.000

FIGURE 5.7. Coefficients of determination for compositional variable abundances vs. imbibition rate test results for quartz phase samples. Variables are sorted in order of magnitude of correlation. R^2 values are considered significant above 0.8. Values between 0.5 and 0.7 are considered moderately significant, and values below 0.5 are considered insignificant. Significant values are marked in green, moderate values in yellow, and insignificant values in gray.

Overall Water Imbibition assessment

Compositional variables in opal-A and quartz phase samples demonstrated remarkably similar direction and magnitude of control of water imbibition test results (see appendix: Imbibition Rates vs. Compositional Variables), though the correlation strength was insignificant in all cases. A single controlling parameter of water imbibition remains unidentified and may not have been measured in this study. No single element

measured produced a moderate relationship with sample wettability to water in any phase set. In most element and oxides measured, opal-A abundances are comparable to opal-CT and quartz samples. Opal-CT samples (along with opal-A phase samples) are distinct from quartz phase samples in their low abundance of barium and distinguished from both of the other silica phase groups in their limited range of sodium oxide. However, the presence of Ba and greater abundance of NaO in the opal-A and quartz phase samples does not appear to directly relate to water imbibition rates. These later two silica phase groups do possess a greater range of composition than the opal-CT phase samples, though. Thus raising the possibility that an unmeasured parameter, such as illite clay or another elemental component, is key here.

Overall Oil Imbibition assessment

Tested samples of all silica phases had a greater range of variation in imbibition times and greater statistical correlation with nearly all compositional variables in oil imbibition tests than water imbibition tests. Nonetheless, opal-A and quartz-phase samples still demonstrated insignificant correlation (<0.50) with all measured compositional variables. Opal-A distribution patterns are randomly scattered, or show little variation across the entire range of composition. The former pattern indicates that the variable has no measureable control on the test result, and the latter indicates that the compositional parameter varies significantly, with negligible effect on imbibition rate. Opal-CT and quartz phase samples demonstrate similar trends to each other with changes in many compositional element abundances. Biogenic and diagenetic silica and SiO_2 both experience positive relationships with oil imbibition rates, while almost all other compositional variables produce a decrease in oil imbibition rate with increase in weight

percent of each variable. This indicates that the more purely siliceous reservoir rocks demonstrate greater wettability to oil and decreased inhibition of its imbibition.

Contact Angles

No trend analyses for compositional variation controls on contact angle tests for the opal-A silica phase group are available from this study, as only a single sample of impermeable opal-A hyalite was available for this test. The strength of relationships between opal-CT and quartz samples with compositional variables in the contact angle tests is weighted heavily by the low number of samples in this test. Furthermore, the compositional variation in these nearly pure samples is small, for some elements or oxides barely exceeding the analytical uncertainty. Therefore, little confidence can be given to the significance of correlations of contact angle with composition. The R^2 value is equal to one minus the squared error of the linear best fit line divided by the total variance in the test result (y) ($R^2 = 1- [SE_{line}/SE_y]$). When the total variance in test results is much larger than the squared error of the best fit line (which is more easily accomplished with fewer samples), the R^2 value is high. Additional tests could prove the correlations that presently appear significant to actually be less so. Similarly, correlations that appear insignificant with few samples could be proven underestimated with more data.

Opal-CT Phase Samples

Only a few correlations of moderate strength were revealed between compositional variables and water contact angle tests. The important variables in this test were phosphate, ferric oxide, zirconium, barium and montmorillonite clay (Figures 5.8a, 5.9 and 5.10). Each of these variables demonstrated a negative relationship with fluid

contact angle for both oil and water except Zr; indicating an increase in wettability toward both oil and water with the increase in these components. Zirconium had a unique response in that it produced higher contact angles, or reduced wettability toward both water and oil with the increase in weight percent of this element for each sample. Potassium oxide, magnesium oxide, titanium oxide, silicon dioxide, detritus, and biogenic and diagenetic silica all showed significant control on oil contact angle (Figures 5.8b, 5.11, 5.12, 5.13). Diagenetic silica and SiO_2 each cause higher contact angles, or decrease wettability to oil and water with their increase in abundance per sample. All other significant scoring components listed produced higher contact angles with increase in abundance (Figure 5.8b). These results indicate that there is a decrease in wettability toward oil with an increase in siliceous content of each sample. This trend is contrary to oil imbibition results.

Ferric oxide, phosphate, and montmorillonite clay all demonstrated moderate and negative correlation with oil and water contact angles in this test. This indicates that these variables increase the wettability of siliceous rock to both fluids.

Quartz Phase Samples

Strontium and zirconium both acted as significant statistical controls on water contact angle for quartz phase samples, while montmorillonite is responsible for only a moderate amount of contact angle variation (Figures 5.14a, 5.15). All three of these components caused an increase in water contact angle, or decrease in wettability to water with increase in their respective weight percents.

Opal-CT H_2O Contact Angle	
Variable	R^2
P_2O_5	- 0.769
Zr	+ 0.542
Ba	- 0.540
Fe_2O_3	- 0.533
Montmorillonite	- 0.527
V	- 0.396
Detritus	- 0.191
TiO_2	- 0.163
MgO	- 0.139
K_2O	- 0.139
Y	- 0.128
CaO	+ 0.113
MnO	+ 0.041
Sr	+ 0.040
Biog-Diag Si	+ 0.040
SiO_2	+ 0.003
Na_2O	0.000

Opal-CT Oil Contact Angle	
Variable	R^2
K_2O	- 0.955
Detritus	- 0.952
Biog-Diag Si	+ 0.947
TiO_2	- 0.940
MgO	- 0.833
SiO_2	+ 0.831
Fe_2O_3	- 0.688
Montmorillonite	- 0.634
P_2O_5	- 0.633
MnO	- 0.612
V	- 0.377
Y	- 0.351
Sr	- 0.338
Na_2O	- 0.295
Zr	+ 0.119
Ba	- 0.117
CaO	- 0.027

FIGURE 5.8a (LEFT) AND 5.9b (RIGHT). Coefficients of determination for compositional variable abundances vs. contact angle test results for opal-CT phase samples. R^2 values are considered significant above 0.8. Values between 0.5 and 0.7 are considered moderately significant, and values below 0.5 are considered insignificant. Significant values are marked in green, moderate values in yellow, and insignificant values in gray.

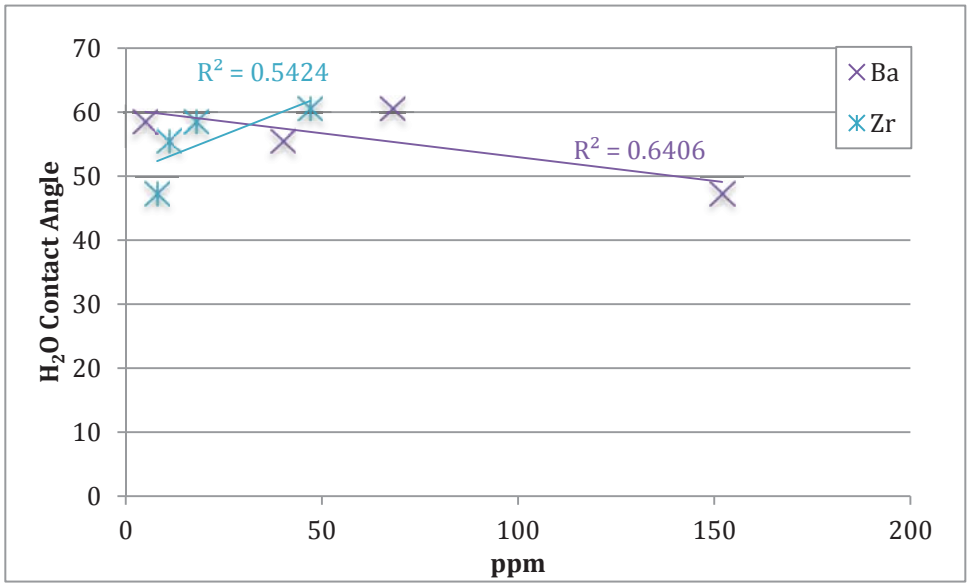

FIGURE 5.9. Moderate R^2 correlations between water contact angles and element abundances for opal-CT phase samples.

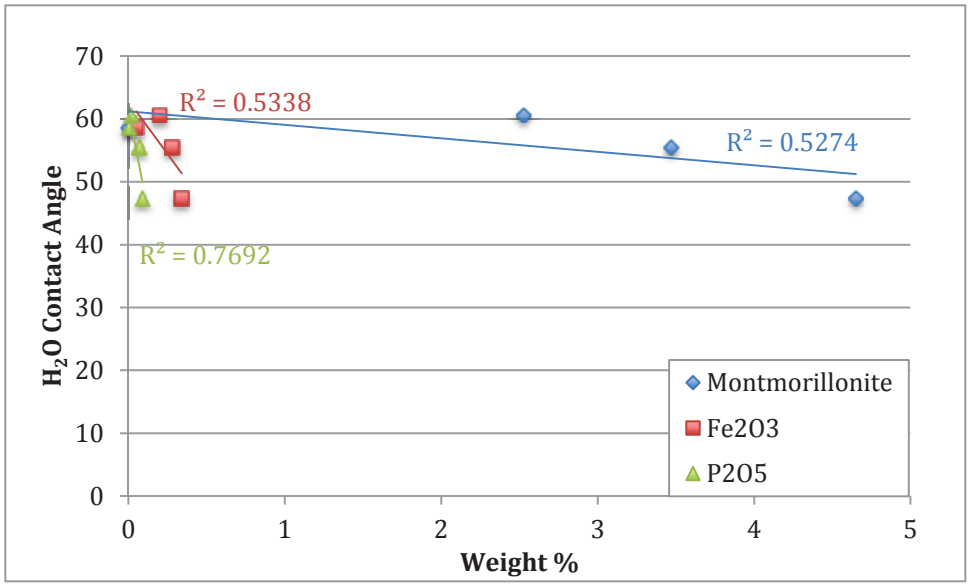

FIGURE 5.10. Moderate R^2 correlations between water contact angles and oxide abundances for opal-CT phase samples.

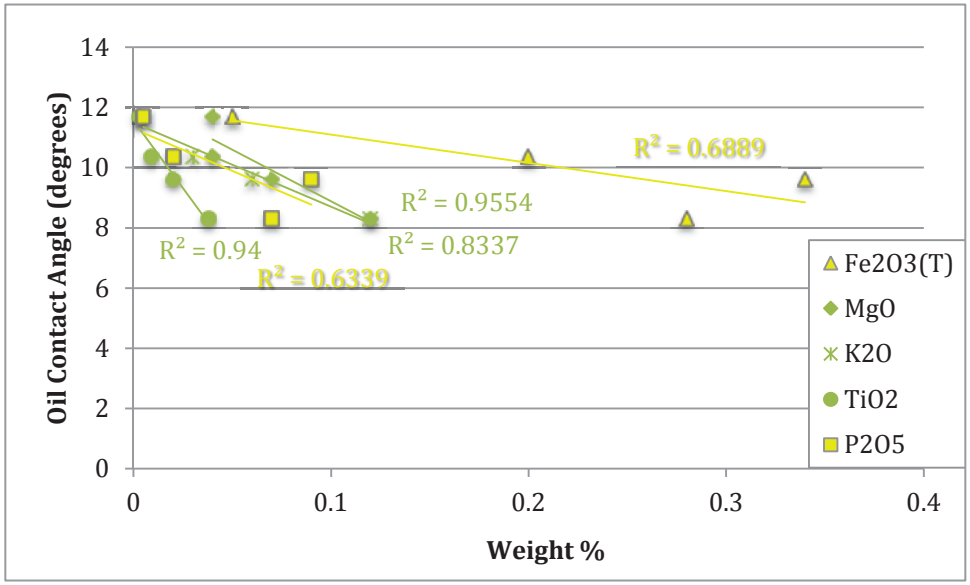

FIGURE 5.11. Significant and moderate R^2 correlations between oil contact angles and oxide abundances for opal-CT phase samples. Green symbol color indicates a significantly correlated compositional variable ($R^2 \geq 0.8$) and yellow indicates a moderate correlation ($0.5 \leq R^2 < 0.8$).

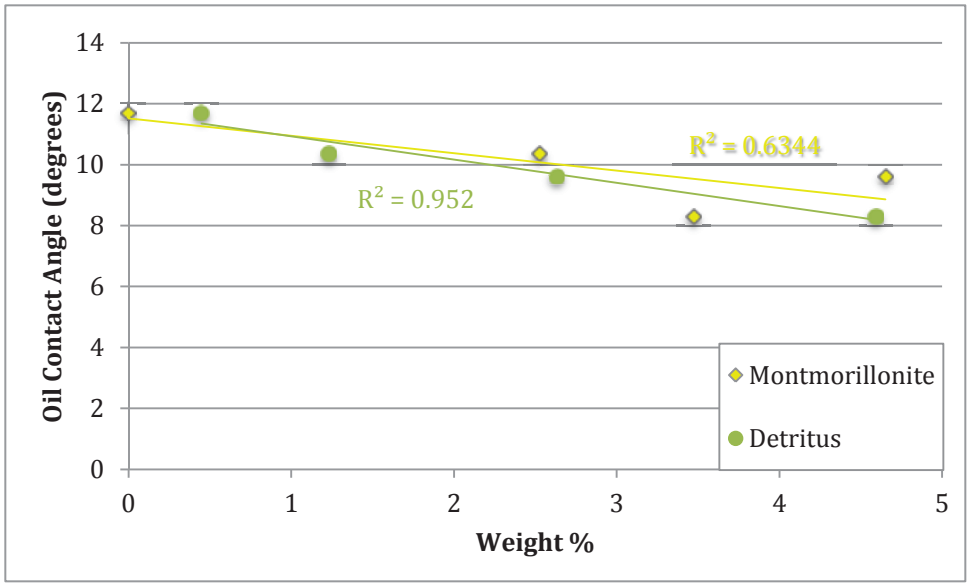

FIGURE 5.12. Significant and moderate R^2 correlations between oil contact angles vs. clay and detritus for opal-CT phase samples. Green symbol color indicates a significantly correlated compositional variable ($R^2 \geq 0.8$) and yellow indicates a moderate correlation ($0.5 \leq R^2 < 0.8$). Detritus is equal to ($5.6*Al_2O_3$) from Isaac's (1980) equation for Monterey Formation siliceous rocks in the Santa Barbara Basin.

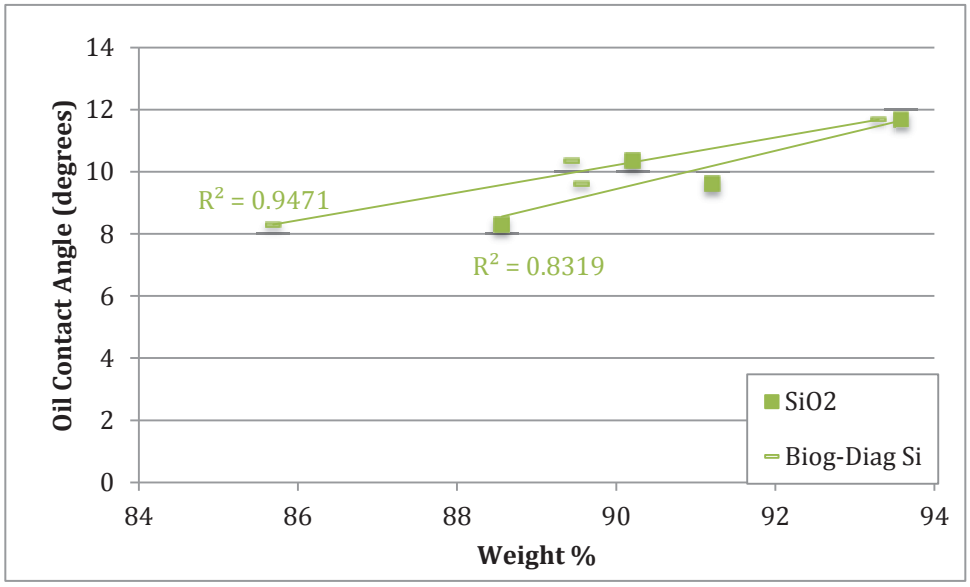

FIGURE 5.13. Significant R^2 correlations between oil contact angles vs. silica-based compositional variables for opal-CT phase samples. Biogenic and diagenetic silica is equal to SiO_2-($3.5*Al_2O_3$) from Isaac's (1980) equation for Monterey Formation siliceous rocks in the Santa Barbara Basin.

Diagenetic silica, silicon dioxide, and montmorillonite clay were each highly significant predictors of oil contact angle values for quartz phase samples, all producing a negative correlation with oil contact angle (Figure 5.16). Siliceous and detrital material have generated opposite responses in all other tests in our study. The fact that montmorillonite clay and siliceous variables demonstrate the same relationship with oil contact angle in these tests is very likely due to 1) the extremely small range of oil contact angle results for quartz samples (9.316 – 10.131), and 2) the error in the measurement of montmorillonite clay exceeding its variation between samples. As described above, the low number of samples has the potential to produce artificially inflated correlation values. Under conditions of minimal variation in data, these trends may even be projected in the wrong direction. Predictors of moderate strength include magnesium oxide, titanium oxide, ferric oxide, yttrium, and vanadium (Figure 5.14b, 5.17 and 5.18). All moderate relationships with oil contact angle were positive except for yttrium, which demonstrated decreased oil contact angles with increased weight percent. Diagenetic silica and SiO_2 both produce higher oil contact angles with increasing weight percent. All other significant and moderately significant variables have a negative relationship with oil contact angle, increasing each sample's wettability to oil with increasing weight percent. This trend also appears contradictory to imbibition wettability tests.

Quartz H_2O Contact Angle	
Variable	**R^2**
Sr	+ 0.893
Zr	+ 0.893
Montmorillonite	+ 0.569
Ba	+ 0.482
SiO_2	+ 0.459
CaO	+ 0.430
Biog-Diag Si	+ 0.359
K_2O	+ 0.319
Na_2O	+ 0.190
MnO	+ 0.177
Detritus	+ 0.142
Fe_2O_3	+ 0.073
MgO	+ 0.036
TiO_2	+ 0.036
Y	- 0.036
V	+ 0.036
P_2O_5	0.000

Quartz Oil Contact Angle	
Variable	**R^2**
Biog-Diag Si	- 0.979
SiO_2	- 0.940
Montmorillonite	- 0.877
MgO	+ 0.594
TiO_2	+ 0.594
Y	- 0.594
V	+ 0.594
Fe_2O_3	+ 0.513
Detritus	+ 0.400
MnO	+ 0.355
Na_2O	+ 0.338
K_2O	+ 0.206
CaO	+ 0.122
Ba	+ 0.090
Sr	- 0.027
Zr	- 0.027
P_2O_5	0.000

FIGURE 5.14a (LEFT) AND 5.15b (RIGHT). Coefficients of determination for compositional variable abundances vs. contact angle test results for quartz phase samples. Variable are sorted in order of magnitude of correlation. R^2 values are considered significant above 0.8. Values between 0.5 and 0.7 are considered moderately significant, and values below 0.5 are considered insignificant. Significant values are marked in green, moderate values in yellow, and insignificant values in gray.

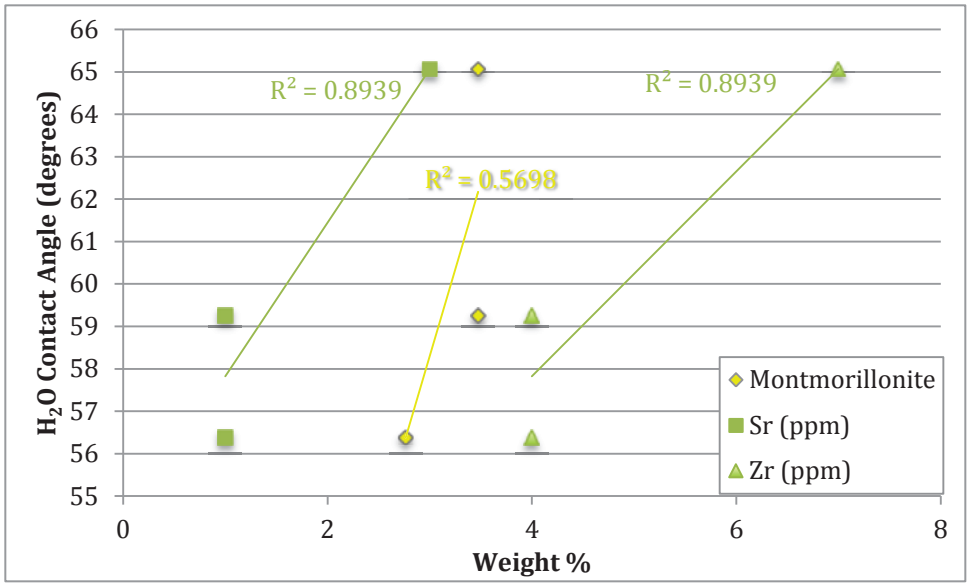

FIGURE 5.15. Moderate and significant R^2 correlations between water contact angles vs. compositional variables for quartz phase samples. Note that Sr and Zr are shown in ppm units for display. Green symbol color indicates a significantly correlated compositional variable ($R^2 \geq 0.8$) and yellow indicates a moderate correlation ($0.5 \leq R^2 < 0.8$).

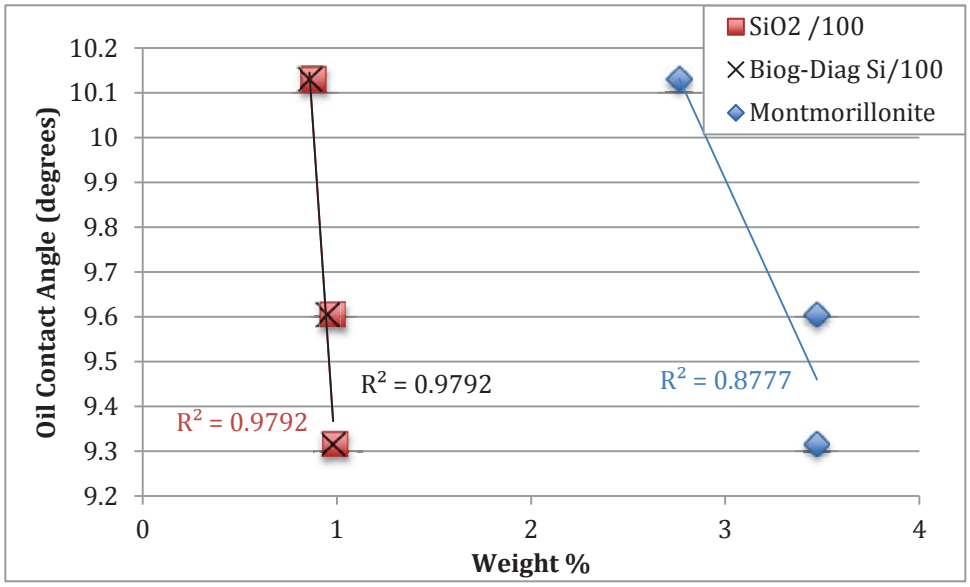

FIGURE 5.16. Significant R^2 correlations between oil contact angles vs. silica-based variables and clay for quartz phase samples. Relationship between montmorillonite may be artificially inflated and incorrectly directed do to error in measurement exceeding the variation between samples, combined with very close oil contact angle measurements.

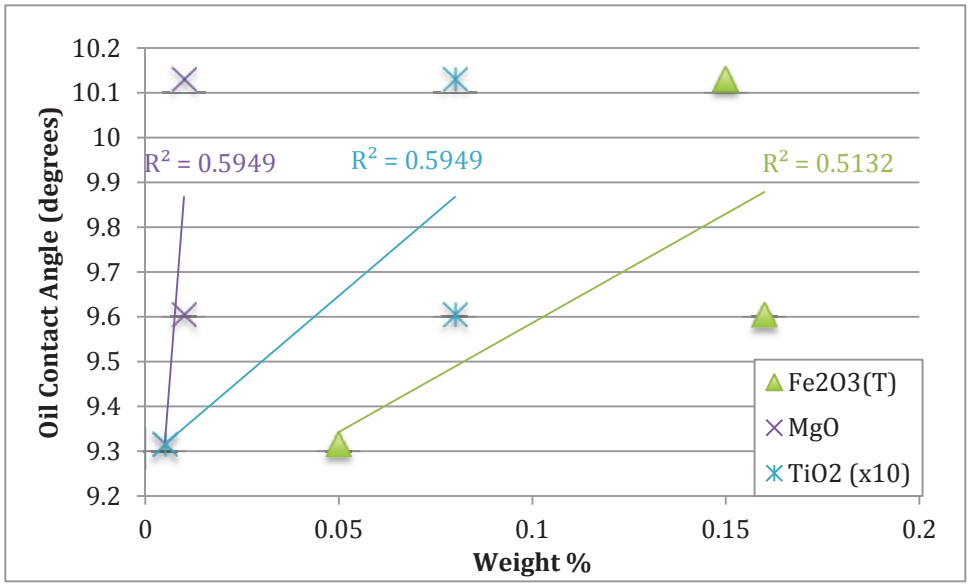

FIGURE 5.17. Moderate R^2 correlations between oil contact angles vs. oxides for quartz phase samples.

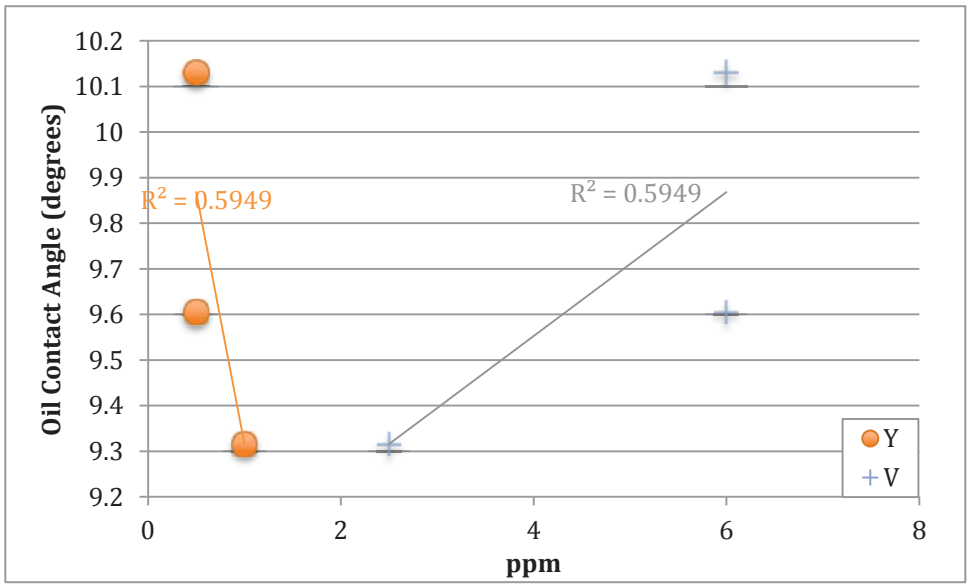

FIGURE 5.18. Moderate R^2 correlations between oil contact angles vs. compositional variables for quartz phase samples.

Principal Component Analysis

PCA is useful for finding the variables most responsible for the variance in a data set, as well as determining commonalities in variable behavior. In the single regression analyses conducted above, each variable was analyzed independently for its relationship to wettability test results. While this may reveal some relationships that may otherwise be obscured, it also may provide misleading trends that attribute variance to a variable that is not truly responsible for it, but behaves similarly to one that is. PCA works by finding a plane through a cloud of data that extends along the greatest amount of variation. A second plane, perpendicular to the first, is projected, explaining the second greatest variation in data. This process is repeated as many times as there are variables, so that there are as many principal components as there are variables. A principal component vector does not correspond directly to a variable, but variables that most closely follow the direction of the principal component are associated with that vector, including its strength of impact on data variability and relationships with any proximal variables. PCA was used in this study to identify compositional trends, similarities and differences between silica phase groups in the sample set, and finally to determine if those factors that were responsible for the greatest variation in sample composition were also responsible for variation in wettability test results.

The significance of a variable to the spread of a dataset in PCA is determined by calculating an eigenvalue. This value rates the amount of variance in the data set caused by that variable. These eigenvalues are plotted along an x-axis in descending order of magnitude. The number of significant principal components in a data set is determined by analysis of the produced chart, known as a "scree plot" (Figure 5.19). One method is

to find the "elbow" or significant decrease in slope of the line and mark that as the cutoff of significant principal components (Johnson and Wichern, 2007). Another method, called the "broken stick" method, calculates the most highly probable length of a stick of length 1 unit broken into n pieces, where n is the number of variables in the data set. If the eigenvalue of a principal component is much greater than the length of the stick segment, then the component is determined significant (Joliffe 2002, Legendre & Legendre, 1998, as cited in Zuur, 2007). Both the elbow (more ambiguous) and the broken stick method indicate that for this study, only two principal components are necessary to explain 75% of the total variance in compositional data from this sample set. The contribution of other variables to data variance is insignificant.

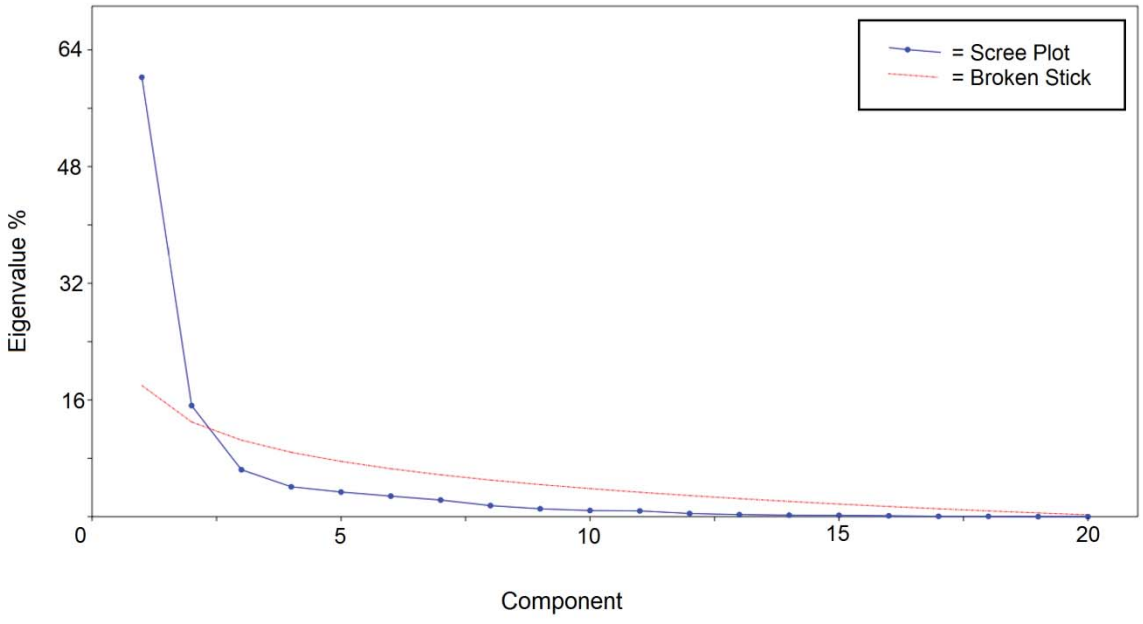

FIGURE 5.19. Scree plot produced by PAST software PCA.

The biplot in figure 5.20 shows that the main variables corresponding to principal component 1, and thus responsible for the greatest variance in the data set, are biogenic & diagenetic silica and SiO_2 (closely related), which are negatively associated with TiO_2, Al_2O_3 and its derivative - detritus, Fe_2O_3, Sc, K_2O and Y. All silica phase groups show a similar distribution along this axis. The PC2 axis, which is responsible for the second greatest variation in compositional data is controlled by measurements of montmorillonite clay, which is negatively related to CaO, Sr, Ba, V, and P_2O_5. This axis also reveals a pronounced distinction between silica phase groups. 82% of all opal-A samples have higher measured montmorillonite weight percentage than all samples of the quartz and opal-CT silica phase groups among core samples. This relationship may largely result from compositional differences between the different members from which the samples were acquired and also would be amplified by increases in silica content of porcelanites with silica diagenesis as suggested by Murray et al. (1992) and Behl and Garrison (1994). Actual montmorillonite values for opal-A are likely somewhat underestimated in measurement due to limitations of the measurement method, so the distinction is probably even more pronounced than the data analysis suggests.

It is notable that montmorillonite values plotted similarly to Al_2O_3 and detritus (a multiple of aluminum oxide). This validates the measurement method used to determine the smectite clay's weight percent via XRD peak height. The contrast in position of these detritus-related variables to CaO, P_2O_5, Ba, and Sr is expected and confirms the validity of element and oxide measurements. These components are largely associated with authigenic precipitates that fill interstitial pore space in sediment, diluting primary detrital and biogenic material.

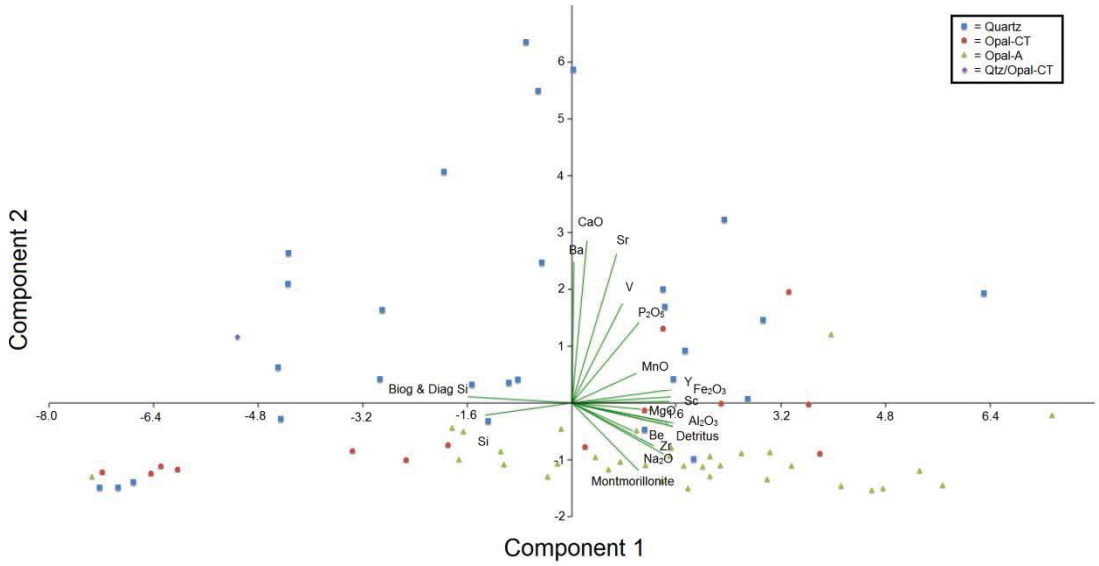

FIGURE 5.20. Biplot produced by PAST software PCA.

PCA Comparison with Wettability Test Results

Plots of PCA scores for PC1 and PC2 versus wettability test results confirm the conclusions of the linear regression analysis described above for water imbibition rates; namely that there is no single observed variable or set of variables that is principally responsible for the change in water imbibition times amongst tested samples (Figures 5.21 and 5.22). The responsible variable could be a compositional element that was not measured in this study, or it could potentially be an uncontrolled variable in the test method that was not fully understood or accounted for. It may be of note that if three outlier points in the quartz phase sample results are removed from the PC2 versus water imbibition rate chart (Figure 5.22) a comparatively significant trend emerges where

imbibition rates decrease linearly with PC2 scores. This would mean that quartz phase samples with higher montmorillonite weight percent and lower abundances of CaO, Sr, Ba, V, and P_2O_5 are more wetting to water and less prone to inhibit imbibition. This is reasonable because most clays are perpetually charged due to uneven cation substitution. Their electric charge readily attracts polar water molecules and may even promote water imbibition rates (Moore, 1960 and Schampera and Dultz, 2011). Opal-A samples form a seemingly random distribution over the PC1 axis when plotted against H_2O imbibition test results, indicating that variables described by PC1 (biogenic and diagenetic silica and SiO_2, which are negatively associated to TiO_2, Al_2O_3 and its multiple - detritus, Fe_2O_3, Sc, K_2O and Y) are not controls of water imbibition rates. Opal-CT samples are also distributed over the PC2 axis with a weak correlation to water imbibition time.

PCA results revealed stronger relationships with oil imbibition than with water. Along the PC1 axis, a similarity in composition between silica phase groups is evident, as is also a clear distinction in imbibition rates (Figure 5.23). Opal-A phase samples required a significantly longer amount of time to imbibe the applied drop of oil than samples of the opal-CT and quartz phases. While the major measured difference between these phase groups is revealed by PCA to be the montmorillonite content (and corresponding positive PC2 variables), a clear correlation between montmorillonite and oil imbibition rates did not emerge within the opal-A sample group itself.

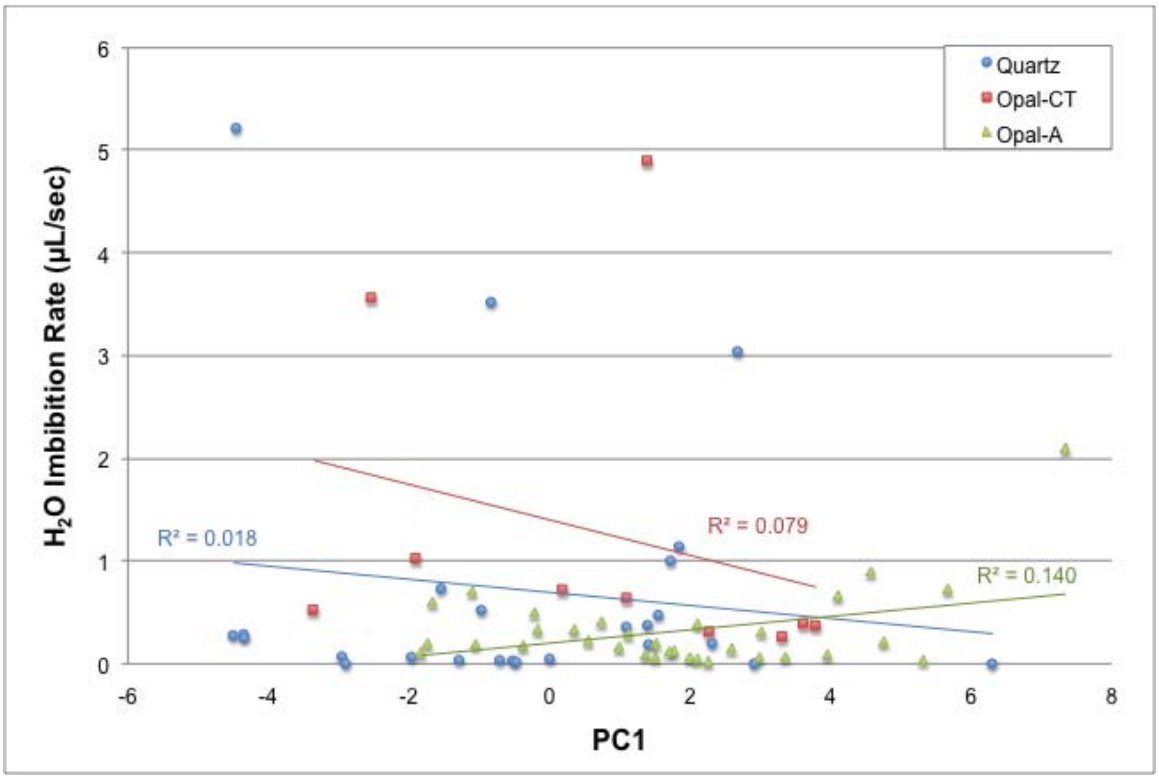

FIGURE 5.21. PC1 vs. H_2O imbibition. Note insignificant R^2 correlation values.

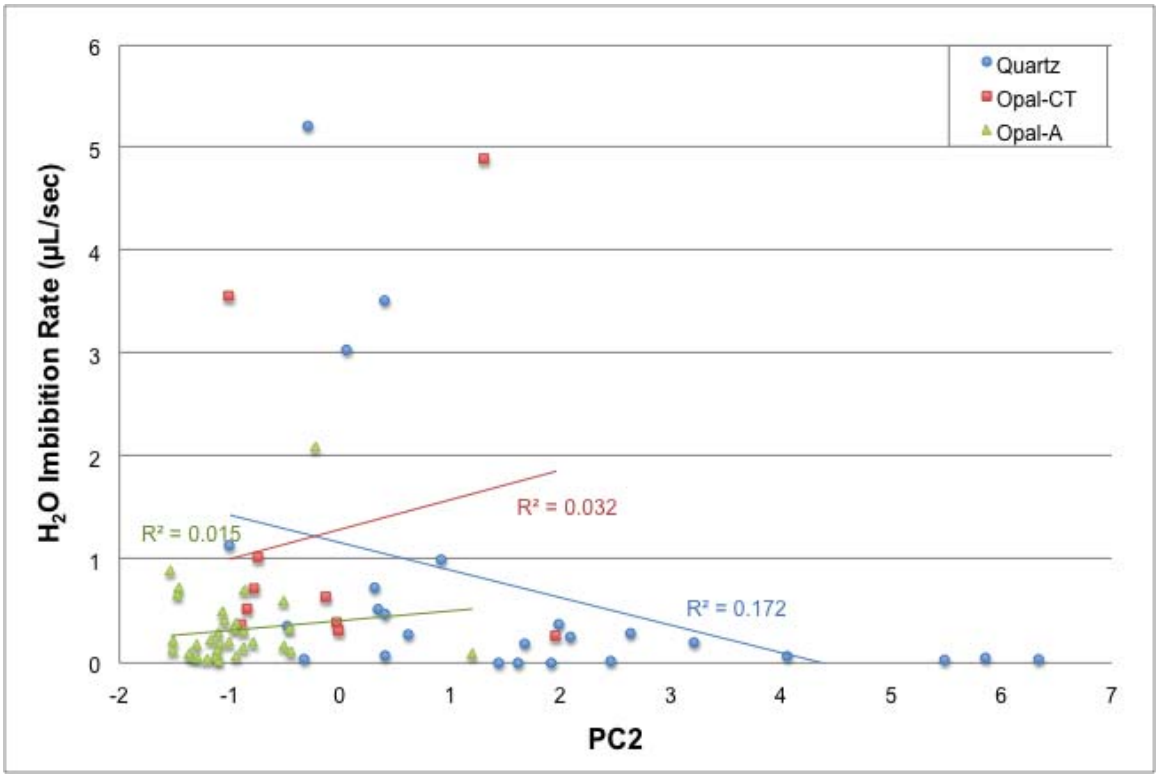

FIGURE 5.22. PC2 vs. H_2O imbibition. Note insignificant R^2 correlation values.

Montmorillonite, therefore, cannot be directly credited for the change in imbibition rates between silica phase groups unless confirmed by further study. Opal-CT phase samples did produce both a moderate and near moderate trend of increasing imbibition time with increase in PC1 and PC2 scores, respectively. The moderate trend along the PC1 axis describes the tendency of montmorillonite clays, detritus, and other PC1 positive scoring variables (Al_2O_3, Fe_2O_3, Sc, K_2O and Y) to reduce the wettability of each sample toward oil.

The plot of PC2 values against oil imbibition rates (Figure 5.24) shows most clearly the distinction in results of this test between silica phase groups. While opal-A samples are distinguished for their negative PC2 scores (montmorillonite content) where the other two groups are primarily positive (less smectite clay, more CaO, Sr, Ba, V, and P_2O_5), there is still no trend of oil imbibition test result change with compositional variation within the group. Both opal-CT and quartz phase samples demonstrate no clear trend of alteration in average oil imbibition times, regardless of their variation in PC2 compositional variables (montmorillonite, CaO, Sr, Ba, V, and P_2O_5).

PC1 scores did not produce any significant relationships with water contact angle test results (Figure 5.25). This seems to indicate that purity of siliceous content and detrital content (with other PC1 variables) are not significant controls on water contact angle. It is important to note that the strength of this interpretation could be limited by the extremely narrow compositional range of the samples tested. Each sample tested is a chert or pure mineral precipitate, so there is minimal variation in detritus or siliceous purity, which are the primary variables responsible for the direction of the PC1 axis.

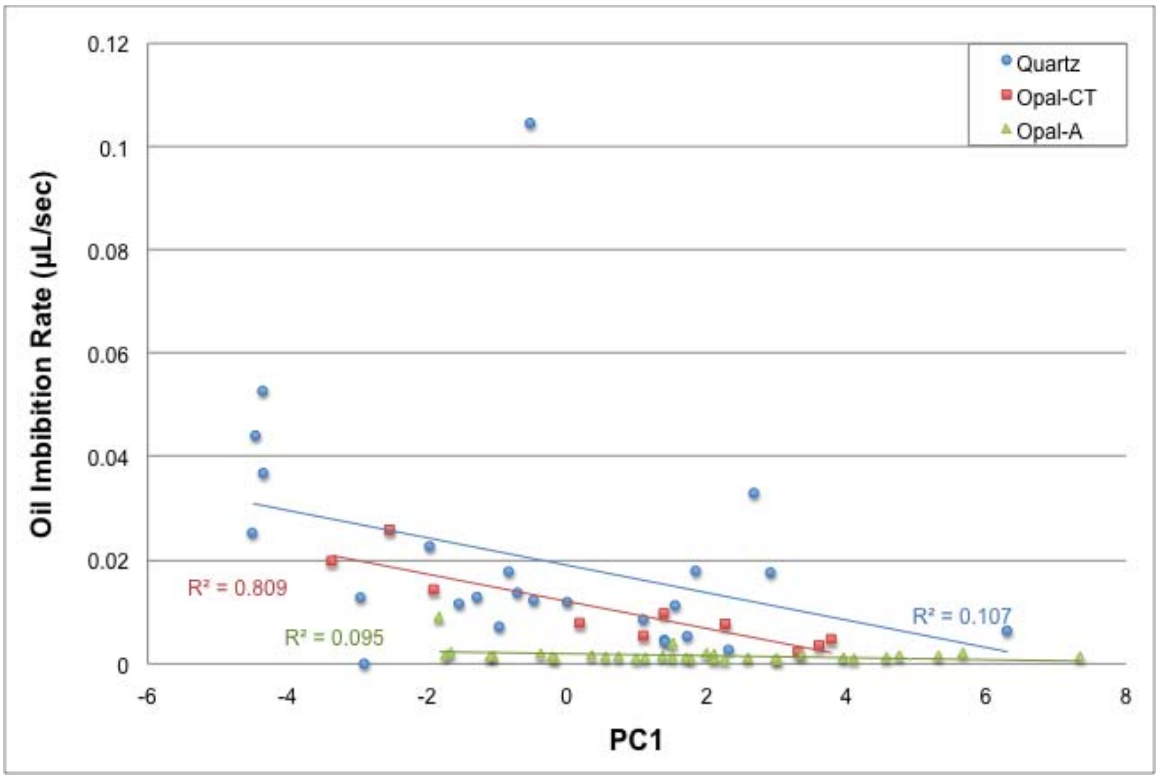

FIGURE 5.23. PC1 scores grouped by silica phase vs. oil imbibition rate.

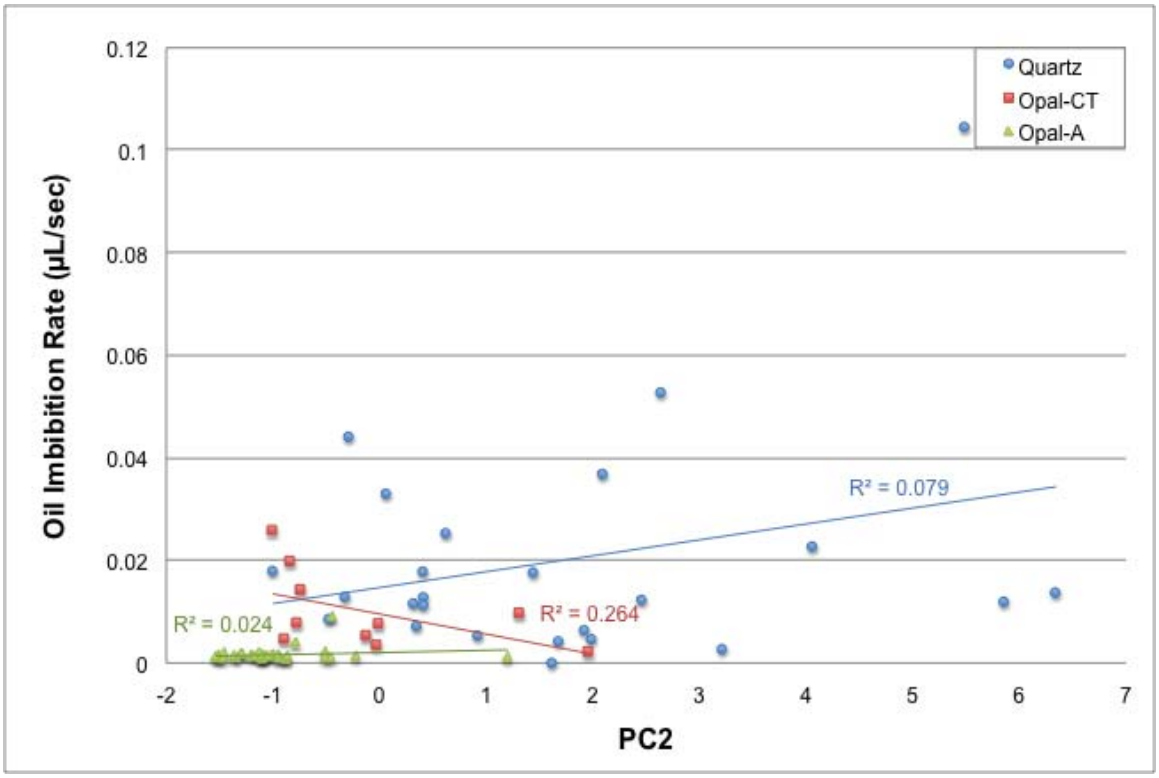

FIGURE 5.24. PC2 scores grouped by silica phase vs. oil imbibition rate.

When water contact angles are plotted against PC2 scores, two significant trends emerge. Both quartz and opal-CT phase samples demonstrate a decrease in water contact angle with increasing PC2 score (Figure 5.26). This signifies increased wettability to water with decrease in weight percent montmorillonite and corresponding increase in abundance of CaO, Sr, Ba, V, and P_2O_5. The relationship is significant for opal-CT phase samples and moderately so for quartz phase samples.

Oil contact angles demonstrated significant response trends when plotted against both PC1 and PC2. The increase in abundance of the positive PC1 variables including detritus, montmorillonite, Al_2O_3, Fe_2O_3, Sc, K_2O and Y, led to an increase in oil drop contact angle with each sample (Figure 5.27). This trend indicates that these variables affect a reduced wettability to oil in siliceous rocks, and that more purely siliceous rocks have a greater wettability to oil. Plotted along the PC1 axis, opal-CT samples exhibited more wetting to oil when they had more positive PC1 scores – that is, more montmorillonite clay, detritus, and related elements and oxides, and a lower weight percent of purely siliceous (biogenic and diagenetic) material. Opal-CT samples do not show a significant trend along the PC2 axis (Figure 5.28).

Multiple Regression Analysis

Multiple regression functions similarly to single regression analysis. For a single regression, a line of best fit (minimum squared error) is found between one dependent variable (y, or in our case, the wettability test result) and one predictor variable, which would be a compositional variable in the current study.

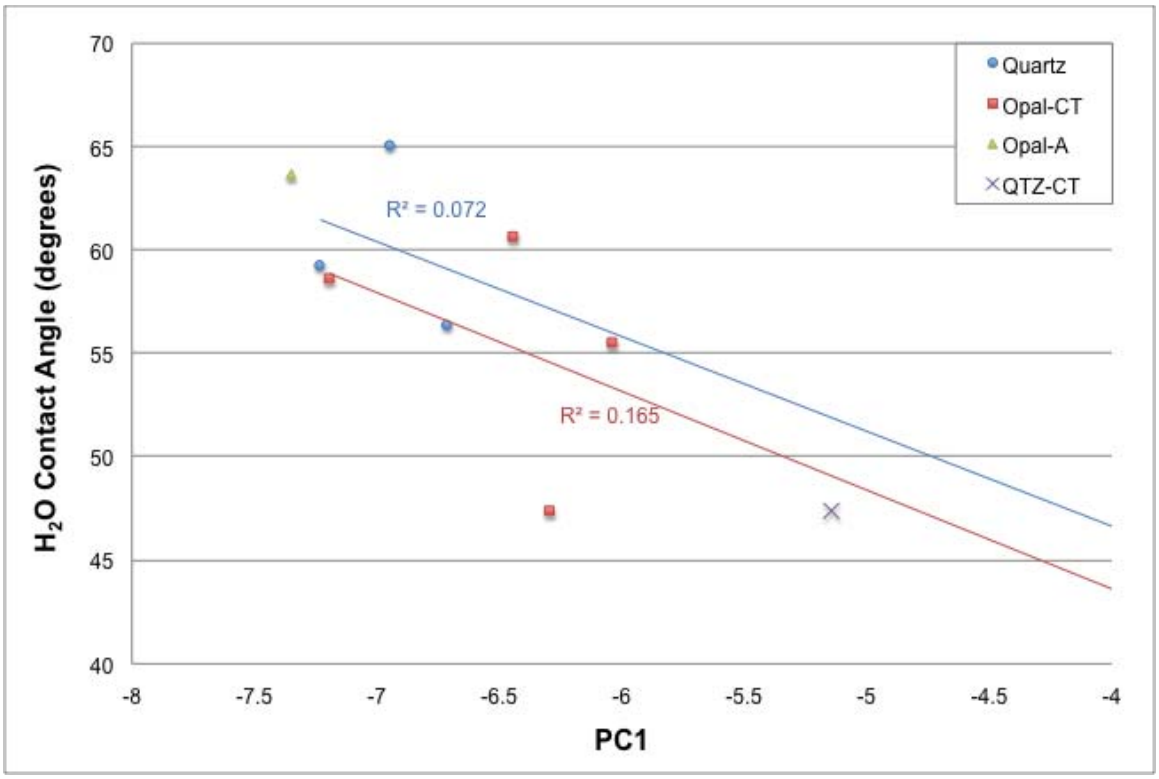

FIGURE 5.25. PC1 vs. water contact angle.

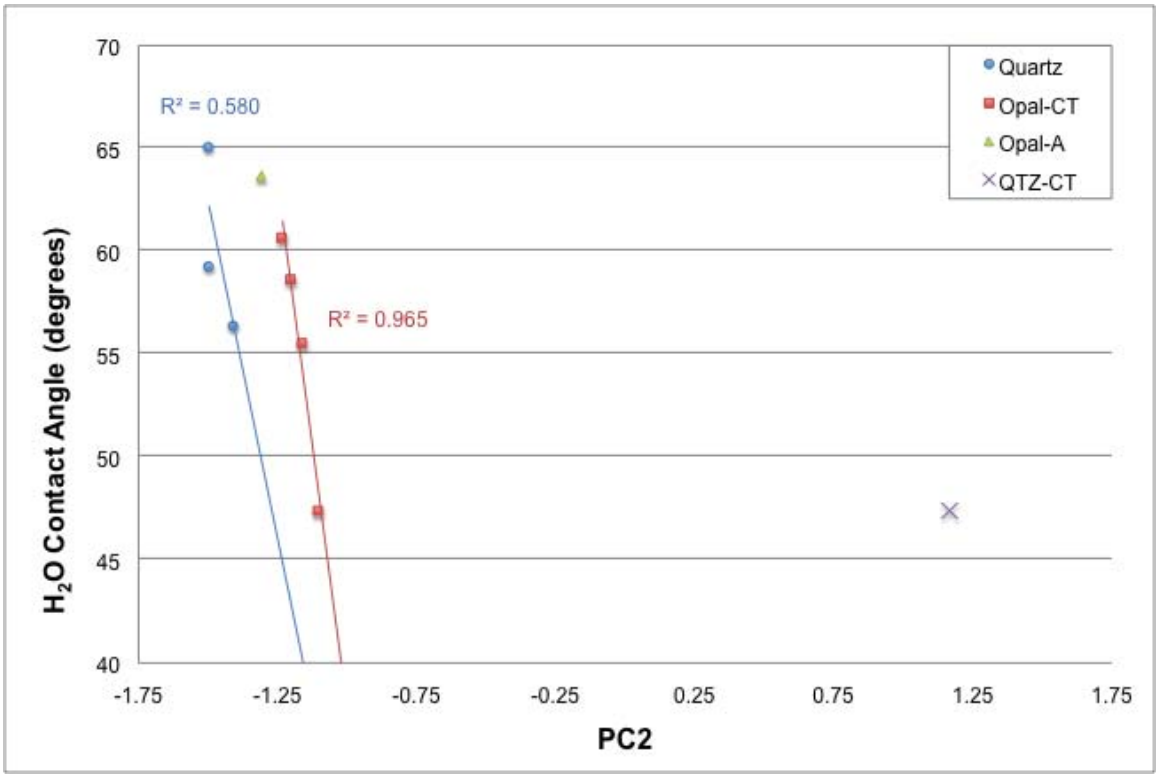

FIGURE 5.26. PC2 vs. water contact angle.

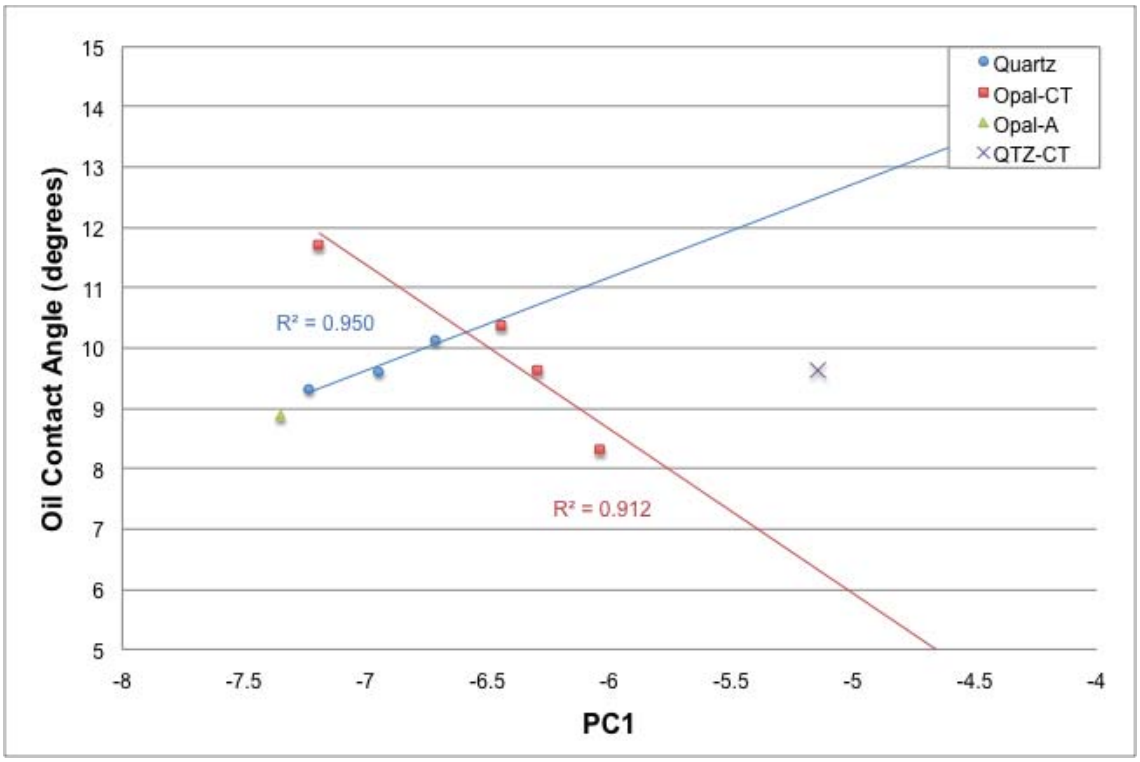

FIGURE 5.27. PC1 vs. oil contact angle.

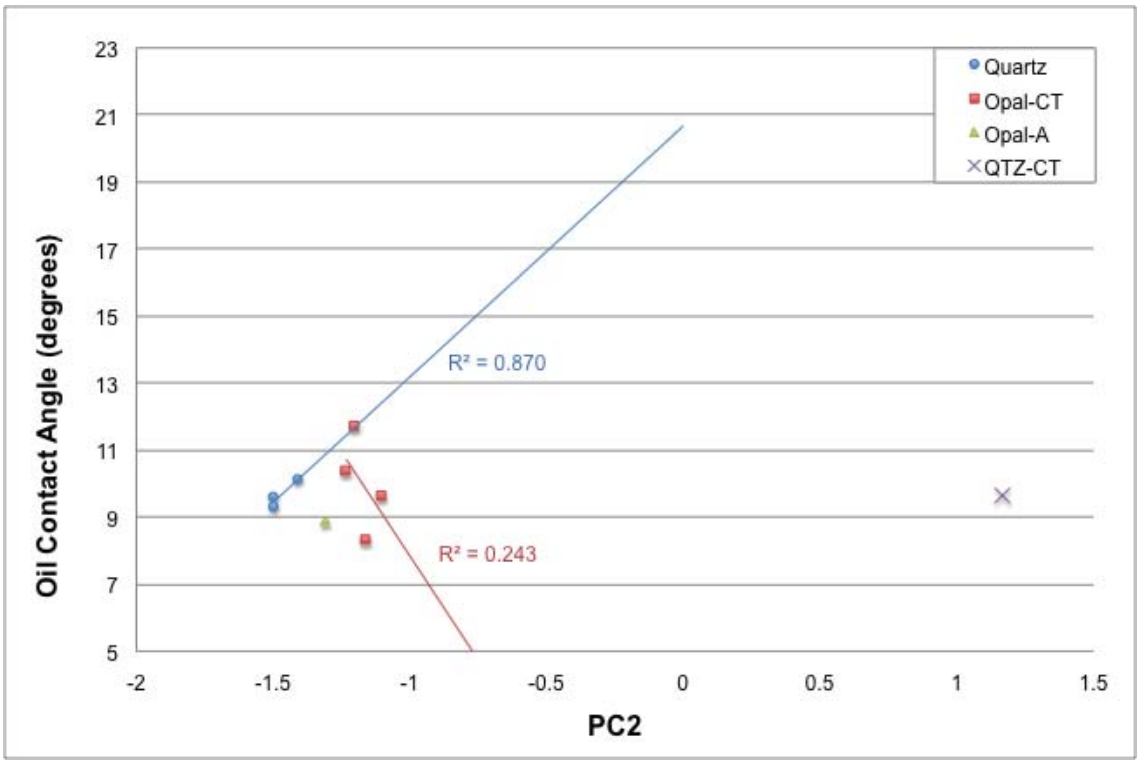

FIGURE 5.28. PC2 vs. oil contact angle.

In multiple regression, a plane of best fit is found for the data by finding the least squared error between a single dependent variable – again, a wettability test result – and multiple predictor variables. Scores are attributed to each variable depending on their predictive power for the model. For our study, we limit the predictor variables to PC1, PC2, PC1*PC2 (an interaction term), and silica phase as a qualitative grouping factor. The number of compositional variables would nullify the regression analysis results if each of the 20 variables were entered into the model. The input of the PCA results as the variables in the multiple regression model determines if those variables which are most responsible for the variance of composition in all samples are also responsible for the change in imbibition test results. Not enough samples were tested to perform a meaningful multiple regression analysis on contact angle results.

When PC1, PC2, and their interaction term: PC1*PC2 were analyzed as predictor variables against the dependent variable of H_2O imbibition time in a multiple regression model, the results resembled those of the single regression analyses. PC2 and silica phase group were the only two variables to score as significant predictors of water imbibition rate. The similar behavior of these variables in our model is expected, due to the fact that PC2 was the most pronounced distinguisher between silica phase groups. The comparative significance of these variables in this model is nullified by the overall lack of predictive power of the model itself, however. All variables combined were only determined to explain approximately 25% percent of the variance in water imbibition rate, overall.

A similar multiple regression analysis as above, but with oil imbibition times as the dependent variable, generated a much more powerful model that is able to explain

almost 81% (R^2 adjusted value) of the variation in test results. By this model, significant predictor variables were PC1 scores, PC1*PC2 interaction values, and silica phase. The coefficients for PC1 and PC1*PC2 were positive, indicating that increasing values for these variables led to higher oil imbibition times, which agrees with the single regression analysis of PC1 vs. oil imbibition time. This also confirms relationships with PC1 variables (biogenic and diagenetic silica, SiO_2, TiO_2, Al_2O_3, detritus, Fe_2O_3, Sc, K_2O and Y) plotted against oil imbibition time in single regression analysis. Individually, these variables produced only a moderate correlation at best with oil imbibition (see tables 6.1, 6.2, and 6.3 for single regression R^2 values). Multiple regression analysis shows that while each of these variables' independent predictive power is low, their cooperative predictive power is substantial for this data set.

Comparison with Previous Work

Imbibition tests in this study agree with the Takashi and Kovcek (2010), Montgomery and Morea (2001), and Toronyi (1997) that Monterey Formation rocks are moderately to strongly water wet across all stages of silica diagenesis. Unfortunately, due to the compositional differences between rocks of different silica phase groups in our study, any change in wettability to water and oil between silica phase groups was not statistically distinguishable, though overall oil imbibition rates decreased from quartz to opal-CT to Opal-A in our study. Such an alteration is logical. Each stage of the process of diagenesis from opal-A to opal-CT to quartz involves removal of water from the crystal lattice, which is likely to affect the propensity of the siliceous material to attract polar water molecules. If this difference exists, it was overshadowed by wettability

differences induced by differences in compositional variables other than SiO_2, especially detritus and clay content.

Average water contact angles on quartz samples in our study agreed with water contact angles on synthesized quartz of 54±6° (Suzuki et al., 2014). Our contact angles were higher than those measured by Sumner et al., (2004), which were <10° for glass and 22±4° for quartz. Our higher contact angles could be a product of a less pure gas phase surrounding the samples testing. This would agree with the assessment by Iglauer et al. (2014) that contact angles on quartz in "clean" environments are between 0 and 30°, and that contact angle tests conducted in contaminated environments are artificially inflated. A "contaminated" environment in this case refers to any quartz sample that is not first submersed in a 5:1 solution of water and ammonium hydroxide, then rinsed with chloroform, 2-propanol, and ethanol in succession, then treated with UV- ozone for 30 minutes. The high contact angles for quartz samples in our study could also be a result of cleaning each sample with hexane between each wettability test. This cleaning was necessary to remove all hydrocarbons from tested samples before retesting, as hydrocarbon pretreatment is known to increase a surface's wettability to other hydrocarbons (Somenon and Rodke, 1983, as cited in Sayyouh et al., 1990).

Our oil imbibition tests confirm Moore's (1960) findings that clays are naturally water wet and increase the wettability of a formation to water when present. Moore's experiments involved sandstone, but the behavior of clays toward water in siliceous reservoirs is identical.

New information from our study involves the wetting interactions between oil and clay in siliceous reservoirs. While clay increases a rock surface's wettability to water in a

siliceous reservoir, it acts as an inhibitor to flow for oil. This phenomenon may be a product of the much higher viscosity of oil, but is likely also highly related to the lack of response to neutrally charged hydrocarbons to charged clay particles in contrast to the strong attraction between clay cations and polarized water molecules.

CHAPTER 6

CONCLUSIONS AND SYNTHESIS

This thesis reports the first published, systematic attempt to measure variation in wettability to water and oil of the highly siliceous rocks that occur within the Monterey Formation and related facies around the Pacific Rim. Specialized approaches were necessary to develop to test these high-porosity, low-permeability rocks. Samples of all three silica phases—opal-A, opal-CT and quartz— were tested over a range of secondary compositions for wettability by rate of imbibition and contact angle. Probably due to the complex compositional variability of even these carefully selected samples, the results of these tests do not paint a simple picture and are, in part, contradictory. Nonetheless, some relationships have become evident, as outlined below.

Opal-A phase samples exhibited lower rates of imbibition of oil (less wettability) than both diagenetic phase groups – opal-CT and quartz – among samples with comparable detrital content. This relationship did not hold for water imbibition.

Of all the tested rocks, opal-CT phase samples produced the statistically strongest relationships of imbibition-quantified wettability to the tested fluids and compositional variation with the relative abundance of various proxies for detritus to silica being the best predictors of behavior. This is especially true for both imbibition and contact angle tests for oil.

Water imbibition tests provided no distinguishing trends of wetting between silica phases that were not better explained by compositional variability between samples. No compositional trends produced statistically significant trends in water imbibition rates within any of the individual silica phase groups (Figure 6.1). Opal-A samples showed very weak trends of increased wettability to water with increased abundance of proxies for detritus or decreased biogenic silica.

Oil imbibition tests showed with moderately significant R^2 values ($0.5 < R^2 < 0.8$) that opal-CT phase rocks were more wetting to oil with increase purity of siliceous content and more inhibitive of oil imbibition with increased detritus with moderate R^2 significance, and a similar direction, but very weakly significant relationship for opal-A and quartz phase samples (Figure 6.2). Opal-CT samples also demonstrated decreased wettability to oil with increased TiO_2, Ba and Fe_2O_3, with moderate R^2 correlation. Trends in oil wettability with composition were weak, with R^2 values below 0.5, for opal-A and quartz phase samples from oil imbibition tests.

In contrast to the imbibition results, the robustness of trends identified from the contact angle tests are limited by the very small range in composition in the tested samples due to the necessity of having relatively pure, dense samples for these tests. Water contact angle tests showed that opal-CT phase samples had increased wettability to water with increased montmorillonite clay, Ba, P_2O_5, and Fe_2O_3 (Figure 6.3). Quartz samples showed decreased wettability to water with increased montmorillonite clay.

Oil contact angle tests showed some opposing trends between quartz and opal-CT phase samples, with opal-CT exhibiting reduced wettability to oil with increased siliceous purity and quartz samples showing decreased wettability to oil with increased detritus

(Figure 6.4). Opal-CT phase samples also showed significant decrease in wettability to oil with increased TiO_2 and moderate increase wettability to oil with montmorillonite clay, P_2O_5, and Fe_2O_3. Quartz samples showed moderate trends of increased wettability to oil with increased TiO_2 and Fe_2O_3.

	Opal-A	Opal-CT	Quartz
Silica	−	+	+
Detritus	+	−	No trend
Montmorillonite	+	−	No trend
Titantium	+	−	−
CaO	+	+	−
Barium	+	No trend	−
P_2O_5	+	−	−
Fe_2O_3	+	−	−

(Strongly) More wetting:	+	*(Strongly) Less wetting:*	−
(Moderately) More wetting:	+	*(Moderately) Less wetting:*	−
(Weakly) More wetting:	+	*(Weakly) Less wetting:*	−

FIGURE 6.1. Water imbibition test trends for geologically significant compositional variables. R^2 values are considered significant above 0.8. Values between 0.5 and 0.7 are considered moderately significant, and values below 0.5 are considered insignificant.

	Opal-A	Opal-CT	Quartz
Silica	+	+	+
Detritus	−	−	−
Montmorillonite	−	−	−
Titantium	−	−	−
CaO	+	−	+
Barium	−	−	+
P_2O_5	−	−	−
Fe_2O_3	−	−	−

(Strongly) More wetting: +
(Moderately) More wetting: +
(Weakly) More wetting: +

(Strongly) Less wetting: −
(Moderately) Less wetting: −
(Weakly) Less wetting: −

FIGURE 6.2. Oil imbibition test trends for geologically significant compositional variables. R^2 values are considered significant above 0.8. Values between 0.5 and 0.7 are considered moderately significant, and values below 0.5 are considered insignificant.

	Opal-A	Opal-CT	Quartz
Silica	N/A	−	−
Detritus	N/A	+	−
Montmorillonite	N/A	+	−
Titantium	N/A	+	−
CaO	N/A	−	−
Barium	N/A	+	−
P_2O_5	N/A	+	No trend
Fe_2O_3	N/A	+	−

(Strongly) More wetting: +
(Moderately) More wetting: +
(Weakly) More wetting: +

(Strongly) Less wetting: −
(Moderately) Less wetting: −
(Weakly) Less wetting: −

FIGURE 6.3. Water contact angle test trends for geologically significant compositional variables. R^2 values are considered significant above 0.8. Values between 0.5 and 0.7 are considered moderately significant, and values below 0.5 are considered insignificant.

	Opal-A	Opal-CT	Quartz
Silica	N/A	−	+
Detritus	N/A	+	−
Montmorillonite	N/A	+	+
Titantium	N/A	−	−
CaO	N/A	+	−
Barium	N/A	+	−
P_2O_5	N/A	+	No trend
Fe_2O_3	N/A	+	−

FIGURE 6.4. Oil contact angle test trends for geologically significant compositional variables. R^2 values are considered significant above 0.8. Values between 0.5 and 0.7 are considered moderately significant, and values below 0.5 are considered insignificant.

CHAPTER 7

FUTURE WORK

The discovery by this study that silica phase in Monterey Formation reservoir rocks is less important to reservoir wettability than non-matrix compositional differences is an important one. Furthermore, the relationships of wettability to specific secondary components is intriguing, but not entirely consistent between compositional proxies. Consequently, the findings of this study raise a number of questions that were not able to be answered with this sample set and experimental design.

Samples for this study were collected from cores from subsurface reservoirs so that changes due to surficial weathering processes were eliminated from influencing test results. Unfortunately, this study was only able to obtain samples of rocks for different diagenetic stages (opal-A, opal-CT and quartz) that were from distinct members on the Monterey Formation that had different secondary compositions. This limitation restricted the ability to make direct comparison between different silica phase rocks that were of similar composition. For future work, it is recommended that samples spanning all silica phase range should be collected from the same location or same stratigraphic member as much as possible in order to prevent wettability differences caused by non-silica-based components. In an optimal situation, samples should be collected down-dip within the same oil field or structure, where the same stratigraphic member of the Monterey

Formation is buried to greater depth and diagenetic stage, making sure to acquire samples over the same compositional range.

Second, the imbibition test method showed that the impact of clays on the wettability of siliceous reservoir rocks is profound. A more robust assessment of the abundance and type of clays present in tested rock samples will be critical to better defining and quantifying the impact of clays on tested samples. This assessment should include a measurement of illite clay, which was not quantified in this study, as well as a more absolutely quantitative measurement of montmorillonite clay.

Contact angle measurements are likely the most effective and direct test of wettability variation related to silica phase change. This study was limited to just a few samples of opal-CT and quartz chert plus one sample of opal-A hydrothermal hyalite. A larger sample selection with numerous relatively pure samples of every silica phase that uses the contact angle method will provide sufficient results to provide statistical confirmation or refutation of differences between silica phases and other trends exhibited in this study for minor compositional variation.

REFERENCES

REFERENCES

Abdallah W., Buckley, J.S., Carnegie, A. Edwards, J., Herold, B., Fordham, E., Graue, A., Habashy, T., Seleznev, N., Signer, C., Hussain, H., Montaron, B., and Ziauddin, M., 2007, Fundamentals of wettability: Oilfield Review, v.19, p.2.

Anderson, W.G., 1987, Wettability Literature Survey – Part 4: Effects of wettability on capillary pressure, Journal of Petroleum Technology, v. 36, p. 1283-1300.

Bachmann, J., Ellies, A., and Hartge, K.H., 2000, Development and application of a new sessile drop contact angle method to assess soil water repellency, Journal of Hydrology, v. 231–232, p. 66-75.

Barclay, S.A., and Worden, R.H., 2000, Effects of reservoir wettability on quartz cementation in oil fields: *in* Quartz Cementation in Sandstones, ed. R.H. Worden and S. Morad, Special Publication of the International Association of Sedimentologists, Blackwell Science, v. 29, p. 103-117.

Behl, R.J., and Garrison, R.E., 1994, The origin of chert in the Monterey Formation of California (USA), Siliceous, phosphatic and glauconitic sediments of the Tertiary and Mesozoic, *in* Proceedings of the 29th International Geological Congress, Part C, p. 101-132.

Berg, S., Cense, A.W., Jansen, E., and Bakker K., 2010, Direct experimental evidence of wettability modification by low salinity, Petrophysics , v.51, no. 5, p. 314-322.

Bhat, S.K., and Kovscek, A.R., 1998, Permeability modification of diatomite during hot-fluid injection, Journal of Petroleum Technology, v. 50, no. 9, p. 98-100.

Buckley, J.S., 1998, Wetting alteration of solid surfaces by crude oils and their asphaltenes, *in* La Production des fluides de gisements en conditions extremes Production of reservoir fluids in frontier conditions, Revue de l'Institut Francais du Petrole, v. 53, no. 3, p. 303-312.

Chandrasekhar, S., and Mohanty, K.K., 2013, Wettability alteration with brine composition in high temperature carbonate reservoirs, SPE Annual Technical Conference and Exhibition, SPE - 166280 - MS

Civan, F., 2004, Temperature dependence of wettability related rock properties correlated by the Arrhenius equation, Petrophysics, v. 45, no. 4, p. 350-362.

Collister, J., Ehrlich, R., Mango F., and Johnson G., 2004, Modification of the petroleum system concept; Origins of alkanes and isoprenoids in crude oils, AAPG Bulletin, v. 88, no. 5, p. 587-611

Compton, J.S., 1991, Origin and diagenesis of clay minerals in the Monterey Formation, Santa Maria Basin area, California, Clays and Clay Minerals, v. 39, p. 449-466

Depalo, A., and Santomaso, A.C., 2013, Wetting dynamics and contact angles of powders studied through capillary rise experiments, Colloids and Surfaces A, Physicochemical and Engineering Aspects, v. 436, p. 371-379

deZabala, E., 1999, Core analyses and rock properties: Estimating initial oil saturation in the Antelope shale, *in* M. Morea, ed., Advanced reservoir characterization in the Antelope shale to establish the viability of CO2 enhanced oil recovery in California's Monterey Formation siliceous shales: Annual Technical Progress Report, Project DE-FC22-95BC14938, National Petroleum Technology

Fernø, M.A., Haugen, Å., and Graue, A., 2011, Wettability effects on the matrix–fracture fluid transfer in fractured carbonate rocks: Original Research Article, Journal of Petroleum Science and Engineering, v. 77, no. 1, p. 146-153.

Freedman, R., Heaton, N., Flaum M., Hirasaki, G.J., Flaum, C., and Huerlimann, M., 2003, Wettability, saturation, and viscosity from NMR measurements: SPE Journal, v. 8, no. 4, p. 317-327.

Garrison, R.E., 1992, Neogene lithofacies and depositional sequences associated with upwelling regions along the eastern margin of the Pacific, *in* Pacific Neogene; Environment, Evolution, and Events: Tsuchi, Ingle, Ryuichi, James C.: Tokyo, Japan, University of Tokyo Press, v. 92, p. 43-69.

Gupta, R., and Mohanty, K.K., 2011, Wettability alteration mechanism for oil recovery from fractured carbonate rocks: Transport in Porous Media, v. 87, no. 2, p. 635-652.

Iglauer, S., Salamah, A., Sarmadivaleh, M., Liu, K. and Phan, C., 2014, Contamination of silica surfaces: Impact on water-CO2-quartz and glass contact angle measurements. International Journal of Greenhouse Gas Control, v. 22, p. 325-328.

Isaacs, C.M., 1980, Diagenesis in the monterey formation examined laterally along the coast near Santa Barbara, California [microform], Dissertation Abstracts International, v. 41-02, sec. B, p. 0498.

Johnson, R.A., and Wichern, D., 2007, Applied Multivariate Statistical Analysis, sixth ed.: New Jersey, Pearson Prentice Hall, p. 445.

Jolliffe, I., 2002, Principal component analysis: Wiley Stats Ref: Statistics Reference Online

Karabakal, U., and Bagci, S., 2004, Determination of wettability and its effect on waterflood performance in limestone medium: Energy & Fuels, v. 18, no. 2, p. 438-449.

Keller, M.A., and Isaacs, C.M., 1985, An evaluation of temperature scales for silica diagenesis in diatomaceous sequences including a new approach based on the Miocene Monterey Formation, California, *in* Origins, transport, and deposition of fine-grained sediments; 1984 SEPM Research conference, Part II - Geo-Marine Letters, v. 5, p. 31-35.

Kirdponpattara, S., Phisalaphong, M., and Newby, B. Z., 2013, Applicability of Washburn capillary rise for determining contact angles of powders/porous materials, Journal of Colloid and Interface Science, v. 397, p. 169.

Kovscek, A.R., Vega, B. and Urdaneta, A.H., 2010, The effect of temperature and oil viscosity reduction on water imbibition of diatomite: *in* Geological Society of America, Cordilleran Section, 106th annual meeting; American Association of Petroleum Geologists, Pacific Section, 85th annual meeting; Society of Petroleum Engineers, Western Region, 80th annual meeting, Abstracts with Programs - Geological Society of America, v. 42, no. 4, p. 73-93

Kumar, K., Dao, E., and Mohanty, K.K., 2005, AFM study of mineral wettability with reservoir oils, Journal of Colloid and Interface Science, v. 289, p. 206-217.

Lamparter, A., Bachmann, J., Woche, S.K., and Goebel, M.O., 2013, Biogeochemical interface formation; Wettability affected by organic matter sorption and microbial activity: Dissolved organic matter in soil, Vadose Zone Journal, v. 13.

Lau, E.V., Gan, S. Ng, H.K., and Poh, P.E., 2014, Extraction agents for the removal of polycyclic aromatic hydrocarbons (PAHs) from soil in soil washing technologies, Environmental Pollution, v. 184, p. 640-649.

Legendre, P. and Legendre, L., 1998, Numerical Ecology. Second English Edition: Elsevier, Amsterdam.

Lemke, H., and Schwochau, K., 1992, Wettability of petroleum reservoir rock minerals: *in* Proceedings of the 7th International Symposium on Water-Rock Interaction; Moderate and high temperature environments, *in* Proceedings - International Symposium on Water-Rock Interaction, v. 2, no. 7, p.1243-1245

Madden, M.P., and Strycker, A.R., 1988, Thermal processes for light oil recovery: Annual Report, Work Performed Under Cooperative Agreement No. FC22-83FE60149, for the U.S.

Mann, U., 1994, An integrated approach to the study of primary petroleum migration, *in* Geofluids; origin, migration and evolution of fluids in sedimentary basins, Geological Society Special Publications, v. 78, p. 233-260.

Matyasik, I., Lesniak, G., Such, P., and Mikolajewski, A., 2010, Mixed wetted carbonate reservoir; origins of mixed wettability and affecting reservoir properties, Annales Societatis Geologorum Poloniae, v. 80, no. 2, p. 115-122.

Mohanty, K., and Kathel, P., 2013, EOR in tight oil reservoirs through wettability alteration, *in* Proceedings, SPE Annual Technical Conference and Exhibition

Montgomery S.L., and Morea, M.F., 2001, Antelope Shale (Monterey Formation), Buena Vista Hills Field; advanced reservoir characterization to evaluate CO2 injection for enhanced oil recovery, AAPG Bulletin, v. 85, p. 561-585.

Moore, J.E., 1960, Clay mineralogy problems in oil recovery—Part 2, How to combat swelling clays: Petroleum Engineer for Management, v. 32, no. 3, p. B-78.

Murray, R.W., Buchholtz ten Brink, M.R., Gerlach, D.C., Russ III, G.P., and Jones, D.L., 1992, Rare earth, major, and trace element composition of Monterey and DSDP chert and associated host sediment; assessing the influence of chemical fractionation during diagenesis, Geochimica et Cosmochimica Acta, v. 56, no. 7, p. 2657-2671.

Nowak, E., Combes, G., Stitt, E.H., and Pacek, A.W., 2013, A comparison of contact angle measurement techniques applied to highly porous catalyst supports, Powder Technology, v. 233, p. 52-64.

Odusina, E.O., Sondergeld, C.H. and Rai, C.S., 2012, An NMR study of shale wettability: Presented at the Canadian Unconventional Resources Conference, Alberta, Canada, 30 October-1, SPE-147371-MS.

Rodríguez-Valverde, M.A., Cabrerizo-Vílchez, M.A., Rosales-López, P., Páez-Dueñas, A., and Hidalgo-Álvarez, R., 2002, Contact angle measurements on two (wood and stone) non-ideal surfaces, Colloids and Surfaces A: Physicochemical and Engineering Aspects, v. 206, no. 1–3, p. 485-495.

Sayyouh, M.H., Dahab A.S., and Omar, A.E., 1990, Effect of clay content on wettability of sandstone reservoirs, Journal of Petroleum Science & Engineering, v. 2, p. 119-125.

Schampera, B., and Dultz, S., 2011, The effect of surface charge and wettability on H2O self diffusion in compacted clays, Clays and Clay Minerals, v. 59, no. 1, p. 42-57.

Seth, M., Hatzikiriakos, S.G., and Clere, T.M., 2001,The effect of surface energy of boron nitride powders on gross melt fracture elimination: Society of Plastics Engineers ANTEC 2001 Proceedings, Session T12: Polymer Modifiers and Additives, p. 2634-2638.

Shedid, S.A., and Ghannam, M.T., 2004, Factors affecting contact-angle measurement of reservoir rocks, Journal of Petroleum Science and Engineering., v. 44, p. 193-203.

Somenon, W.H. and Rodke, C.J., 1983, Role of clay in EOR of petroleum from some California sand, Journal of Petroleum Technology, v. 35, p. 643-654.

Sumner, A.L., Menke, E.J., Dubowski, Y., Newberg, J.T., Penner, R.M., Hemminger, J.C., Wingen, L., Brauers, T., and Finlayson-Pitts, B.J., 2004, The nature of water on surfaces of laboratory systems and implications for heterogeneous chemistry in the troposphere, Physical Chemistry, Chemical Physics, v. 6, p. 604-613.

Susana, L., Campaci, F., and Santomaso, A. C., 2012, Wettability of mineral and metallic powders: Applicability and limitations of sessile drop method and Washburn's technique, Powder Technology, v. 226, p. 68-77.

Suzuki, T., Takahashi, K., Kawasaki, M., and Kagami, T., 2014, Specific surface free energy of as-grown and polished faces of synthetic quartz, Journal of Crystallization Process and Technology, v. 4, p. 177-184.

Takahashi, S., and Kovscek, A.R, 2010, Spontaneous countercurrent imbibition and forced displacement characteristics of low-permeability siliceous shale rocks, Journal of Petroleum Science and Engineering, vol. 71, p. 47-55.

Takahashi, S., and Kovscek, A.R., 2010, Wettability estimation of low-permeability, siliceous shale using surface forces, Journal of Petroleum Science and Engineering v. 75, p. 33-43.

Tennyson, M.E., Cook, T.A., Charpentier, R.R., Gautier, D.L., Klett, T.R., Verma, M.K., Ryder, R.T., Attanasi, E.D., Freeman, P.A., and Le, P.A., 2012, Assessment of remaining recoverable oil in selected major oil fields of the San Joaquin Basin, California: U.S. Geological Survey Fact Sheet 2012-3050

Thakker, M., Karde, V., O Shah, D., Shukla, P., and Ghoroi, C., 2013, Wettability measurement apparatus for porous material using the modified Washburn method, Measurement Science and Technology, v. 24, p. 125902.

Toronyi, R.M., 1997, Advanced reservoir characterization in the Antelope Shale to establish the viability of CO2 enhanced oil recovery in California's Monterey Formation siliceous shales, National Technical Information Service, v. 703, p. 605-6000.

U.S. Energy Information Administration, 2014, Annual Energy Outlook 2014; With Projections to 2040, Report Number: DOE/EIA-0383ER(2014).

van Oss, C.J., and Giese, R.F., 1995, The hydrophilicity and hydrophobicity of clay minerals, Clays and Clay Minerals, v. 43, p. 474-477.

Zelenev, A.S., Champagne, L.M., and Hamilton, M., 2011, Investigation of interactions of diluted microemulsions with shale rock and sand by adsorption and wettability measurements: Colloids and Surfaces A, Physicochemical and Engineering [60] Aspects, v. 391, p. 201-207.

Zhou, D., Jia, L., Kamath, J., and Kovscek, A.R., 2001, Countercurrent imbibition processes in diatomite, Journal of Petroleum Technology, v. 53, p. 44.

Zuur, A.F., Ieno, E.N. and Smith, G.M. (2007) Analysing Ecological Data: Springer, New York.